

SITES FOR WIND-POWER INSTALLATIONS:
Physical Modeling of the Influence of Hills,
Ridges and Complex Terrain on
Wind Speed and Turbulence

by

R. N. Meroney and V. A. Sandborn
Principal Investigators

R. J. B. Bouwmeester, H. C. Chien, M. Rider
Associate Investigators

PART II EXECUTIVE SUMMARY

Fluid Mechanics and Wind Engineering Program
Civil Engineering Department
Colorado State University
Fort Collins, Colorado 80523

June 1978

Prepared for the United States
Department of Energy
Division of Distributed Solar Technology
Federal Wind Energy Program

DOE Contract No. EY-76-S-06-2438, A001

NOTICE

This report was prepared as an account of work sponsored by an agency of the United States Government. Neither the United States nor any agency thereof, nor any of their employees, makes any warranty, expressed or implied, or assumes any legal liability or responsibility for any third party's use or the results of such use of any information, apparatus, product or process disclosed in this report, or represents that its use by such third party would not infringe privately owned rights.

ABSTRACT

Wind-tunnel model measurements have been performed to study the influence of topography profile, surface roughness and stratification on the suitability of various combinations of these variables for wind-power sites. For the range of examined cases (large turbulence integral scales with respect to surface feature scales) the flow is dominated by inviscid dynamics. Hence, the influence of hill shape, surface roughness, and mild stratification can be reliably estimated by simple prediction procedures for the range of situations considered (i.e., horizontal length scales of the order of 1000 meters).

Detailed tables of velocity, turbulence intensity, pressure, spectra, etc., have been prepared to guide numerical model design and experimental rule of thumb constrictions. Cases include hill slopes from 1:2 \rightarrow 1:20, neutral and stratified flows, two- and three-dimensional symmetric ridges, six alternate hill and escarpment shapes, and a variety of windward versus leeward slope combinations to evaluate ridge separation characteristics. In addition, one comparison program over complex terrain consisting of both field and laboratory measurements has been completed.

The final product of this investigation is a summary of criteria to be satisfied for potential sites. Included was validation that certain criteria are satisfied which ensure similitude between the laboratory experiment and the atmospheric situation being modeled. The laboratory data were verified by comparison with field measurements in a well documented case of flow over known terrain. Emphasis was placed on effects of surface layer separation and topography scales larger than turbulence integral scales, i.e., hills small with respect to atmospheric surface layer depth.

ACKNOWLEDGMENT

The authors wish to express their appreciation to Drs. William Pennell and Ronald Drake of Battelle, Pacific Northwest Laboratories, for their technical review and advice, to Ms. Pamela Partch for her careful editorial review and criticism, and to Mrs. Louise Warren for her patience during typing many revisions of this report. Special thanks is given to George Tennyson and Louis Divone of the Department of Energy Wind Systems Branch for their support and advice.

TABLE OF CONTENTS

<u>Chapter</u>	<u>Page</u>
ABSTRACT	iii
ACKNOWLEDGMENTS	iv
LIST OF TABLES ,	vii
LIST OF FIGURES	viii
LIST OF SYMBOLS	x
1.0 INTRODUCTION	1
1.1 PROCEDURES FOR COMPLETING OBJECTIVES	1
1.2 ORGANIZATION OF THIS REPORT	3
2.0 WIND CHARACTERISTICS IN COMPLEX TERRAIN	4
2.1 TWO- AND THREE-DIMENSIONAL SLIGHT OR MODERATE RELIEF HILLS	4
2.2 ADIABATIC AND BAROSTROPHIC FLOW OVER MOUNTAINOUS TERRAIN	5
2.2.1. Neutral Airflow Over Mountainous Terrain	6
2.2.2 Stratified Airflow Over Mountainous Terrain	6
2.3 WINDS ENHANCED BY PASSES, SADDLES, GAPS, CANYONS AND GORGES	7
2.4 REVIEW OF PHYSICAL MODELING EXPERIENCE OF WIND CHARACTERISTICS OVER IRREGULAR TERRAIN	8
3.0 CRITERIA FOR LABORATORY SIMULATION OF WIND CHARACTERISTICS OVER IRREGULAR TERRAIN	17
3.1 BASIC EQUATIONS AND ASSUMPTIONS	17
3.2 PERFORMANCE ENVELOPE FOR WIND TUNNEL MODELING OF AIRFLOW OVER TERRAIN	22
3.3 TIME AND SPACE DOMAIN APPROPRIATE FOR PHYSICAL MODELING OF WECS SITE CHARACTERISTICS.	23
4.0 EVALUATION OF FIELD AND LABORATORY DATA	32
4.1 INFLUENCE OF TWO-DIMENSIONAL RIDGES ON WIND SPEED AND TURBULENCE	32
4.1.1 Effect of Ridge Shape	33
4.1.2 Effects of Turbulence	36

TABLE OF CONTENTS (continued)

<u>Chapter</u>		<u>Page</u>
	4.1.3 Effects of Surface Roughness	37
	4.1.4 Effects of Thermal Stratification	39
	4.1.5 Parameterization of Speedup	40
	4.1.6 Prediction of the Velocity Distribution at the Crest of a Ridge	41
	4.1.7 The Effect of Finite Hill Width	41
4.2	INFLUENCE OF THREE-DIMENSIONAL HILLS OR RIDGES OF WIND SPEED AND TURBULENCE	42
	4.2.1 Laboratory Measurement Program	44
	4.2.2 Results and Conclusions	44
4.3	INFLUENCE OF COMPLEX TERRAIN ON WIND SPEED AND TURBULENCE	45
	4.3.1 Joint Physical Modeling to Field Measurement Comparison Study	45
	4.3.2 Validation Results and Conclusions	48
5.0	SUMMARY AND RECOMMENDATIONS	76
5.1	FLOW CHARACTERISTICS PERCEIVED FROM GENERIC HILL AND RIDGE STUDIES	76
5.2	SIMILITUDE CONSTRAINTS	78
5.3	NUMERICAL MODELING IMPLICATIONS PERCEIVED FROM LABORATORY DATA	79
5.4	RECOMMENDATIONS FOR PHYSICAL MODELING METHODOLOGY FOR WECS SITING	80
	REFERENCES	82

LIST OF TABLES

<u>Table</u>		<u>Page</u>
2-1	Experimental Data of Flow Over Hills, Ridges and Escarpments	10
2-2	Site Classification as Suggested by Frenkiel (1962) . . .	12
2-3	Laboratory Simulation of Flow Over Irregular Terrain . .	13
3-1	Typical Boundary Layer Wind Tunnel Characteristics . . .	25
3-2	Typical Field Characteristics	26
3-3	Typical Wind Tunnel and Field Parameter Range	27

LIST OF FIGURES

<u>Figure</u>		<u>Page</u>
2-1	Methods in Which Terrain Features Affect Atmospheric Motions	16
3-1	Performance Envelope for Physical Modeling of Shear Flows Over Complex Terrain	28
3-2	Scale Definitions and Different Processes With Characteristic Time and Horizontal Scales	29
3-3	A Classification of the Effects of Terrain on Atmospheric Motions	30
3-4	Physical Modeling Domain Among Time and Space Scales for WECS Site Selection	31
4-1	Mean Velocity and Static Pressure Contours Over Triangular Hills	51
4-2	The Effect of Downwind Slope on Vertical Velocity Profiles Downwind of the Crest	52
4-3	The Effect of Opposite Wind Directions	53
4-4	Criterion for Flow Separation Over Two-Dimensional Hills	54
4-5	Upstream Approach Profiles for Numerical Inviscid Flow Calculation	55
4-6	Fractional Speedup Ratios Predicted From Numerical Inviscid Flow Calculations	56
4-7a 4-7b	Contour of Longitudinal Turbulence Intensity With Superimposed Streamlines.	57
4-8	Mean Velocity Contours Over Triangular Hills	59
4-9	Static Pressure Contours Over Triangular Hills	59
4-10	Approach Velocity Profiles for Numerical Inviscid Flow Calculations	60
4-11	Fractional Speedup Ratios Predicted From Numerical Inviscid Flow Calculations	61
4-12	Contour of Longitudinal Turbulence Intensity With Superimposed Streamlines	62

LIST OF FIGURES (continued)

<u>Figure</u>		<u>Page</u>
4-13	Fractional Speedup Ratio Over the Ridges	63
4-14	The Effect of Upwind Slope on the Speedup Factor for $\alpha_o = 0.13$	64
4-15	The Effect of Downwind Slope of the Speedup Factor for $\alpha_o = 0.13$	65
4-16	Mean Velocity Profiles Over a Ridge With Finite Width	66
4-17	Mean Velocity Profiles Over a Ridge With Finite Width	67
4-18	Flow Pattern Around a Rectangular Block With Reattachment of the Free Shear Layer	68
4-19	Schematic of the Vortex-Containing Wake of a Hemisphere	69
4-20	Boundary Layer Wind Tunnel, Department of Mechanical Engineering, University of Canterbury	70
4-21	Models of Rakaia River Gorge Region Looking Northwest .	71
4-22	Portable Tower and Anemometer Rakaia River Gorge Field Experiment	72
4-23	Vertical Section G-G Isotachs, Terraced Model	73
4-24	Vertical Section G-G Isoturbs, Terraced Model	74
4-25	Scatter Diagram Field Test Data, December 28 versus Contoured Model Data	75

LIST OF SYMBOLS

<u>Symbol</u>	<u>Definition</u>	<u>Dimensions</u>
A	Amplification factor	
c_p	Specific heat capacity	$L^2 T^{-1} \theta^{-2}$
C_f	Skin friction coefficient	
Ek	Eckert number	
Eu	Euler number	
g	Gravitational constant	LT^{-2}
h	Hill height - base to crest	L
H	Shelter belt height	L
I_{ij}	Turbulence intensities	
k	von Karman constant	
K_H	Eddy diffusivity for heat	$L^2 T^{-1}$
K_m	Eddy diffusivity for momentum	$L^2 T^{-1}$
k_T	Thermal conductivity	$MLT\theta^{-3}$
L	Hill half width: distance from crest to half height	L
L_d	Downwind hill length = 2 L	L
L_{mo}	Monin Obukhov scaling length	L
L_o	Characteristic length	L
L_u	Upwind hill length = 2 L	L
ℓ	Scorer parameter = $g\beta/U_o^2$	L
L_{u_x}	Longitudinal integral scale	L

LIST OF SYMBOLS (continued)

<u>Symbol</u>	<u>Definition</u>	<u>Dimensions</u>
n	Frequency	T^{-1}
Pr	Prandtl number	
p	Pressure	$ML^{-1}T^{-2}$
Q_H	Heat flux	M/T^3
r	Sample correlation coefficient	
$R(\tau)$	Autocorrelation function $\frac{\overline{u'u'}(\tau)}{\overline{u'^2}}$	
Re	Reynolds number	
Ri	Richardson number	
Ro	Rossby number	
Ri_B	Bulk Richardson number	
ΔS	Fractional speedup factor	
$S(n)$	Energy spectrum function	
T	Temperature	θ
u'_1	Velocity fluctuation	LT^{-1}
\bar{u}	Mean velocity	LT^{-1}
U	Characteristic velocity	LT^{-1}
u_*	Friction velocity	LT^{-1}
x, y	Variables in linear regression	
z_0	Roughness length	L

LIST OF SYMBOLS (continued)

<u>Symbol</u>	<u>Definition</u>	<u>Dimensions</u>
<u>Greek</u>		
α	Velocity profile index	
β	Volumetric compressibility (Thermal)	θ^{-1}
δ	Boundary layer thickness	L
η	Vorticity	T^{-1}
θ	Potential temperature	θ
λ	Roughness scale	L
μ	Absolute viscosity	$ML^{-1}T^{-1}$
ν	Kinematic viscosity	L^2T^{-1}
ρ	Mass density	ML^{-3}
ψ	Stream function	L^2T^{-1}
τ	Shear stress	$ML^{-1}T^{-2}$
Ω	Coriolis parameter, rotational velocity	T^{-1}

Subscripts

h	Length scales to hill height
G	Geostrophic level
o	Characteristic scale
δ	Length scales to boundary layer depth
m	Model
p	Prototype

1.0 INTRODUCTION

This report summarizes the results of a laboratory program designed to systematically study the major interactions of wind and topography. Its primary purpose was to provide information of use to wind-power site selection; however, the results will also be of interest to those involved in architectural planning, wind loading on buildings, forest blowdown, ballistics, snow drifting, and environmental control.

More specific objectives have been:

1. To determine local wind profiles and turbulence over two- and three-dimensional hills or ridges as influenced by hill or ridge profile, upwind surface roughness, stratification, hill slope or aspect ratio, and downslope hill configurations which influence separation or reattachment;
2. To identify the pertinent similarity parameters and scaling conditions to assure adequate replication of the kinematics and dynamics of the complex terrain flow field;
3. To verify those similarity and physical modeling techniques selected by comparing measurements against a well documented field investigation;
4. To interpret the results of this physical modeling program in terms of their implications for Wind Energy Conversion Systems (WECS) siting; and, finally,
5. To recommend under which conditions it would be appropriate to consider physical modeling of a specific site during a siting strategy.

1.1 PROCEDURES FOR COMPLETING OBJECTIVES

The laboratory method consists of obtaining velocity and turbulence measurements over a scale model of selected terrain placed in a simulated atmospheric flow. The wind characteristics of the simulated atmospheric flow are chosen to reproduce the wind profile shape and length scales of the equivalent prototype situation. Since field profiles are rarely available in advance, velocity profiles and turbulence characteristics are chosen to fit an equivalent class of conditions as recorded by earlier investigators over terrain of similar roughness.

A wide range of natural wind characteristics can be simulated by means of the unique Meteorological Wind Tunnels which have been used for this research. Characteristics of major concern are magnitudes and spatial distribution of mean velocity, turbulence scales and turbulence spectra of winds approaching the wind power sites. Verification that natural wind characteristics are simulated to a high degree of approximation by the long-test-section type wind tunnel has been reported by Cermak (1975).

A review of physical modeling similarity requirements has been previously reported by Meroney et al. (1976, 1977, 1978). To consolidate the consensus of this program Section 3.0 of this report summarizes the similarity criteria specified by dimensional and inspectional analyses.

Measurements have been made of wind speed, turbulence intensity, static pressure, skin friction, and spectra over a number of general two-dimensional hill shapes. Measurement techniques are described in Meroney et al (1976a, 1976b, 1977), and Bouwmeester et al (1978). Data are tabulated in detail in Meroney et al. (1976b), Bouwmeester et al. (1978), and Rider and Sandborn (1977a) for neutral stratification measurements in the Meteorological Wind Tunnel (MWT). Additional measurements over a set of 6 different hill shapes made in the smaller Transpiration Wind Tunnel (TWT) are described by Rider and Sandborn (1977b). A set of measurements associated with stratified flow over two-dimensional hills has been compiled into Appendix C in Meroney et al. (1978b). An added set of measurements investigating the flowfield when the down slope hill varies in incipient separation are described by Bouwmeester et al. (1978). A detailed evaluation of the WECS siting significance and fluid dynamics implications of all two-dimensional measurements are contained in the report by Bouwmeester, et al. (1978), which is a companion report to this summary. Three-dimensional flowfield data are provided in tabulated form by Chien et al. (1978). Their interpretation will be discussed in Section 4.3 of this report.

A validation study was performed through a joint effort between Colorado State University, U.S.A., and University of Canterbury, New Zealand. The results of this program have been described by Meroney et al. (1978a) in another companion report of this series on WECS siting. During the validation study both terraced and contoured models of the Rakaia River Gorge region were prepared to an undistorted geometric scale of 1:5000. The contoured model was examined for three, separate, surface-roughness conditions: a surface textured to represent typical paddock grass roughness only, the same surface with zero-porosity shelterbelts added, and the same surface with porous shelterbelts added.

The field program first considered the results of climatological measurements correlated by Cherry (1976) as part of the New Zealand Wind Energy Task Force (NZWETF) survey of Wind Energy Resources in New Zealand. (A phase II program is currently (1974-1978) gathering further data in the Rakaia River Gorge region at a number of additional sites in the Rakaia Gorge area.) On two spring days selected for strong adiabatic down-valley windflow, three teams of investigators surveyed up to 27 sites on either side and within the river gorge. Measurements consisted of wind speed and direction at a 10 meter height on lightweight portable towers. All measurements were completed during the course of a five-hour wind event and normalized against continuous records taken from a permanent anemometer station maintained by the New Zealand Wind Energy Task Force. The laboratory simulation results were compared

with the available field data by means of statistical correlation and scatter diagrams. The model and field results were used to assess the value of the laboratory experiments for assisting WECS siting field programs.

1.2 ORGANIZATION OF THIS REPORT

This report provides a summary of the concensus of all other reports prepared under this contract. A brief review of the various aspects of meteorology over complex terrain such as effects of terrain on wind structure and laboratory simulation are presented first in Chapter 2.0. The required assumptions, equations, and similitude parameters which govern the air flow over complex terrain are established in Chapter 3.0 by examining the reducing the basic equations governing the atmosphere in the planetary boundary layer. A performance envelope for a typical meteorological wind tunnel suggests operational constraints that place bounds on the use of the laboratory model as a predictive tool.

A discussion of both laboratory and field results are found in Chapter 4.0. These include mean wind profiles, longitudinal turbulence intensities, spectra, correlations, fractional speedup factor, pressure distributions, wind veering angles, and shelterbelt aerodynamics, as influenced by hill shape, roughness, stratification, end effects, separation, etc. Conclusions and recommendations concerning the program objectives are provided in Chapter 5.0.

2.0 WIND CHARACTERISTICS IN COMPLEX TERRAIN

One can divide the terrain perturbed influence of the atmospheric motion on wind power into four areas:

- a) variation of wind speed over uniform terrain,
- b) local wind circulations,
- c) flow over slight or moderate relief, and
- d) flow over high mountains.

Each of these areas has received attention from past investigators. Indeed, a wealth of information exists on category a, the understanding of which has recently been summarized in an American Meteorological Society monograph (Haugen, 1973). However, if there is an abrupt change in roughness and heating for even flat terrain, major changes can occur as considered under category b, local wind circulations.

Local wind circulations may be driven by nonhomogeneities in roughness, temperature, or pressure. A good deal has been learned recently in the laboratory about thermal and roughness inhomogeneities (Yamada and Meroney, 1971; Kahawita and Meroney, 1973; Cermak and SethuRaman, 1973; Huang and Nickerson, 1972; Meroney et al., 1974). Saddle points, passes, or gaps offer possibilities for enhanced winds especially if they are open to a prevailing wind direction. Such local effects can greatly enhance energy potential; yet, they do not usually show up in national wind survey results.

Areas c and d are discussed with greater detail in Sections 2.1 and 2.2 respectively.

2.1 TWO- AND THREE-DIMENSIONAL SLIGHT OR MODERATE RELIEF HILLS

Flow over slight or moderate relief may result in enhanced wind speeds as a result of wind "overshoot" or "speedup." A few field measurement programs over terrain features were carried out specifically to estimate wind power potential (Putnam, 1948; Golding, 1955; Frenkiel, 1962-63; Frenkiel, 1963; Archibald, 1973; Hewson, 1973). These results are to a large degree site specific and do not cover a wide enough range of terrain types to allow more than a very limited and qualitative generalization to other situations. In fact the combination of hill features, roughness, upstream topographies, and stabilities studied even appear to lead to a set of contradictory conclusions (Davidson et al., 1964). A number of additional field and laboratory investigations of flow over topography have been completed, which were not specifically oriented toward wind power site selection. The characteristics of a number of these studies together with typical results have been compiled into Table 2-1. These studies, which span some 46 years and more than seven countries include gentle hills, cones, ridges, escarpments, and mountains. A number of the laboratory studies included, or were performed in conjunction with, field measurements.

Meroney et al. (1976a, 1976c) discussed briefly the reliability and implications of these studies with regard to wind turbine site evaluation. Experience gleaned from these studies included in Table 2 with regard to wind site evaluation over low to medium height ridges or hills suggests the following:

1. Ridges should be perpendicular to the principal wind direction, but high velocities are not likely on upwind foothills.
2. Hilltops should not be too flat, and slopes should extend all the way to the summit.
3. A hill on the coast is more likely to provide high winds than an inland hill surrounded by other hills, i.e., unobstructed upwind.
4. Speedup is greater over a ridge of given slope than over a conical hill of the same slope.
5. Speedup over a steep hill decreases rapidly with height above the hill crest.
6. The optimum hill slope is probably between 1:4 and 1:3 based on optimum speedup and the presence of a uniform velocity profile.
7. Topographical features in the vicinity of the hill produce the structure of the flow over it.
8. Frenkiel (1962 and 1963) ranks sites based on the uniformity of the summit wind profile. He suggests ranking which has been incorporated into Table 2-2.
9. Hills with slopes greater than 1:3 should probably be avoided because of gustiness associated with flow separation.
10. Vertical wind speed above a summit does not increase as much with height above ground as over level terrain.

2.2 ADIABATIC AND BAROSTROPHIC FLOW OVER MOUNTAINOUS TERRAIN

Upwind of an abrupt, steep mountain chain such as the Southern Alps, New Zealand, the air is often blocked, the wind is reduced, and only a weak flow along the base of the mountain exists. Downwind of the mean divide winds may be enhanced by convergence and channeling effects. It is true such sites often produce very high winds of large gustiness; yet, future designs for wind power generators may permit use of this extremely energetic wind. Mountains may alter atmospheric airflow

characteristics and motion in a number of different ways. These effects can generally be grouped into those due to inertial-viscous interactions associated with a thick neutrally stratified shear layer and to thermally induced interactions associated with stratification or surface heating.

2.2.1 Neutral Airflow Over Mountainous Terrain

Near-neutral or adiabatic atmospheric boundary layers will exist over mountains during situations when winds are high due to intense synoptic pressure fields, when continuous cloud banks impede surface heating, and when sharp terrain features produce separation eddies which mix the flow field vigorously in the vertical. Such a situation is shown schematically as case a, Figure 2-1.

When the static stability is neutral, airflow over mountains creates pressure gradients in the flow direction, which together with surface friction, may produce separation, flow reversal, and reattachment. Separation eddies at the windward or leeward side of a mountain can alter the effective shape of the mountain resulting in a modified wind profile at the crest. Scorer (1978) described eight different variations of the separation phenomenon. He notes that separation may be changed in character by insolation, blocking, diabatic changes, and three-dimensional effects.

Meroney et al. (1976c) summarized experimental data available from field and laboratory structures over hills, ridges, and escarpments (see Table 2-1). Orgill (1977) surveyed wind measurements programs that have used wind networks (2 to 60 measurements sites) to identify data suitable for calibrating WECS siting methodologies. Out of the 139 field programs 3 relate to an isolated mountain, 7 to mountain-plain flows, and 20 to complex topography.

2.2.2 Stratified Airflow Over Mountainous Terrain

Stratification has a strong effect upon flow over and around hills. The intensity of an inversion may influence both wind velocity and direction. If inversions are frequent, acceleration of air around the hillside rather than over the hilltop may lead to larger annual average velocities away from the hill crest. Stratified flow over mountain ridges may also lead to lee waves or helm winds. There is very extensive literature dealing with orographic induced waves, but since most of it deals with cloud systems and upper atmosphere character far from the surface, it is not very helpful for windmill site analysis. Over mountain ridges speedup effects as well as speeddown effects may be observed. These effects seem to depend on the orography, slope, roughness, stability, and insolation. Thus one sees maximum winds,

not on the highest peak, but frequently at some lower level (for example, the behavior of the Hump of Mt. Washington (Putnam, 1948)).

2.3 WINDS ENHANCED BY PASSES, SADDLES, GAPS, CANYONS AND GORGES

Certain terrain forms are more wind energy rich than others because they tend to channel and enhance wind speeds. Many of the locations that lay wisdom associates with high winds are related to such terrain features as passes, saddles, gaps, canyons, and gorges. Windy Gap, Wyoming (Marrs and Marrwitz (1977)), Nuuanu Pali Pass, Oahu, (Hardy (1977)), the Tehachapi Mountain saddle, California, (Lindley (1977) or Traci et al. (1977)), or even Wind Whistle near the Rakaia Gorge, New Zealand, are pertinent examples.

Mountain passes, saddles, and gaps are usually the more accessible and lowest notches across a mountain barrier or between two or more distinct mountains. Canyons or gorges refer to a longer opening in otherwise complex topography usually associated with a river or erosion channel and normally having high, steep, side walls.

These types of topographic configuration have been suggested as good wind energy sites because they produce enhanced wind speeds. The increased wind speeds are the results of a venturi or jet effect as the air is forced around the sides of mountains or hills and through the opening. As Davidson et al. (1964) remarks, this speedup will occur both day and night provided the prevailing wind is strong enough. There appears to be no special set of criteria to judge the efficacy of a given venturi-shaped surface feature. In addition to height, width, or length of a saddle, gap, or pass one might expect that elevation, shape, approach condition, and roughness are significant. Scorer (1952) discusses some data from Gibraltar, Liu and Linn (1976) report on laboratory measurements in stratified flow near an idealized mountain saddle.

Valleys or canyons are generally V shaped as a result of vigorous stream erosion or U shaped as a result of glacial movement. Sometimes a steep sided gorge may exist through glacial morrain and lower hills, which lie at the end of the broader U shaped valley. This is the case for the Rakaia River Gorge studied in a companion volume of this Final Report. A broad U shaped valley lies between the Mt. Hutt range and the Big Ben Range. This valley has an average breadth of 10,000 meters. The gorge which is the dominant feature of the valley exit has a typical width of 1500 meters (see Figure 2-5).

The airflow pattern in any particular valley will depend upon the large scale airflow or gradient wind above the valley and its direction with respect to the valley. Atmospheric stability, geometry of the valley, surface roughness, and insolation are all critical to the general

flow circulation. As mentioned earlier the physical situation studied for the Rakaia Gorge was limited to time periods in which the wind was moderate to strong and the direction was parallel to the valley.

Detailed wind information for gaps and gorges is lacking. Some information from studies by Clements and Barr (1976) for flow in Los Alamos Canyon suggests that in high gradient wind conditions canyon floor winds are even less than the surrounding mesa top wind levels. Davidson (1961) reported observations from eight valleys in New England. Although recognizing the possibility of venturi effects for valleys whose axis are along the prevailing wind directions he concludes wind speeds in most valley locations in the zone of the westerlies are less than they would be over flat terrain.

2.4 REVIEW OF PHYSICAL MODELING EXPERIENCE OF WIND CHARACTERISTICS OVER IRREGULAR TERRAIN

In view of the extreme difficulties in obtaining practically useful results in the area of meteorology over complex terrain it is natural that physical model experiments on the laboratory scale have been used to explore the possibilities of simulating the flow over irregular terrain.

Laboratory simulation of flow over irregular terrain presents many problems such as

1. the specification of criteria for similitude between model and prototype,
2. the adoption of restrictive assumptions associated with physical limitations of the laboratory apparatus,
3. the accurate measurement of flow variables to construct pertinent parameters, and
4. the necessity of verifying the model approach with actual field measurement.

Chapter 3.0 considers the equations and assumptions required to define appropriate similitude criteria. Although not all investigators agree on details most would concur that the dominant forcing mechanisms in the atmosphere surface layer can now be identified and are understandable.

Nonetheless, when using physical models often only parts of a problem may be realistically simulated and many simplifying, but not necessarily invalidating, assumptions are made through necessity. In some cases these restrictions relate to current facility limitations.

Section 3.2 considers a performance envelope for the typical, large, boundary-layer wind tunnel and its ability to deal with the task of WECS siting over a range of terrain size and scaling ratio.

Finally, reasonable concern exists that quite often adequate field data are not available in order to check the model results. In this work, the second method of research, the field program, was incorporated into the test plan in order to provide pertinent observations that would assist in evaluating the laboratory simulation and the accuracy of laboratory measurements.

Most topographic model studies have been made with neutral flow while barostromatic airflow has just recently been investigated in the wind tunnel. However, an effort was made in 1941 by Abe to study flow over Mt. Fuji with an airstream stratified by solid carbon dioxide. Table 2-3 gives a listing of terrain models which have been studied and the type of flow used.

A neutral airflow although the most convenient to simulate, may only apply to the actual field conditions in very special atmospheric conditions, i.e., during periods of neutral stability through deep layers of the atmosphere. A barostromatic airflow attempts to simulate the normal temperature stratification one observes in the atmosphere, i.e., an increase of potential temperature with height. This type of airflow is difficult to produce realistically because of the required temperature or density stratification.

TABLE 2-1. EXPERIMENTAL DATA OF FLOW OVER HILLS, RIDGES, AND ESCARPMENTS

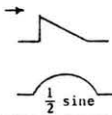


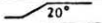
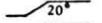
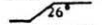

AUTHOR	METHOD	SHAPE RAMP OR HILL	h L	STABILITY	α	z ₀ h	u ₀ [*] u ₀ (L)	MEASUREMENTS REPORTED								
								p	u	u'	τ	w'	E _u (k)	-C _p _{max}	ΔS	S
Field & Warden (1929-1930)	wind tunnel	Gibraltar	-1.10	N	-0	--	--		x	x			--	--	--	
	field		-1.10	N					x	x			--	--	--	
Putnam (1948) (Petterssen, 1961)	field	Pond	1.27	--	.3	.05	--		x				--	--	0.84	
		Glastenberg	--	--	.3	--	--		x				--	--	1.04	
	wind tunnel	Mt. Washington	.61	--	.3	.05	--		x				--	--	1.47	
		Pond	1.27	N	-0				x				--	--	1.29	
		Glastenberg	--	N	-0				x				--	--	1.44	
	Mt. Washington	.61	N	-0				x				--	--	1.30		
Golding (1955)	field	Costa, Orkney U.K.	0.3-0.6	--	--	--	--		x				--	--	--	
		Vestra Field, U.K.	0.2	--	--	--	--		x				--	--	--	
Frenkiel (1961)	field	Hreiba Ridge, Israel	0.25	N,S	0.15	1.4x10 ⁻⁴	--		x	x			--	--	--	
		Givat Hamere Hill, Israel	-0.57	N,S	0.15	9x10 ⁻⁵	--		x	x			--	--	--	
Halitsky et al. (1962-1963)	wind tunnel	Bear Mtn., NY	-0.46	N	--	--	--		x	x	x		--	--	--	
Chang (1966)			1.0	N	.15		.036	x	x	x			.33	.27	1.0	
Plate & Lin (1965)	wind tunnel		1.0	US*	.19	1.5x10 ⁻⁴		.033	x	x			--	.24	1.15	
			2.0	N	.15			.036	x	x	x			.33	.35	1.1
			0.5	N	.15			.036	x	x	x			.33	.35	1.0
			0.8	N	.15	1.5x10 ⁻⁴		.035	x	x	x	x		.55	.76	1.38
				US**	.19			.032	x	x			--	--	--	
Cermak & Peterka (1966)	wind tunnel	Pt. Arguello, CA	0.11	N	0.25	--	--		x				--	--	--	
			0.11	S ^{ΔΔ}	0.25	--	--		x				--	>3.0	1.25	
Meroney & Cermak (1967)	wind tunnel	San Nicolas Is., CA	0.12	N	0.14	1.2x10 ⁻²	.032		x	x	x		--	--	--	
			0.12	S ^{ΔΔ}	0.20	--	--		x				--	--	--	
Lin & Binder (1967)	wind tunnel		0.67	S					x				--	--	1.2	
			1.33	S		Lee Waves			x				--	--	2.6	
Garrison & Cermak (1968)	wind tunnel	San Bruno Mtn., CA	-0.43	S	0.16	2.5x10 ⁻³	.125		x				--	0.5	1.07	
Hsi et al. (1968)	wind tunnel	Green River, UT	-.09	N	0.14	2x10 ⁻⁴	--		x				--	--	1.14	
Boryland et al. (1968)	field		0.1	N	--	--	--		x				--	0.25	--	
										x				--	0.1	1.1
Zrajevsky, Doroshenko & Chepik (1968)	wind tunnel	"	"	N	-0	--	--		x				--			
Kitabayashi et al. (1971)	wind tunnel	Elk Mtn., WY	0.35	N	0.21	7x10 ⁻³	0.149		x	x			--	0.37	1.04	
				S ^{***}	0.32	--	--		x				--	0.29	1.29	

TABLE 2-1.(CONTINUED) EXPERIMENTAL DATA OF FLOW OVER HILLS, RIDGES, AND ESCARPMENTS

AUTHOR	METHOD	SHAPE RAMP OR HILL	h L	STABILITY	α	z ₀ h	u ₀ u ₀ (L)	MEASUREMENTS REPORTED					-C _p max	ΔS	S	
								p	u	u'	τ	w'				E _u (k)
Eliseev (1971)	field	Razdan Valley, USSR	0.61	N	--	--	--	x					--	0.35	--	
Orgill & Cermak (1971)	wind tunnel	Climax, CO	.10	N	0.25	3.0x10 ⁻⁴	--	x	x	x	x	x	--	1.86	1.18	
			.10	S	ΔΔΔ	--	--	--	x				--	0.67	1.00	
			.10	N	0.57	--	--	--	x	x	x		--	1.20	0.75	
de Bray (1973)	wind tunnel		0.72	N	0.14	--	--	x					--	0.41	1.13	
			0.5	N	0.14	--	--	--	x				--	0.34	1.07	
			--	N	0.14	--	--	--	x				--	0.30	1.04	
			--	N	0.11	--	--	--	--							
Freeston (1974)	wind tunnel		0.72	N	0.14	--	--	x	x				0.40	0.38	1.10	
			1.67	N	0.14	--	--	--	x	x			0.90	0.45	1.16	
			3.46	N	0.14	--	--	--	x	x			1.00	0.18	0.94	
			0.5	N	0.14	--	--	--	x	x			0.50	0.34	1.07	
			--	N	0.14	--	--	--	--	x	x			0.40	0.30	1.04
Bowen & Lindley (1974)	field		0.98	N	0.1	5x10 ⁻⁵	0.102	x					--	0.39	1.06	
			=	US	0.45	1x10 ⁻²	--	x					--	1.13	1.16	
			0.98	N	0.18	4x10 ⁻³	0.160	x					--	0.40	1.12	
Meroney et al. (1976)	wind tunnel		=	N	0.18	5.3x10 ⁻³	0.160	x					--	0.47	1.10	
			1.0	N	0.14	9x10 ⁻⁵	.032	x	x	x	x	x	x	0.25	0.71	1.07
			0.67	N	0.14	"	"	x	x	x				.26	0.79	1.15
			0.50	N	0.14	"	"	x	x	x				0.93	1.41	1.53
			0.33	N	0.14	"	"	x	x	x	x	x	x	0.77	1.11	1.35
0.10	N	0.14	"	"	x	x	x	x	x	x	0.15	.40	0.90			

$$C_{p_{max}} = \frac{\Delta p}{\frac{1}{2} \rho u_0(\delta)^2}, \Delta S = u(z)/u_0(z), S = \frac{u(z)}{u_0(z+hL/L)}$$

- * Ri_{δh} = -.016
- ** Ri_{4h} = -.019
- *** Ri_δ = 1.70
- Δ Field comparisons available
- ΔΔ Ri_δ = 0.30
- ΔΔΔ Ri_h = 6.0

TABLE 2-2. SITE CLASSIFICATION AS SUGGESTED BY FRENKIEL (1962)

QUALITY	$R = U_{40m}/U_{10m}$	POWER COEFFICIENT α	SLOPE	h/L
Optimum	$R < 1.05$	0.0	1:3.5	0.57
Very Good	$1.05 < R < 1.10$	0.07	1:6 smooth regular	0.35
Good	$1.1 < R < 1.15$	0.1	1:10	0.20
Fair	$1.15 < R < 1.21$	0.14	1:20 smooth 1:6 regular	0.10
Avoid	$1.21 < R$	>0.14	$>1:20$ $<1:2$	<0.05 >1.0

TABLE 2-3. LABORATORY SIMULATION OF FLOW OVER IRREGULAR TERRAIN

AUTHOR/(DATE)	TOPOGRAPHIC SITE	PROBLEM STUDIED	TYPE OF AIR FLOW	MAXIMUM HEIGHT OF RISE (m)	LENGTH SCALE RATIO	SIMILITUDE CRITERIA						
						$\delta/\Delta H$	$\frac{1}{\alpha}$	$\frac{z_0}{\Delta H} \times 10^4$	$\frac{\overline{U^2}}{U_0^2}$	$\frac{U_x}{U_0}$	$\frac{L_x}{\Delta H}$	Ri
▲1 Field & Warden (1929-1930)	Rock of Gibraltar	Topographic effects & turbulence	Neutral	520	5,000	0	0					
▲2 Abe (1941)	Mt. Fuji, Japan	Mountain clouds and topographic effects	Barostromatic (dry ice)	4,000	50,000							not accurate
▲3 Putnam (1948)	Pond Glastenberg, Mt. Washington	Topographic effects	Neutral	300 850 1,154	5,280 8,280 5,280							
4 Suzuki & Yabuki (1956)	Idealized hills	Mountain lee waves	Barostromatic (brine solution)			0	0					
5 Long (1953, 1954, 1955)	Idealized hills	Mountain lee waves	Barostromatic (brine solution)			0	0					13-94.0
▲ Long (1959)	Sierra Nevada Mountains, Calif.	Mountain lee waves	Barostromatic (brine solution)	2,750	75,000	0	0					12-300
6 Nemoto (1961)	Enoshima & Akashi Channel, Japan	Turbulence & Velocity Profiles	Neutral	60	600 3,300/ 10,000		1.0		0.20		1.33	
▲7 Halitsky, Toleiss, Kaplin & Magony (1962-63)	Bear Mountain, New York	Turbulence & wake patterns	Neutral	390	1,920	1.25			0.16			
8 Briggs (1963)	Rock of Gibraltar	Turbulence Patterns	Neutral	520	5,000	0	0					
9 Halitsky, Magony & Halpern (1964-65)	Mountains near Manchester, Vermont	Topographic effects	Neutral									
10 Plate & Lin (1965)	Idealized hill	Velocity & turbulence in wake	Neutral Unstable			3-9 3-5	0.15 0.19	1.5 1.5	0.14	0.032 0.032		0.02
11 Chang (1966)	Idealized hill	Velocity & turbulence in wake	Neutral			2	0.15	1.5				
▲12 Cermak & Peterka (1966)	Pt. Arguello, California	Topographic effects & diffusion	Barostromatic Neutral	500 500	12,000 12,000	9.0 9.0	0.25 0.25					0.31
▲13 Meroney & Cermak (1967)	San Nicolas Island, California	Topographic effects & diffusion	Neutral & Barostromatic	275 275	6,200 6,200	12.6 12.6	0.14 0.20	0.20		0.032		0.30
14 Lin & Binder (1967)	Idealized mountain	Mountain lee waves	Barostromatic									4-25

▲Field observations available.

TABLE 2-3. (CONTINUED) LABORATORY SIMULATION OF FLOW OVER IRREGULAR TERRAIN

AUTHOR/(DATE)	TOPOGRAPHIC SITE	PROBLEM STUDIED	TYPE OF AIR FLOW	MAXIMUM HEIGHT OF RISE (m)	LENGTH SCALE RATIO	SIMILITUDE CRITERIA						
						$\delta/\Delta H$	$\frac{1}{\delta}$	$\frac{z_0}{\Delta H} \times 10^4$	$\frac{U^*}{U_0}$	$\frac{U^*}{U_0}$	$\frac{L_x}{\Delta H}$	Ri
15 Garrison & Cermak (1968)	San Bruno Mountain, California	Topographic effects	Neutral Barostromatic (dry ice)	400	6000/4800	3.7	0.16	25	0.125		0.32 0.32	
				400	6000/4800	3.7	0.16	25				
				400	5000/2400	1.9						
16 Hsi, Binder & Cermak (1968)	Green River, Utah	Topographic effects	Neutral	65	800	6.0	0.14	2				
17 Zrajevsky, Doroshenko & Chepik (1968)	Idealized hill	Topographic effects	Neutral									
18 Kitabayashi, Orgill & Cermak (1971)	Elk Mountain, Wyoming	Topographic effects, Barostromatic diffusion	Neutral Barostromatic (dry ice)	1200	9600	2.0	0.21	70	0.149		1.70	
				1200	9600	2.0	0.32					
19 Orgill, Cermak & Grant (1971)a	Eagle River, Chalk Mountain Area, Colorado	Topographic effects, diffusion	Neutral Barostromatic (dry ice)	1950	9600	4.0	0.25	3	0.28 0.50 0.05 0.60		6.0	
				1950	9600	2.0						
20 (1971)b	San Juan Mountains, Colorado	Topographic effects, diffusion	Neutral Barostromatic	2250	14,000 hor.	2.0	0.35		0.15 0.20			
				2250	9,600 ver.	2.0						
21 Mori, Miyata, & Mitsuta (1971)	Mt. Takakura, Japan	Topographical effects	Neutral	300	5000							
22 Meroney, Chaudhry (1971-72)	Rocky Flats, Colorado	Topographic effects & diffusion	Neutral	140	1000	3.0	0.14	2	0.13			
23 de Bray (1973)	Idealized ramps & escarpments	Speedup	Neutral	-		3.0	0.14		0.12 0.15			
				-		3.0	0.11					
				-		0.05 3.0	0.15					
24 Sacre (1973)	Idealized ramps & hills	Speedup	Neutral									
25 Counihan (1973)	Idealized ramps & hills		Neutral			8, 12 23			0.10			
26 Hewson, et al (1973-75)	Yaquina Head, Oregon	Speedup for WECS	Neutral	15	300	1.7						
27 Freeston (1974)	Idealized hill escarpments	Speedup	Neutral				0.14					
28 Meroney & Cermak (1974-1975)	Mississippi River, Lansing, Iowa	Topographic effects & diffusion	Neutral Barostromatic	150	400	2.0	0.27	60			1.0	
				150	400	2.0	0.70	60				
29 Bowen & Lindley (1974)	River banks & coastal beach, New Zealand	Speedup	Neutral	10,13	200-250	4.5	0.18	0.5	0.18	0.16		
30 Liu & Lin (1976)	Idealized Saddle Mountain Garfield, Utah	Topographic effects & diffusion	Barostromatic Barostromatic (brine solution)	1480	10,000						0-58 9-36	

*Field observations available.

TABLE 2-3. (CONTINUED) LABORATORY SIMULATION OF FLOW OVER IRREGULAR TERRAIN

AUTHOR/(DATE)	TOPOGRAPHIC SITE	PROBLEM STUDIED	TYPE OF AIR FLOW	MAXIMUM HEIGHT OF RISE (m)	LENGTH SCALE RATIO	SIMILITUDE CRITERIA						
						$\delta/\Delta H$	$\frac{1}{\alpha}$	$\frac{z_0}{\Delta H} \times 10^4$	$\frac{\overline{U^2}}{U_0^2}$	$\frac{U_x}{U_0}$	$\frac{L_{u_x}}{\Delta H}$	Ri
31 Meroney,etal (1976) (1977) (1978)	Idealized hills Shapes: 2d 2d 3d	Topographic effects for WECS	Neutral			10.0	0.14	1.0	.15	0.032		
			Barostromatic			10.0		1.0				
			Neutral			10.0		0.14				
▲ 32 Kitabayashi (1977)	Idealized hills	Stagnant flows	Barostromatic			3.0						0.19-2.78
33 Peterson & Cermak (1977-78)	Geysers Area, California	Topographic effects of diffusion	Neutral	700	1920	2.5		7.0				
34 Cermak & Mutter (1977-78)	Kahe, Oahu	Topographic effects of diffusion	Neutral	900	6500							
▲ 35 Govind, et al. (1977-78)	Kingston, Tennessee	Topographic effects of diffusion	Neutral	150	800							
36 Riley, Liu & Geller (1976)	Idealized hill 3-d	Topographic effects of diffusion	Barostromatic (brine solution)	1480	10,000							5-288
▲ 37 Meroney etal (1978)	Rakaia Gorge, New Zealand	Topographic effects for WECS	Neutral	200	5000	2.5	0.15	1.0	.13	0.03	0.75	

▲ Field observations available.

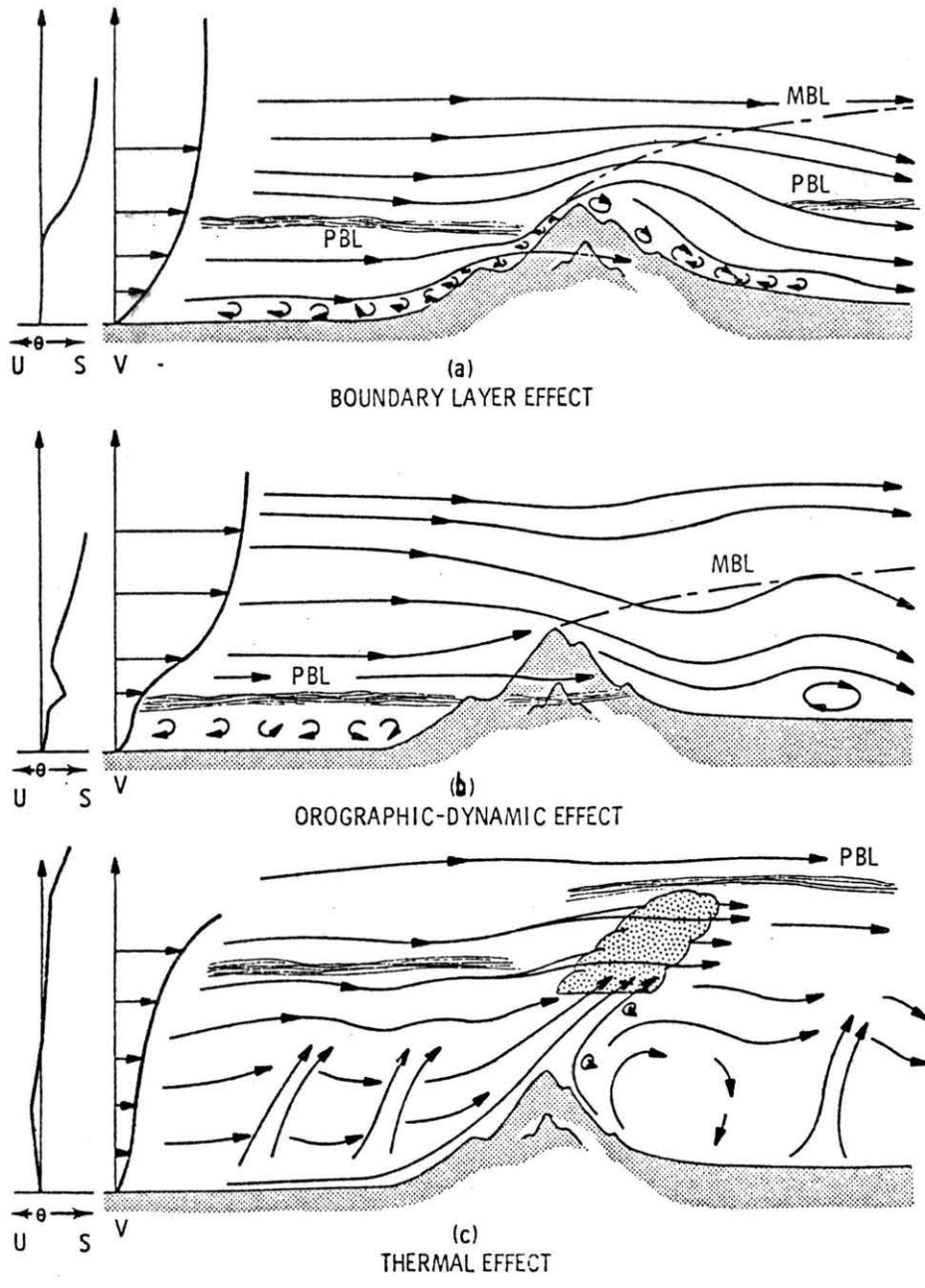


Figure 2-1. Methods in Which Terrain Features Affect Atmospheric Motions

3.0 CRITERIA FOR LABORATORY SIMULATION OF WIND CHARACTERISTICS OVER IRREGULAR TERRAIN

The basic tool of laboratory simulation is similitude or similarity, defined as a relation between two mechanical (or flow) systems (often referred to as model and prototype)* such that by proportional alterations of the units of length, mass, and time, measured quantities in the one system go identically (or with a constant multiple of each other) into those in the other. In order that the flow in any laboratory model should be of value in interpreting or predicting the observed flow in the atmosphere, it is essential that the two flow systems should be dynamically, thermally and kinematically similar. This means that it must be possible to describe the flow in the two systems by the same equations after appropriate adjustments of the units of length, time and other variables.

A number of authors including Cermak (1966, 1970, 1975), McVehil et al. (1967), Bernstein (1965), and Snyder (1972) have derived the governing parameters for atmospheric heat, mass, or momentum transport by dimensional analysis, similarity theory, and inspectional analysis. Another group justify similitude by considerations of turbulence theory and recent reviews of full scale wind data which present the characteristics of the prototype atmospheric wind on a parametric basis (Nemoto (1961, 1962), Counihan (1969, 1973), Cook (1977), and Melbourne (1977)). Although all investigators do not agree concerning details, most would concur that the dominant mechanisms can now be identified and are understandable. The following paragraphs review similitude criteria as they relate to adiabatic atmospheric shear flow over irregular terrain. Consideration of the scales and turbulence spectra developed in atmospheric and aerodynamic boundary layers guide the choice of scales desired in atmospheric simulation. Restrictive assumptions are discussed and a typical performance envelope for large wind tunnel facilities is provided to guide subsequent use of wind tunnels as a model tool for WECS siting in irregular terrain.

3.1 BASIC EQUATIONS AND ASSUMPTIONS

The basic equations necessary for considering atmospheric motions are the following:

Equation of turbulent momentum transfer,
Continuity equation,
Equation of state,
Poissons equation,

*Prototype--actual airflow involving full scale

Model--airflow involving smaller scale than prototype but usually with geometrically similar boundaries

Equation of turbulent heat transfer,
 Equation of heat transfer from the surface boundary, and
 Equation of turbulent scalar transfer.

These equations together with the appropriate boundary conditions have been summarized in Appendix A of Meroney et al. (1978).

For complete flow similarity in two systems of different length scales, geometrical, kinematical, dynamical and thermal similarity must be achieved. In addition, boundary conditions upstream, in the upper atmosphere, and downstream should also be similar.

Geometrical similitude exists between model and prototype if the ratios of all corresponding dimensions in model and prototype are equal. This is realized by using an undistorted scale model of the prototype geometry. Kinematic similitude exists between model and prototype if the paths of homologous moving particles are geometrically similar and if the ratio of the velocities of homologous particles are equal. Dynamic similitude exists between geometrically and kinematically similar systems if the ratios of all homologous forces in model and prototype are the same. Thermal similitude exists if the temperature or density stratification are similar.

The proper similitude parameters governing the phenomena of interest may be established by dimensional analysis, similarity theory or inspectional analysis. No attempts will be made here to give a comprehensive description of each of these methods since several good discussions are available in various textbooks and publications. The pertinent parameters for steady, turbulent, near neutral airflows are:

$$Ro = \frac{U_o}{L_o \Omega_o} \quad (\text{Rossby Number}) \quad (3-1)$$

$$Re = \frac{U_o L_o}{\nu} \quad (\text{Reynolds Number}) \quad (3-2)$$

$$Ri = \frac{\Delta T_o}{T_o} \frac{L_o}{U_o^2} g_o \quad (\text{Richardsons Number}) \quad (3-3)$$

$$Pr = \frac{\mu}{c_p k} \quad (\text{Prandtl Number}) \quad (3-4)$$

$$Ek = \frac{U_o^2}{c_p \Delta T_o} \quad (\text{Eckert Number}) \quad (3-5)$$

$$Eu = \frac{\Delta p_o}{\rho U_o^2} \quad (\text{Euler Number}) \quad (3-6)$$

The foregoing requirements must be supplemented by the stipulation that the surface-boundary conditions and the approach-flow characteristics be similar for the atmosphere and its model. Surface-boundary-condition similarity requires similarity of the following features:

- a. surface-roughness distribution with "aerodynamically rough" behavior,
- b. topographic relief, and
- c. surface-temperature distribution.

Similarity of the approach-flow characteristics requires similarity of the following flow features:

- a. distributions of mean and turbulent velocities,
- b. distributions of mean and fluctuating temperatures,
- c. longitudinal pressure gradient (should be zero), and
- d. equality of the ratio of inversion depths if the flow is thermally layered.

As a result of similarity of boundary conditions and approach flow characteristics, one may expect equality in approach flow turbulence quantities such as:

$$I_{ij} = \frac{\sqrt{\overline{(U_i U_j)}}}{U_o} \quad - \text{Turbulence intensities} \quad (3-7)$$

$$\text{or } \frac{\sqrt{\overline{T'^2}}}{\Delta T_o}$$

$$\frac{z_o}{L_o}, \frac{L_{u_x o}}{L_o}, \frac{L_{m o}}{L_o}, \frac{\delta_o}{L_o} \quad - \text{Turbulence Length Scales,} \quad (3-8)$$

$$Re_t = \frac{U_o L_o}{K_m} \quad - \text{Turbulence Reynolds Number, and} \quad (3-9)$$

$$Pr_t = \frac{K_m}{K_H} - \text{Turbulence Prandtl Number} \quad (3-10)$$

Sometimes investigators go directly to the resulting turbulence parameter of interest to justify a simulation methodology thereby emphasizing that only results are relevant.

If all the foregoing requirements were met simultaneously, all scales of motion ranging from micro to mesoscale, 10^{-3} to 10^5 m, could be simulated within the same flowfield for a given set of boundary conditions. However, all of the requirements cannot be satisfied simultaneously by existing laboratory facilities, and partial or approximate simulation must be used. This limitation requires that atmospheric simulation for a particular wind-engineering application must be designed to simulate most accurately those scales of motion which are of greatest significance for that application. By considering each similarity requirement separately, it is possible to determine for what flow features "exact" similarity is lacking between the laboratory and the atmospheric boundary layer.

The effects of equal Rossby numbers cannot be obtained in non-rotating wind tunnels. The laboratory boundary layer is an adequate model for atmospheric flow when Coriolis forces are not significant for the application, or the turning is small. The Rakaia Gorge area, for example, has a characteristic length of 20 km, northwesterly winds are at least 20 m/sec at gradient wind height, and $\Omega_0 = 9 \times 10^{-5} \text{ sec}^{-1}$ at $\phi \approx 40$ degree latitude; hence $R_0 \approx 11$, i.e., the inertial effects are an order of magnitude greater than the Coriolis term. Indeed, Hoxit (1973) and Scorer (1978) observe that most of the time the air is not in equilibrium with Coriolis forces due to thermal winds.

Equal Reynolds numbers are also not attainable. However, this does not seriously limit capabilities for modeling the atmospheric boundary layer over irregular terrain at high wind speeds, since the significant flow characteristics are but weakly dependent on Reynolds number. Essentially all natural surfaces are "aerodynamically rough;" hence, flow structure will be similar if the scaled-down roughness has a sufficiently large size to prevent the formation of a laminar sublayer. Generally the requirement for fully rough flow is $\frac{U_* \lambda}{\nu} > 100$

(Sutton) or $\frac{U_0 L_0}{\nu} > 10^4 - 10^6$. The Rakaia Gorge model considered herein satisfied both these criteria. Duplication of the main streamline features, regions of turbulent eddies, and structure of turbulence thus becomes dependent upon geometric similarity and equivalence of

relevant length scale ratios, such as z_0/L_0 , $\frac{L_{u_{x_0}}}{L_0}$, etc.

Equal gross or local Richardson numbers can be obtained in specially designed wind tunnels. Batchelor (1953) has established that if the flowfields are such that the pressure and density everywhere depart by only small fractional amounts from the values for an equivalent atmosphere in adiabatic equilibrium and if the vertical length scale of the velocity distribution is small compared to the scale height of the atmosphere, the Richardson number distribution governs dynamical similarity. Unfortunately, these conditions are only normally satisfied in the first 100 m of the planetary boundary layer.

The gradient Richardson number is defined by

$$Ri = \frac{g}{\bar{\theta}} \frac{\left(\frac{\partial \bar{\theta}}{\partial z}\right)^2}{\left(\frac{\partial u}{\partial z}\right)^2} \quad (3-11)$$

Batchelor has emphasized that no single local, variable quantity can be used as a similarity parameter. Similarity parameters can have meaning only when they characterize the gross features of the flow. When a gross or bulk Richardson number is desired to describe the thermal influence over a layer of thickness, Δz , the following form is convenient

$$Ri = \frac{g}{\bar{\theta}} \frac{\Delta \bar{\theta}}{(\Delta u)^2} \Delta z \quad (3-12)$$

In the case of the model airflow the potential temperature may be replaced by temperature or density.

The atmosphere for purposes of simulation was assumed to be in a neutral state over the Rakaia Gorge for the cases investigated.

This implies $Ri \equiv 0$ or $\frac{\partial \theta}{\partial z} \Big|_{\text{field}} \equiv \frac{\partial T}{\partial z} \Big|_{\text{model}} = 0$ for the temperature distribution in the field and wind tunnel. No measurements over the boundary layer depth were available at the gorge on the days examined; however, Orgill et al. (1971a & b) reports that for a day when the sky was totally overcast with moderate to light precipitation and surface

winds were strong and gusty at Camp Hale, Colorado, near-neutral stability conditions were observed through a depth of 2400 m. This depth exceeded the highest mountains in the area. Such a situation closely describes weather conditions during the Rakaia Gorge field experiments.

The Prandtl numbers and Euler numbers are essentially equal for flows in the laboratory and the atmosphere. The Eckert number is equivalent to a Mach number squared, which is small compared to unity for both laboratory and atmospheric flows.

3.2 PERFORMANCE ENVELOPE FOR WIND TUNNEL MODELING OF AIRFLOW OVER TERRAIN

The viability of a given simulation scenario is not only a function of the governing flow physics but the availability of a suitable simulation facility and the measurement instrumentation to be employed. It would seem appropriate, therefore, to suggest bounds for the range of field situations which can reasonably be treated by physical modeling.

A number of boundary layer wind tunnels exist at various laboratories. Generally these tunnels range in size from facilities with cross-sections of 0.5 m x 0.5 m to 3 m x 4 m. Several of these facilities are equipped with movable side walls or ceilings to adjust for model blockage. By utilizing a variety of devices such as vortex generators, fences, roughness, grids, screens, or jets a fairly wide range of turbulence integral scales can be introduced into the shear layer. Varying surface roughness permits control of surface turbulence intensity, dimensionless wall shear, and velocity profile shape. Density stratification can be induced by means of heat exchangers, use of different molecular weight gases, or latent heat adsorption or release during phase changes. Table 3-1 suggests parameter values for typical wind tunnels familiar to the authors. The probability range of the equivalent parameters in the atmospheric surface layer are tabulated in Table 3-2. A comparison between field and laboratory parameter ratios are summarized in Table 3-3.

When one combines various operational constraints into a performance envelope, a clear picture appears of the performance region for wind-tunnel facilities. Figure 3-1 is such a performance envelope prepared for a large facility such as the Environmental Wind Tunnel at Colorado State University. The criteria selected to specify operations ranges are:

Maximum model height ($h \leq 0.5$ m)

Minimum convenient model height ($h \geq 0.02$ m)

Minimum Reynolds number ($Re_h = \frac{U_o h}{\nu} \geq 10,000$)

Maximum model integral scale ($L_{u_x} \leq 0.5$ m)

Minimum model integral scale ($L_{u_x} \geq 0.05$ m)

Minimum model measurement resolution ($\Delta z \geq 0.1$ mm)

Maximum model boundary depth ($\delta \leq 2$ m)

Minimum model boundary depth ($\delta \geq 0.1$ m)

Since field values for some parameters are uncertain the prototype value of δ and L_{u_x} are assumed to range over complex terrain

as follows

300 m < δ < 1000 m, and

100 m < L_{u_x} < 1000 m.

Not all previous laboratory studies meet such similitude restrictions, some experiments were performed to meet objectives other than similitude of turbulence or mean velocity profiles; nevertheless, a number of the studies listed in Table 2-3 are indicated on Figure 3-1 by number. In almost all cases noted values fall within the indicated operational envelope or just outside the predicted region.

Based on Coriolis force considerations, Snyder (1972) suggests a 5 km cut off point for horizontal length scales for modeling diffusion under neutral or stable conditions in relatively flat terrain. Mery (1969) suggests a 15 km limit, Ukejurchi et al. (1967) suggest 40 to 50 km, and Cermak et al. (1966) and Hidy (1967) recommend 150 km. A middle road value would be that of Orgill et al. (1971a) who suggest for rugged terrain in high winds that a length scale of 50 km is not unreasonable.

Assuming an upper value of length scale ratio of 10,000 and a tunnel length of 25 m a distance of 50 km is well within the capacity of existing facilities to contain in the windward direction. Assuming a lateral width restriction of 4 m suggests a 40 km lateral maximum for the field area modeled.

3.3 TIME AND SPACE DOMAIN APPROPRIATE FOR PHYSICAL MODELING OF WECS SITE CHARACTERISTICS

The joint consideration of time and space scales modeled in atmospheric boundary-layer wind tunnels may be overlaid upon the characteristic time and horizontal scales of atmospheric phenomena. Such an overlay upon the atmospheric scales defined by Orlanski (1975) has been proposed in

Figure 3-2. The wind tunnel may thus study phenomena up to the mesoscale in time and into the β mesoscale in length with reasonable credibility.

When the performance envelope of physical modeling by wind tunnels is superimposed upon the scale effects produced by terrain on atmospheric motions Figure 3-3 is obtained. Only the time scales associated with turbulence or advection over terrain are realistically included in current physical modeling repertoire. The fluctuations in a field of motion associated with diurnal variations in the atmosphere are not developed in models considered to date.

One can, however, synthesize the average statistics of a flow field over longer time periods by associating a given measurement set with a recurring meteorological situation for which climatological probability distribution information is available. Hence it is possible to expend the physical modeling domain to longer time scales as proposed by Orgill (1977a). Two resultant domains in time and space for which physical modeling can provide WECS siting information are displayed on Figure 3-4.

TABLE 3-1. TYPICAL BOUNDARY LAYER WIND TUNNEL CHARACTERISTICS

WIND TUNNEL PROPERTY	RANGE
Tunnel height H_T (m)	0.5 - 2.5
Tunnel width W_T (m)	0.5 - 4.0
Tunnel length L_T (m)	1.0 → 30.0
Boundary depth δ (m)	0.10 → 2.0
Roughness z_o (mm)	0.01 → 15.0
Velocity U_o (m/s)	0.0 → 36.0
Integral scale $L_{u_{x_o}}$ (m)	0.06 → 0.60
Temperature gradient $d\theta/dz$ ($^{\circ}\text{C}/\text{m}$)	0.0 → 200
Hill height h (m)	0.02 → 0.5
Hill half width L (m)	0 → 2
Resolution Δz (mm)	~ 0.1 mm
Surface friction $C_f/2$ (dimensionless)	0.0005 - 0.0040
Richardson number Ri_B (dimensionless)	0.0 → 1.0
Monin-Obukhov length L_{MO} (m)	0.065 → ∞
Turbulence intensity $\sqrt{U'^2}/U_o$	~2.0 - 3.0
Power law coefficient $1/\alpha$ (dimensionless)	0.05 - 0.80

TABLE 3-3. TYPICAL WIND TUNNEL AND FIELD PARAMETER RANGE

DIMENSIONLESS PARAMETER	WIND TUNNEL RANGE	FIELD RANGE
Reynolds number $Re_h = u_o h/\nu$	$0 \rightarrow 7.0 \times 10^5$	$0 \rightarrow 6.0 \times 10^6$
Richardson number $Ri_B = \frac{g(dT/dz)_h}{T U_o^2}$	$-1.0 \rightarrow 1.0$	$-1.0 \rightarrow 1.0$
Prandtl number $Pr = \mu cp/k$	~ 0.72	~ 0.72
Skin friction coefficient or Stanton number $C_f = \frac{\tau_w}{\rho U_o^2} = \left(\frac{u_*}{U_o}\right)^2$ $St = \frac{q}{\rho c_p (\Delta T)_o}$	$0.006 \rightarrow 0.004$	$0.001 \rightarrow 0.004$
Insolation parameter $Fr_I = \frac{U_o^2 T_w}{g(T_w - T_n)L}$	$0.002 \rightarrow \infty$	$2.5 \times 10^{-5} \rightarrow \infty$
Scaling lengths z_o/h	$2 \times 10^{-5} \rightarrow 0.25$	$3.0 \times 10^{-7} \rightarrow 0.15$
δ/h	$0.20 \rightarrow 50.0$	$0.10 \rightarrow 100$
h/L	$0.05 \rightarrow \infty$	$2 \times 10^{-4} \rightarrow \infty$
$(L_{u_x})_o/L$	$0.06 \rightarrow \infty$	$0.001 \rightarrow \infty$
h/H_T	$0.01 \rightarrow 0.15$	--
L_T/L	$0 \rightarrow 30 \rightarrow \infty$	--
h/L_{MO}	$0 \rightarrow 5.0$	$-360 \rightarrow 240$
Power law coefficient α	$0.05 \rightarrow 0.8$	$0.05 \rightarrow 0.7$

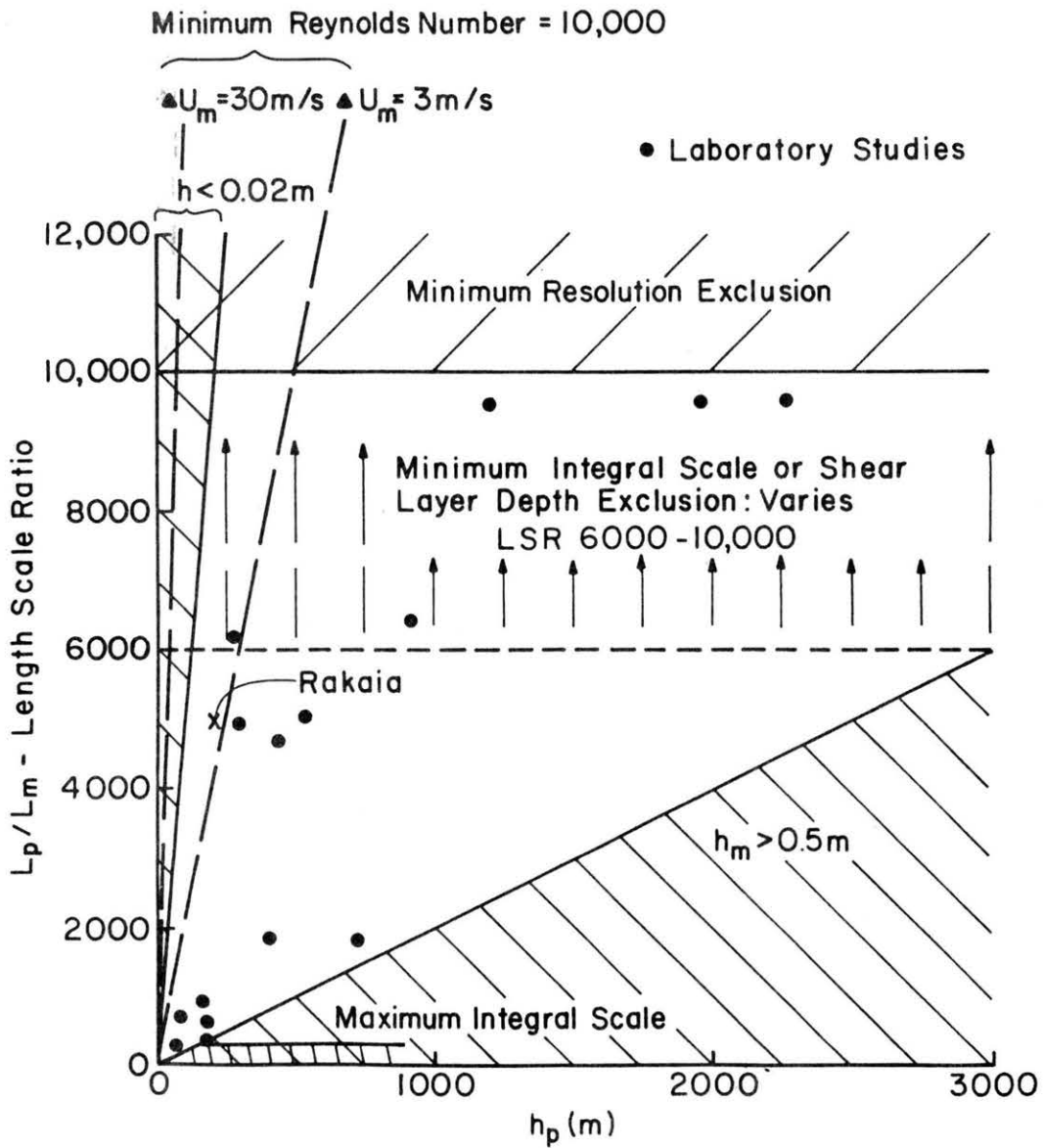


Figure 3-1. Performance Envelope for Physical Modeling of Shear Flows Over Complex Terrain

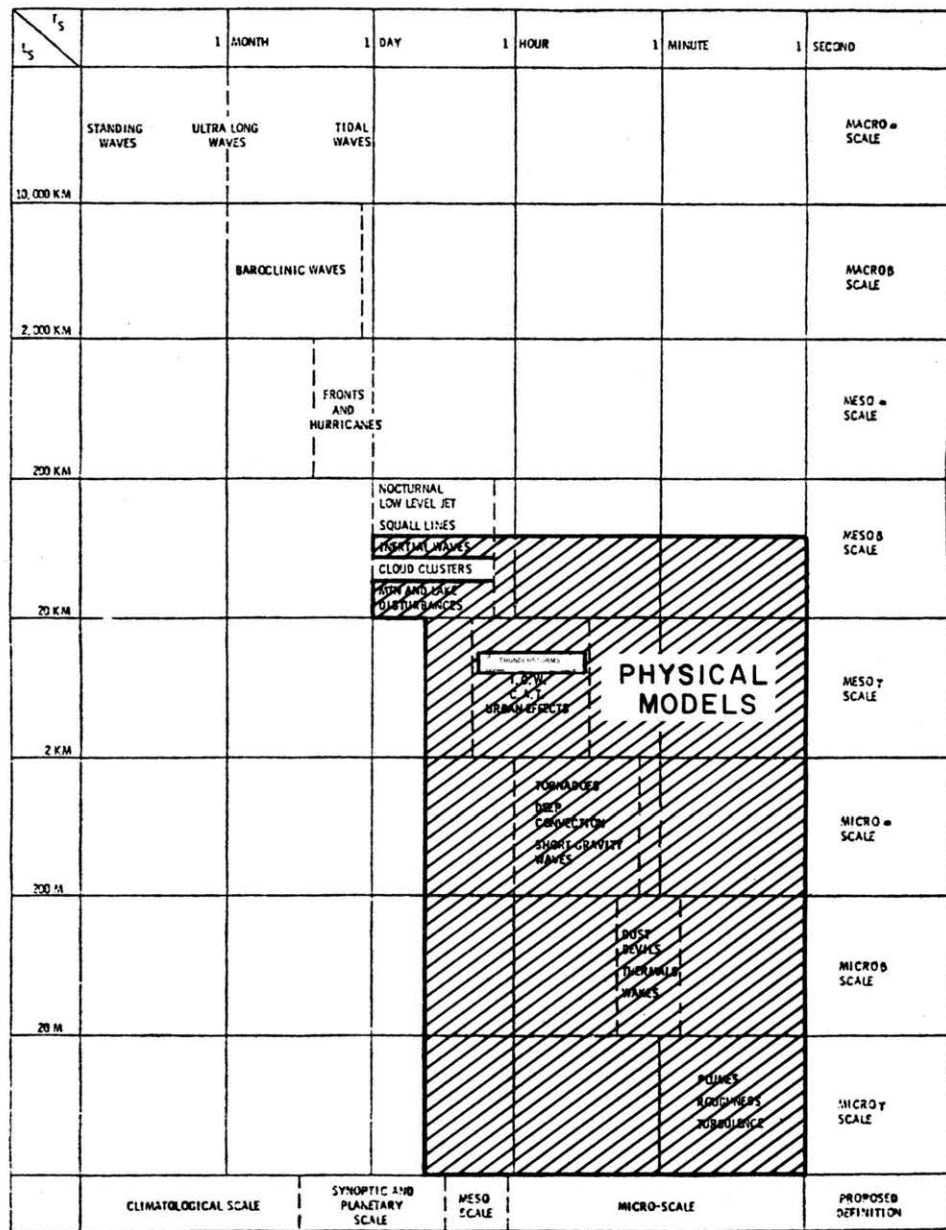


Figure 3-2. Physical Model Regime Overlaid Upon Scale Definitions and Different Processes With Characteristic Time and Horizontal Scales (Orlanski, 1975)

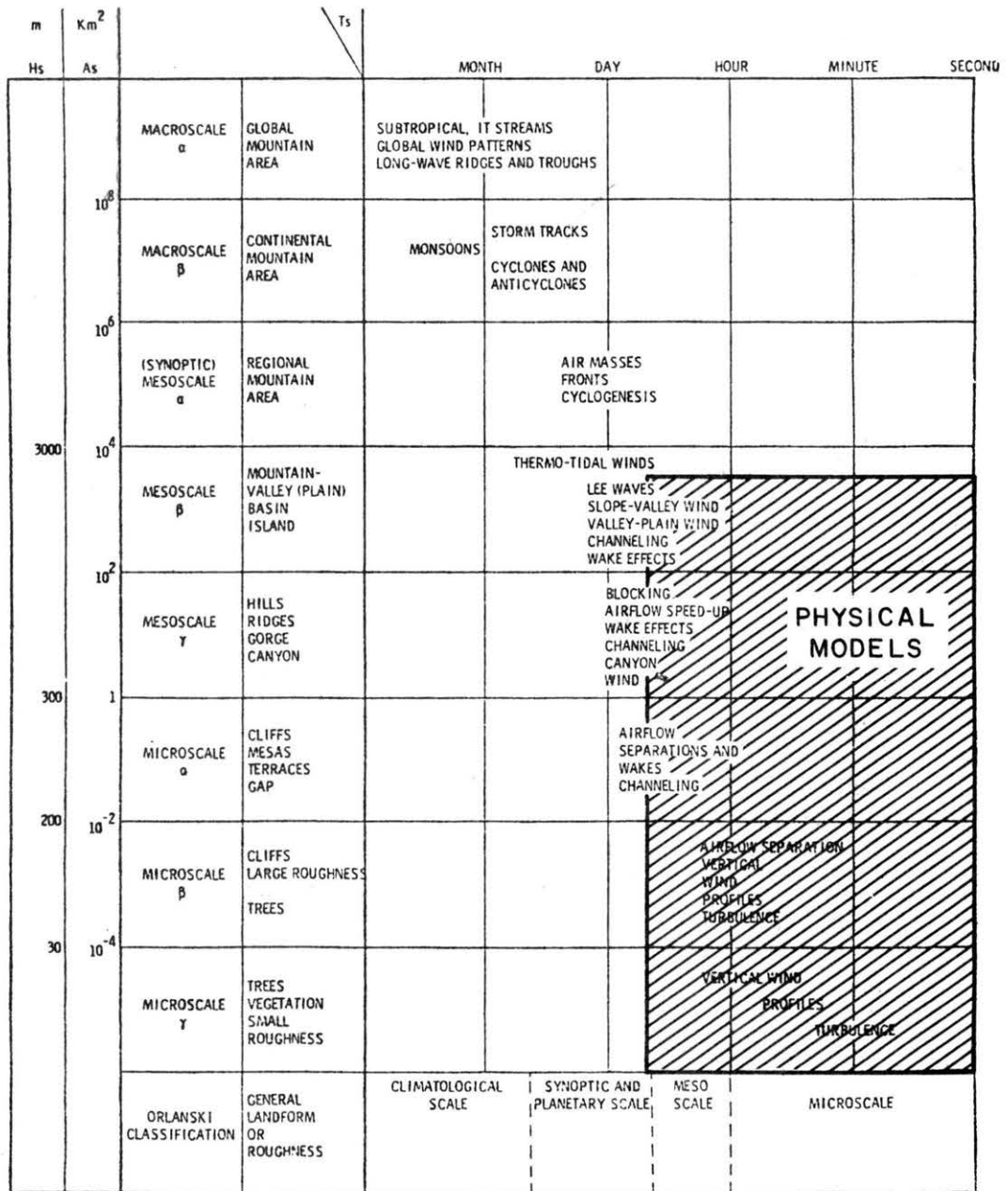
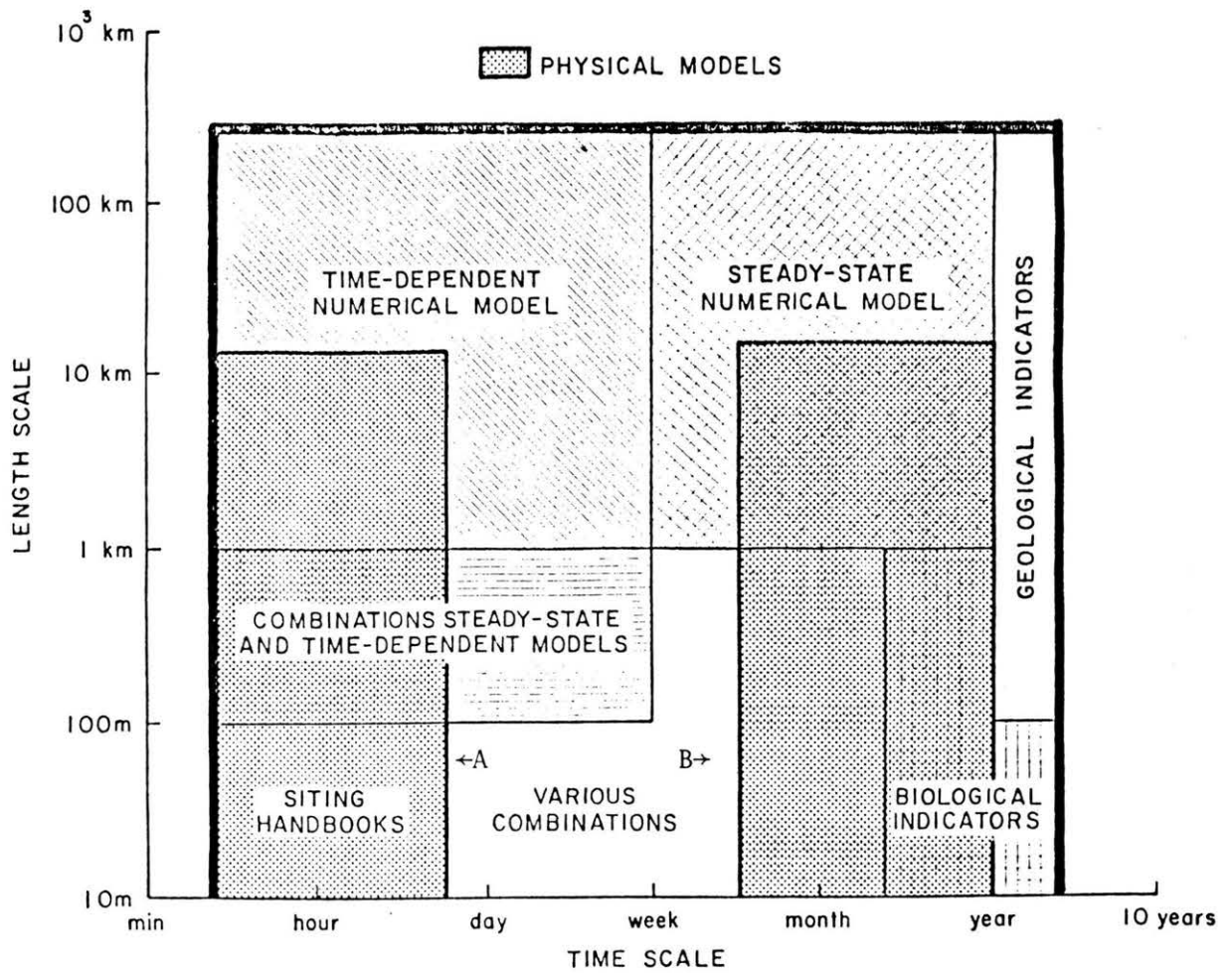


Figure 3-3. A Classification of the Effects of Terrain on Atmospheric Motions. After Orlanski (1975)



- A. Results During a Single Meteorological Episode
- B. Results Averaged and Weighted by Probability Density Distributions

Figure 3-4. Physical Modeling Domain Along Time and Space Scales for WECS Site Selection

4.0 EVALUATION OF FIELD AND LABORATORY DATA

The results and data developed during the program outlined in Sections 1.2 and 1.3 appear separately in a number of individual reports. Bouwmeester et al. (1978) discuss the implications of the extensive program to evaluate flow over two-dimensional ridges. Meroney et al. (1976b) tabulate a large portion of the relevant data; however separate contributions are found in Rider et al. (1977a, 1977b) on turbulence effects and in Chien et al. (1977) on three-dimensional generic hills. Again, Meroney et al. (1978) present the material from a laboratory to field validation effort over complex terrain. Data sets are reproduced as appendices to this document; however no attempt is made herein to discuss all material. Instead, trends, insights and conclusions are emphasized.

4.1 INFLUENCE OF TWO-DIMENSIONAL RIDGES ON WIND SPEED AND TURBULENCE

Measurements of shear-flow perturbations over two-dimensional hill models have been conducted to investigate the effect of terrain features on the mean flow turbulence. Terrain and upstream flow characteristics were varied over a range of parameter values derived from the following dimensional quantities:

- height of the hill; h ,
- hill length at the upwind side of the crest (L_u , L_u being twice the distance L recommended by Jackson and Hunt (1975) taken between the crest and the point at the upwind side where the hill height is $h/2$),
- hill length at the downwind side of the crest (L_d , L_d being defined similarly to L_u),
- detailed hill shape, distinction is made between sharp and round crested hills,
- the boundary layer thickness (δ),
- the surface roughness (z_0),
- the velocity at a height δ ($u(\delta)$),
- the thermal stratification characterized by a representative temperature gradient ($\Delta T/\Delta z$).

From these seven variables plus the kinematic viscosity of air and gravity several nondimensional parameters can be derived, namely:

$$h/L_u, h/L_d, z_o/h, h/\delta, Re = \frac{u(\delta)h}{\nu} \text{ and} \quad (4-1)$$

$$Ri = \frac{g}{T} \frac{\Delta T}{\Delta u^2} h ,$$

where ΔT and ΔU are characteristic changes in temperature and velocity respectively over the layer of thickness h . A seventh parameter is the detailed hill shape.

4.1.1 Effect of Ridge Shape

Wind speed variation over a hill or ridge depend strongly on the upwind and downwind hill slopes. Speedup of the wind is highest for ridge slopes that just avoid flow separation. Such a speedup causes reduction of the minimum static pressure by a separated wake at either the upwind or downwind side of the crest. Figure 4.1a and b present results that show the dramatic change in velocities and static pressures over symmetric triangular hills as a result of flow separation. No flow separation occurs for the hill defined by $h/\delta = 0.1$, $h/L_u = h/L_d = 1/4$; whereas, flow separation occurs for the hill defined by $h/\delta = 0.1$, $h/L_u = h/L_d = 1/3$. It is noted that the static pressure gradients penetrate much deeper into the boundary layer for the 1/3-hill, causing slightly higher velocities in the higher region of the boundary layer.

The character of flow separation occurring at the upwind side of the hill is different from that at the downwind side. The eddy in the downwind separation region interacts strongly with the main flow producing an extended wake in the downwind direction. For steep downwind slopes the separation region may extend to a distance of 10-20 times the obstacle height. The interaction between eddy and main flow at the upwind side is constrained by the presence of the hill. With a slight variation that depends on the parameter h/δ , the upstream separation region does not extend further than two hill heights upwind. Flow separation occurs if $h/L_u > 1/2$.

The location of the flow separation point depends to some degree on the Reynolds number as defined in the previous section. A Reynolds number effect was avoided by studying the phenomenon of flow separation over triangular hill models that fix the separation point at the crest.

In general a round crested hill results in flow separation downwind of the crest. The results obtained for the triangular hill are somewhat conservative if applied to round crested hills.

The extent of the downstream separation region depends strongly on the strength of the eddy just downwind of the separation point. For relatively gentle downwind slopes only weak eddies can develop. Weak eddies permit "early" reattachment of the separating streamline. The effect of h/L_d on the mean velocity field is illustrated in Figure 4-2. For all cases $h/\delta = 0.1$, $h/L_u = 1/2$. The downwind slopes were $h/L_d = 1/0, 1/3, 1/4$, and $1/6$. The boundary layer recovers faster for the smaller values of h/L_d . A larger speedup occurs over the hill crest for $h/L_d = 1/6$. Similar effects may be noticed in Figure 4-3, where vertical velocity profiles are presented at the crest and downwind of hills with $h/L_u = 1/3$, $h/L_d = 1/4$ and $h/L_u = 1/4$, $h/L_d = 1/3$. The figure also illustrates the effect of changing wind directions over 180° .

Most data obtained to study the effect of flow separation on the velocity field were for $h/\delta = 0.1$. Huber et al. (1977) show that the separation phenomenon is not affected by the upstream velocity distribution. Essentially identical downwind separation regions were obtained for a uniform approach velocity profile and for values of $h/\delta = 0.3$.

Flow separation over triangular ridges immersed in typical shear profiles depends primarily on h/L_d and h/L_u . Based on a series of measurements of flow over triangular hills with alternate upwind and downwind slopes, the occurrence of flow separation has been identified. Figure 4.4 shows the relationship between h/L_u and h/L_d and the occurrence of flow separation for triangular hills.

Jackson and Hunt (1975) suggested that perturbations in wind speed be characterized by a fractional speedup ratio, defined as

$$\Delta S_{\text{crest}} = \frac{u_{\text{crest}}(z) - u_o(z)}{u_o(z)} \quad (4-2)$$

where u_o is the upstream velocity distribution, u_{crest} is the velocity profile above the crest, and z is the distance from the surface. By normalizing the increase in wind speed $u_{\text{crest}}(z) - u_o(z)$ with the upstream profile it may be anticipated that the fractional speedup ratio does not strongly depend on the approach velocity distribution.

Numerical calculations were carried out using an inviscid flow model described in Bouwmeester et al. (1978). A series of approach velocity distributions were used to calculate ΔS above the crest. These velocity profiles are defined by

$$\frac{u(z)}{u(\delta)} = \frac{\ln \left(\frac{z}{h} / \frac{z_0}{h} \right)}{\ln \left(\frac{\delta}{h} / \frac{z_0}{h} \right)} \quad \text{for } z < \delta, \text{ and} \quad (4-3)$$

$$\frac{u(z)}{u(\delta)} = 1 \quad \text{for } z > \delta.$$

The hill shape is defined by

$$z_s = \frac{h}{1 + \left(\frac{x}{L} \right)^2} \quad (4-4)$$

where $L = 1/2 L_u = 1/2 L_d$.

Typical upstream approach velocity profiles and corresponding fractional speedup ratio profiles are given in Figure 4-5 and 4-6. For $h/\delta > 1$ the fractional speedup, ΔS_{crest} , becomes independent of h/δ , and for $h/\delta < 1$ the fractional speedup, ΔS_{crest} , is independent of h/δ but depends weakly on z_0/h . (See Section 4.1.3 for a further discussion on the effect of surface roughness.)

The effect of detailed hill shape on the velocity field has been investigated by comparing velocity fields over symmetric triangular hill models with those measured over sinusoidal shaped hill models but with the same slope h/L . Almost identical velocity fields were measured. Rider and Sandborn (1977b) considered alternate hill shapes with the same height and with the same distance from crest to the foot of the hill, where the hill height is zero. The models include full sine wave, half sine wave, triangular, trapezoidal, and box shaped hills. Speedup effects over the crest of the different hill models varied substantially as may be expected since length scale L , as defined previously varied by a factor of two. Moreover, separation regions exist upwind and downwind of the box shaped hill. Nonetheless, hills with similar average slope had similar velocity perturbations.

After the effects of turbulence, surface roughness and thermal stratification are discussed in the following sections a functional relationship between ΔS , h/L_u , h/L_d , z_0/h will be considered in Section 4.1.5.

4.1.2 Effects of Turbulence

When air passes over a hill, the turbulence structure is distorted causing Reynolds stress gradients different from those of equilibrium flow conditions. The result is that the momentum transfer from one streamline to another is not at the same rate, and the total head across streamlines does not decrease uniformly over the height of the atmospheric boundary layer. Bouwmeester et al. (1978) provides an order of magnitude analysis to estimate the total head losses caused by the distortion of the turbulence. The "additional total head" lost at the crest could be expressed as follows

$$\Delta P'_{\text{crest}} = 0 \left[4 r + \frac{h}{\delta} \overline{u'^2}_{\text{max}} \right] \text{ if } \frac{h}{\delta} < 2 \frac{h}{L_u} \quad (4-5)$$

$$\text{and } \Delta P'_{\text{crest}} = 0 \left[\left(2 + \frac{L_u}{\delta} \right) r + \frac{h}{\delta} \overline{u'^2}_{\text{max}} \right] \text{ if } \frac{h}{\delta} > 2 \frac{h}{L_u}, \quad (4-6)$$

where r is the maximum characteristic change in Reynolds stress along a streamline between a point upstream and a point at the crest,

and $\overline{u'^2}_{\text{max}}$ is the maximum Reynolds stress existing in the flow

field. An adequate estimate for $\overline{u'^2}_{\text{max}}$ is the square of the longitudinal turbulence intensity close to the surface.

To evaluate $\Delta P'$ for a particular hill shape, detailed information is required of the turbulence intensities over the hill. Rider and Sandborn (1977) present data on the longitudinal and vertical turbulence intensity variation over two-dimensional hills. For the case $h/\Delta < 2 h/L_u$ (short hills), their data show that the longitudinal

turbulence intensity increases toward the base of the hill, then decreases over the crest. The vertical turbulence intensity shows a decrease at the base of the crest and an increase over the crest. For $h/\delta = 0.1$ and $h/L_u = h/L_d = 1/2, 1/4$ and $1/6$ maximum values of r at

streamlines close to the surface were almost 50% of $\overline{u'^2}_{\text{max}}$. Thus, additional total head losses close to the surface are approximately

$$\Delta P' \approx 2 \overline{u'^2}_{\text{max}} \quad (4-7)$$

With maximum local turbulence intensities of 20% the total head close to the crest may then change by 8%.

The changes of the longitudinal component of the turbulence intensity as affected by hill slope are included in Bouwmeester et al. (1978). Contour plots of longitudinal turbulence intensities superimposed on the streamline pattern for triangular hill models ($h/\delta = 0.1$, $h/L_u = h/L_d = 1/4$ and $h/L_u = h/L_d = 1/20$) are given in Figure 4.7a and b respectively. The figures show that the decrease in turbulence intensity between the base and the crest along streamlines close to the surface is for the 1/4-hill 50% and for the 1/20-hill hill 25% of $\overline{u'^2}_{\max}$. The decrease of r , the characteristic change in Reynolds stress, with height is approximately linear, and is nearly zero at a height L_u above the surface.

The changes of dynamic head close to the surface are as large as 400%. Supposing that the change of additional total head causes an equal change in dynamic head, it may be concluded that the effect of the turbulence on the mean flow at the crest is not significant at least for $h/\delta < 2 h/L_u$. The effect of turbulence may be expected to be somewhat higher for hills with $h/\delta > 2 h/L_u$ (long hills).

Downwind of the crest turbulence production increases and turbulence intensities in this region exceed upstream intensities. Additional total head changes become larger. The relative effect of turbulence changes on the dynamic head increases, since the dynamic head returns to values approximately equal to upstream values. These considerations are illustrated by examining flow over a symmetric hill. According to inviscid flow theory the velocity and static pressure field over a symmetric hill is also symmetric. Therefore the measured degree of flow symmetry or asymmetry gives a direct indication of the effects of turbulence on the mean flow. Contour plots of mean velocity and static pressure are presented in Figure 4.8 and 4.9 respectively. Hill shapes are triangular with $h/\delta = 0.1$, $h/L_u = h/L_d = 1/4$ and $h/L_u = h/L_d = 1/20$ respectively. For the 1/20-hill, a high degree of symmetry exists. The surface pressure patterns at the base of the 1/4-hill shows the largest departure from symmetry.

Inviscid flow theory predicts mean velocity distributions above the crest of hills (that do not cause flow separation) accurately. Somewhat less reliable prediction of the velocity is obtained in the surface region downwind of the crest particularly for hill with $h/L_d < 1/10$.

4.1.3 Effects of Surface Roughness

Two length scale parameters determine the velocity distribution of a fully developed turbulent boundary layer over a surface perturbation,

namely z_0/h and h/δ . In this section the effect of z_0/h on mean velocity and turbulence is discussed assuming h/δ remains constant.

The effect of z_0/h is most significant for small values of h/δ for then mean velocity and turbulence structure are significantly different over a surface layer with a thickness of the order of h . In Figure 4-10 nine velocity distributions are plotted for different combinations of z_0/h and h/δ . The velocity distributions are similar to those displayed in Figure 4-5; however, they have been rearranged for explanatory purposes. The fractional speedup ratios predicted by an inviscid computer code for the velocity distribution set are given in Figure 4-11. Fractional speedup ratios are essentially independent of z_0/h for $h/\delta = 4$, and there is a slight dependency of ΔS on z_0/h for $h/\delta = 0.4$ and $h/\delta = 0.04$. Surface roughness effects as reflected in the approach mean velocity distribution change the fractional speedup ratio at the crest significantly only if $h/\delta < 1$.

The effects of surface roughness on total head losses as reflected in the turbulence structure is most clearly explained by referring to Equations 4-5 and 4-6. $\overline{u'^2}_{\max}$ and r both increase if z_0/h increases. Therefore, one expects the influences of the turbulence on the mean flow will become larger. However, since $\overline{u'^2}_{\max}$ and r do not change by orders of magnitude, as shown on Figure 4-12 it may be expected that inviscid flow theory will predict the mean flowfield accurately upwind of the crest even for the larger surface roughnesses. Downwind of the crest there may be production of turbulence as a result of flow separation.

Only uniform surface roughness has been considered, implying that equilibrium flow conditions exist in the approach wind. Flow separation occurs as a result of increased surface shear stresses over the top of the hill because of speedup of the wind and adverse pressure gradients on the downwind side. Once flow separation takes place the interaction between the eddy in the wake and the main flow will dominate the separation phenomenon. If the approach surface roughness is not uniform location of flow separation or even the occurrence of flow separation may be affected. Consider, for instance, an upwind surface roughness that is larger than the surface roughness over the hill. In this case surface shear stress at the hillcrest may be less than in the case of uniform surface roughness. Consequently, flow separation may occur "later" or may not occur at all. Opposite effects can be expected if the surface roughness over the hill is larger over the hill than upwind. Installation of extensive

windmill hardware on a hill may itself induce earlier flow separation and consequently less speedup of the wind.

4.1.4 Effects of Thermal Stratification

A stably stratified boundary layer was simulated to study its effects on the velocity field over ridges. Triangular ridges with $h/L_u = h/L_d = 1/4, 1/6$ and $h/\delta = 0.1$ were employed. The freestream approach velocity was varied from 2.8 to 8.9 m/sec with a corresponding variation in Richardson number as defined by

$$Ri = \frac{g}{T} \frac{\Delta T}{\Delta U^2} h \quad \text{from } 5.7 \times 10^{-3} \text{ to } 7.0 \times 10^{-2}.$$

Details of the measurements of the mean and turbulent velocities and temperature are given in Appendix C of Meroney et al. (1978b).

The effect of stable thermal stratification on the fractional speedup ratio above the crest is shown in Figure 4-13a and b for the 1/4-hill and the 1/6-hill. There is some evidence that the experimental fractional speedup, ΔS , increases slightly as the stratification becomes more stable; however, the effect may be attributed to changes in approach profile shape with stability. Calculations by Derickson and Meroney (1977) suggest that ΔS will decrease slightly with stability for a given approach profile.

The effect of stably stratified flow on the turbulence is to reduce further the longitudinal velocity component over that originally observed for the neutral flow case for the same ridge shapes. The temperature fluctuation behaves as a passive scalar quantity and does not change as it is convected over the ridge.

The effect of stratified flow on the extent of a separation region is significant although speedup over the crest is not strongly affected. Measurements over a triangular hill with $h/L_u = 1/4$ and $h/L_d = 1/6$ showed that the downwind separation region is significantly elongated. Perhaps since the temperature in the separation region is low as a result of the low wind velocities in this region the heavier air in the separation region resists reattachment of the separation streamline. More details are provided in Bouwmeester et al. (1978).

It is noted that the stratification effects studied do not include effects of an elevated inversion directly above the hill crest. When airflow is constrained to flow between a ridge and an elevated inversion an increase in speedup is likely.

4.1.5 Parameterization of Speedup

The wind velocity distribution over a hill can be described by two parameters (Bouwmeester et al., 1978) namely the amplification factor $A(z_{\text{ref}})$ and the upwind power law exponent α_o . The amplification factor is defined as

$$A(z) = \frac{\bar{u}_c(z)}{\bar{u}_o(z)} \quad (4-8)$$

where \bar{u}_c is the velocity above the crest and \bar{u}_o is the upwind velocity at the same height above the surface.

The wind velocity distribution can be calculated from

$$\bar{u}_c(z) = \bar{u}_o(z) * A(z) \quad (4-9)$$

where

$$A(z) = A(z_{\text{ref}}) \left(\frac{z}{z_{\text{ref}}}\right)^{\alpha_o - \alpha_c} \quad (4-10)$$

and, either,

$$\alpha_c - \alpha_o = \frac{A(h) - 1}{2.3} \quad (4-11)$$

or, alternatively,

$$\alpha_c - \alpha_o = \frac{\log_e A(z_{\text{ref}})}{2.14 - \log_e \left(\frac{z_{\text{ref}}}{h}\right)} \quad (4-12)$$

The fractional speedup ratio is calculated from

$$\Delta S(z) = A(z) - 1 \quad (4-13)$$

The dependence of $A(z_{\text{ref}} = h)$ on upwind and downslopes is given in Figure 4-14 and 4-15 respectively for $\alpha_o' = 0.13$. In order to utilize these results for a different approach velocity distribution (different value of α_o) the following correction formulae should be applied

$$A(h; \alpha_o) = A(h; \alpha_o') \frac{1.15 + \alpha_o}{1.15 + \alpha_o'} \quad (4-14)$$

It is noted that the parameterization yielded satisfactory agreement between the measured velocity distribution over the ridge and the predicted distribution from Equation 4-10. Differences in predicted

and measured velocities were less than 5% (Bouwmeester et al., 1978) in the range $0.1 h < z < \delta$. The prediction method does not seem to be adequate in the surface region, where

$$z < 0.05 h \quad (4-15)$$

In the case that hill height, h , is of the order of the shear layer thickness, δ , the method does not seem to be applicable.

4.1.6 Prediction of the Velocity Distribution at the Crest of a Ridge

There are several procedures that may be followed to assess the velocity distribution over a ridge. Four of these are:

- a) Direct method. Wind tunnel results may be employed directly, particularly if the parameters h/L_d , h/L_u , and h/δ , as well as α_o correspond satisfactorily.
- b) Empirical method. $A(h)$ is estimated from Figure 4-14 or 4.15. α_o should be known from either observation or from the literature (e.g., Davenport, 1960).
- c) Field method. Once α_o is known $A(z_{ref})$ can be obtained from velocity measurements upwind and at the crest at a height z_{ref} . The height should be preferably larger than $0.1 h$.
- d) Numerical method. An inviscid computer code may predict the velocity distribution accurately provided no flow separation occurs.

4.1.7 The Effect of Finite Hill Width

Mean velocities have been measured over the crest of model ridges which have finite width yet identical shape to those considered in the two-dimensional ridge study. Typical velocity profiles over the crest of a hill with a width $W = 9h$, $h/L_u = 1/4$ and $h/L_d = 1/3$ are given in Figure 4-16. The velocities at the center of the hill decrease; whereas, at the extreme ends the velocity profiles are about the same as the two-dimensional profiles.

Under neutral flow conditions significant speedup effect occurs over the full width of a finite width ridge, but stable stratified flow reduces speedup over the ridge significantly. Figure 4-17 shows a set of mean velocity profiles at different locations at the crest. The hill shape is identical to the hill of Figure 4-16.

Particularly at the ends of the crest the speedup is much less. This is caused by the tendency of the dense air to go around the hill rather than over it.

4.2 INFLUENCE OF THREE-DIMENSIONAL HILLS OR RIDGES ON WIND SPEED AND TURBULENCE

A homogeneous "infinite plane" is never seen in nature. Similarly irregular three-dimensional surface obstructions are much more prevalent than the idealized two-dimensional ridge. Because of the large number of irregular geometric shapes, the problem is not amenable to mathematical characterization except for a few simple cases such as flow around spheres or cylinders. Consequently the wind tunnel has frequently been used to investigate scale models of bluff objects.

Early work tended to suggest that fields of turbulence and secondary flow around bluff bodies would be similar to those identified downwind of two dimensional fences or ridges. Hence, a cavity region downwind of separation was hypothesized, which communicated with the extended flow primarily by diffusion and pressure perturbations across free shear layers. Improved visualization techniques have revealed more complex flow pattern.

Wakes generated by hills or other obstacles are generally characterized by increased turbulence, mean velocity defect, and in certain situations by organized, strong vortices with axes generally parallel to the main flow direction. Under certain circumstances, however, the wake may involve mean velocity excess or turbulence defects. The wake generated by a three-dimensional surface-mounted protuberance in a turbulent boundary layer is highly three-dimensional. The characteristics of the wake (the extent of the momentum wake, the strength and extent of the vortex wake, the rate of decay of excesses and defects in the wake, etc.) are highly dependent on the overall obstacle height, the aspect ratio of the obstacle, the hill width-height ratio, the shape (projecting corners, step structure, round portions, etc.), approaching wind azimuth, character of the surrounding terrain (extent of vegetation and other nearby topography, etc.), and in some cases the stability of the approaching wind flow. For these reasons, a simple description or generalization of obstacle wakes does not appear to be possible.

Extensive surveys of the mean velocity and turbulence fields near hemispherical and rectangular block models immersed in a wall shear flow have been described by Hansen and Cermak (1975) and Woo, Peterka, and Cermak (1976). The complex flow patterns which develop around rectangular block models is noted in Figure 4-18. Two flow patterns of the whole flow structure about a rectangular body have been identified: one for reattached flow and one for unreattached flow on the sides of the model. (Note that unlike two-dimensional flow where the same streamline connects the separation to the attachment point, three-dimensional flows usually have no streamline which connects separation and attachment points or lines.)

Measurements downwind of hemispheres are different from the wake of a body in a uniform flow or a momentum wake behind a building in two important ways. First in the far-wake profiles there is a relative maximum in the velocity (or a relative minimum in the velocity deficit) on the wake centerline (see Figure 4-19). A significant portion of the wake contains velocity excesses. The minimum velocity in the lateral profiles is observed at points equally spaced on either side of the wake centerline. The near wake velocity profiles have the shape of a momentum wake. The minimum velocity is observed at the center of the wake. This profile shape is quickly changed into the shape with a local maximum velocity on the wake centerline. Velocity profiles measured in the lower region of the wake show this transition, from a momentum wake profile to what can appropriately be called a vortex wake profile. The profiles measured above the height of the obstacle show a momentum wake character far downwind. But the region, which contains the characteristic vortex wake velocity profiles, slowly grows upward giving almost all the the far wake a vortex wake structures.

The second, and the most surprising, feature of the hemisphere wake is the extreme persistence of the wake. Mean velocity wakes of simple cubes and blocks in turbulent boundary layers reported by other researchers extended at most to distances of the order of 10-15H, but the wake of this hemisphere is clearly evident at $x/R = 69.8$. It is not known how far the wake persisted downwind, but it was apparently greater than 100 radii in the smooth-floor boundary layer.

Separation is generally the dominant feature perturbing flow over surface obstacles; however, thermal stratification or surface heating may further complicate the already confusing flow picture. Hawthorn and Martin (1951) considered flow with vertical velocity and density gradients around a hemisphere attached to a horizontal wall.

For the stable case, vortex lines, which are horizontal and lie perpendicular to the flow far upstream, are held back by the obstacle and are therefore stretched and rotated so that, when seen from above, the vortex vector points upwind on one side and downwind on the other side of the obstacle. This introduces a secondary component, which produces downward motion behind the obstacle.

Over a hot hump, the secondary vorticity generated by gravity is in the opposite direction. Close to the floor where the vertical displacement is negligible the effect is very small; whereas, the effect of the holding back of the vortex lines is a maximum. Consequently, there is on each side a surface below which the vorticity was dominantly produced by gravity. There is therefore an inflow towards the axis of the flow along these surfaces (see Scorer (1978, § 3.6)).

The upwind distortion of vortex lines by the presence of a hill in a stream with shear is responsible for possible separation and the formation of "horseshoe" shaped vortex cells which wrap around the

base of the obstruction. The vortex lines essentially wrap around the obstacle and they are stretched so as to intensify the vorticity (i.e., continuously accumulate at the foot). A general downflow is induced in the hill wake by these vortices tending to increase velocities where a momentum defect might otherwise exist.

A very limited set of three-dimensional hill measurements have been completed as part of the present program. Only hills of modest slope were considered similar to shapes examined during the two-dimensional program described in Section 4.1. Details of the experiment and tabulated data are contained within Appendix D of Meroney et al. (1978b).

4.2.1 Laboratory Measurement Program

A set of velocity distribution measurements were made over an approximate Gaussian shaped hill and over a 1 to 4 slope and a 1 to 3 slope, cone shaped hill. The hills were approximately one tenth the height of the boundary layer thickness. Detailed velocity measurements were made for a freestream velocity of 9.4 m/sec. A limited number of velocity profiles were also taken over the Gaussian hill for a freestream velocity of 15.3 m/sec. As a result of the three-dimensional nature of the hill the local speedup at any particular location will not be as great as that observed for the two-dimensional ridge. The present models will correspond to atmospheric hill heights of the order of 30 to 100 m.

The measurements were taken in the Meteorological Wind Tunnel located in the Fluid Dynamics and Diffusion Laboratory at Colorado State University. Three, 3-dimensional, hills were used for the tests. Numbers were used to distinguish these hills as:

- Hill No. 1 Gaussian hill with crest height:radius = 1:6
- Hill No. 2 Cone shaped hill with crest height:radius = 1:4
- Hill No. 3 Cone shaped hill with crest height:radius = 1:3.

Static pressure measurements were made above and along the surface of each hill. Velocities and velocity fluctuations were sampled with a pitot-static probe, a Kiehl probe, and a conventional hot film anemometer.

4.2.2 Results and Conclusions

Surface oil visualization revealed that over the Gaussian hill (1:6 slope) an area of separation occurs starting near the crest and spreading downwind laterally at about an included angle of 35° . This separation region was fluctuating and nonstationary, and results suggested the presence of organized vortex motions. A speedup ratio of 0.57 was obtained at the crest of the Gaussian hill. It is possible that slightly higher speedup ratios may be obtained in the region just off the crest;

however, the present grid of measurements did not cover the crest region in sufficient detail to indicate a maximum away from the crest. The cone hills obtain maximum speedup ratios of the order of 0.3 at the crest. Compared to the two-dimensional ridges, the isolated three-dimensional hills do not appear to be a great deal better than bluff, two-dimensional ridges.

The present study suggests that the round crest hill will be a better wind power site than the sharp crested cones. The flow visualization suggests that the region around the crest on the shoulders may also produce local highwind velocities. The static pressure measurements on the Gaussian hill appear to indicate the higher velocities over a region of about $h/7$ to $h/2$ radius away from the crest at right angles to the flow direction. Thus, for the rounded three-dimensional hill it may not be necessary to mount the wind turbine directly at the crest. If, however, the prevailing windflow direction varies over large angles, the crest of the hill is suggested as the best location. The separation region on the downstream face of the hill does not quite reach to the crest of the Gaussian hill, but the large fluctuations associated with the separation are evident near the crest. If a choice is available it would appear that two-dimensional ridges are much better as wind velocity amplifiers than the isolated three-dimensional hills.

4.3 INFLUENCE OF COMPLEX TERRAIN ON WIND SPEED AND TURBULENCE

The flow characteristics of regions of complex terrain differ significantly as a function of topographical details and meteorological conditions. For this reason there must be programs designed to distinguish between the generalizations possible as outlined in Sections 4.1 and 4.2 and the site-specific types of flow phenomena.

Meteorological phenomena peculiar to complex terrain include the presence of effects of separation, stable stratification (lee waves), thermally driven mountain-valley winds, and turbulence induced by stratification.

These phenomena produce flow effects which are by no means likely to be additive by linear superposition. Nonetheless it is necessary their flow physics be understood independently as well as together.

A program to study flow over complex terrain which emphasized such aspects for the WECS program is contained in Meroney et al. (1978a). Typical results and conclusions drawn from this material follows.

4.3.1 Joint Physical Modeling to Field Measurement Comparison Study

New Zealand the the United States are both geographically complex, contain many potentially attractive windpower sites, and yet in many

such areas of complex terrain there are "meteorological data" deserts. One such area is the Rakaia River Gorge region on the eastern slope of the Southern Alps in New Zealand. Climatological records obtained from stations somewhat removed from the area suggest moderate to very high wind energy. Extended field measurement programs are invariably expensive and time consuming; hence a survey program was proposed to utilize laboratory simulation of the relevant wind characteristics in a meteorological wind tunnel. To evaluate the validity of laboratory simulation methods and provide a confidence measurement bound for laboratory data, a simultaneous limited field measurement program was organized.

The area studied by means of a laboratory model is located along the Rakaia River as it emerges from the Southern Alps, South Island, New Zealand. The primary terrain features consist of the Rakaia River Gorge which runs generally in a northwest-southeast direction. Gorge walls rise 180 m, surrounding hills rise to 460 m. To the south lies the Mount Hutt range, which climbs to 2188 m. The range parallels the course of the Rakaia River in this area. To the north lies the Rugged Range, but nearby Fighting Hill and Round Hill are the largest features. A model section 6100 m wide by 18,300 m long centered over the Rakaia River Gorge was constructed to a scale of 1:5000.

The construction material was expanded polystyrene bead board cut to 0.61 cm thickness to match 100 ft (30.5 m) map contour intervals. This was mounted in layers on a particle board support sheet. The dimensions of the overall model was approximately 5 m long by 1.22 m wide which includes a 1.22 m terraced section upwind to transition the model to the tunnel floor. To provide a greater upwind fetch of equivalent surface roughness an additional 1.22 m x 2.44 m section of polystyrene bead board was mounted immediately upwind of the transition subsection. The total model length was thus 7.3 meters. A 2.5 cm high trip fence and a square bar turbulence grid were placed upwind of the model to produce the desired similitude characteristics. Plaster was smooth between terrace escarpments and was textured to provide an equivalent surface roughness. This surface roughness was such as to provide a $z_0 \approx 0.01$ mm equivalent to $z_0 = 0.05$ m at full scale.

The hill sides to either side of the Rakaia River are primarily devoted to sheep paddocks. To protect flocks and paddock surface during the high wind event, farmers have planted shelterbelts around most fields. Most of these shelterbelts are mature coniferous tree stands about 20 m high. The tree stands often consist of several rows and appear quite dense. Aerodynamic studies of flow fields behind shelterbelts in New Zealand have been performed by Sturrock (1972). Measurements behind 4 mm high pipe cleaners revealed they simulate the velocity and turbulence field for 1:500 scale very well, hence pipe cleaner shelterbelts were added to the model to simulate the prototype vegetation.

The Rakaia River Gorge model was studied in an Atmospheric Boundary Layer Wind Tunnel as shown in Figure 4-20. The model as it appeared in the tunnel is shown in Figure 4-21. Laboratory measurements include horizontal and vertical profiles of mean wind velocity, longitudinal turbulence, wind direction, turbulence spectra and correlations utilizing hot wire anemometry, pitot-static pressure probes, and cobra pressure probes.

Measurements of wind velocity and directions were desired over the Rakaia River Gorge test region to provide a basis for validation of laboratory methodology and physical modeling. Ideally a network of permanent meteorological instruments would be installed on multiple towers with data recording equipment versatile enough to intercept and record a northwesterly wind event. The cost of capitalization and maintenance of such a network was unfortunately prohibitive. An alternative proposed is to place a simple, lightweight cup anemometer on each of several collapsible pole towers and move the towers frequently during a wind event. The effectiveness of such a procedure will depend upon spatial correlation of wind velocities over the same 100 square km region, the quasi-stationarity of the wind event over a 3 to 6 hour period, and the statistical significance of a 15 minute sample at a given point taken once during a 3 to 6 hour recording period. Recent climatological analysis by Corotis (1977) suggest high correlation (0.76 - 0.83) over distances less than 22 km and high autocorrelation over periods to 3.5 to 7 hours. The criteria for a field station were thus light weight, rapid erection, and low cost. Three masts were constructed to 5 cm diameter thin wall aluminum tube. The tubes were made in two 5 meter sections which could be connected via a simple sleeve joint. Three nylon rope ties were attached at 7.5 m to the upper section and when erected the ties attached to three steel stakes driven at convenient distances from the mast base. The three cup RIMCO anemometers were attached to the top of the mast by a threaded fitting. A 3 lead supply and signal cable led from the anemometer to a power supply and counter module placed at the base of the mast. The entire system was conveniently light and easy to handle. It could be carried on the luggage rack of a passenger car or in the back of a jet boat. Two or three men could erect the tower in 5 minutes and remove it in somewhat less time (see Figure 4-22).

On two spring days, selected for strong adiabatic down valley wind flow, three teams of investigators surveyed up to 27 sites on either side and within the river gorge. Measurements consisted of wind speed and direction at a 10 meter height on lightweight portable towers. All measurements were completed during the course of a five hour stationary wind event and normalized against continuous records taken from a New Zealand Wind Energy Task Force anemometer near terrain center.

4.3.2 Validation Results and Conclusions

A series of contour diagrams were prepared from the laboratory velocity and turbulence intensity measurements into isotach and isoturb charts. Figures 4-23 and 4-24 show a typical pair of such drawings. Note the wide variation in wind speed near ground level between points within the gorge and the nearby hill top. Simultaneously large relative gustiness exists within the river gorge when compared to the hill crest. Horizontal sections prepared for a 10 meter equivalent height reveals the river valley and gorge consistently has lower wind energy than the surrounding ridges.

The laboratory simulation results were compared with the available field data by means of statistical correlation and scatter diagrams. The model and field results were used to assess the value of the laboratory experiments for assisting WECS siting field programs. A thorough search of the literature reveals that few authors have chosen to compare field and model (either numerical or physical) results in other than qualitative terms. Recently Fosberg et al. (1976) compared a numerical model which includes terrain, thermally, and frictionally induced perturbations to seven field data sets. Correlation coefficients determined for the velocity and direction results were 0.60 and 0.62 respectively. These limited results may be used as a context within which to judge the efficacy of the present physical model or as a statement of reasonably current alternative modeling capacity. A typical scatter diagram result is shown in Figure 4-25. Plotted on the scatter diagram are the co-correlation lines of the result of regressions of abscissa against ordinate and ordinate versus abscissa. When $r = +1$ these lines will be colinear, when $r = 0$ the lines will be perpendicular. The lines thus provide visual evidence of the quality of correlation.

Special results and conclusions resulting from this research are

1. Physical modeling can reproduce wind patterns produced by the atmospheric shear layer flowing over complex terrain to within the inherent variability of the atmosphere to produce stationary results;
2. Physical modeling reproduced the relative wind speeds found over complex terrain to rank to sample correlation coefficient levels equal to 0.78 to 0.95;
3. Physical modeling reproduced the individual day to day quantitative wind speeds found over complex terrain to sample correlation coefficient levels equal to 0.70 to 0.76;
4. Physical modeling reproduced the two field day average quantitative wind speeds found over complex terrain to a sample correlation coefficient level equal to 0.81;

5. Physical modeling reproduced the individual day to day site wind directions found on complex terrain to simple correlation coefficient levels equal to 0.65 to 0.67;
6. Adequate physical modeling of adiabatic shear flow over complex terrain requires attention to surface roughness, terrain shape, and vegetation as well as upstream velocity profile, turbulence intensity, and turbulence eddy structure;
7. Over complex terrain local wind speeds may vary by over 100% in a distance of a few hundred meters as a result of terrain shadowing, flow separation, or flow enhancement;
8. In the Rakaia River Gorge area preferred WECS locations are the surrounding hills and ridges, and not the gorge or river bottoms.

In addition to the specific conclusions related above, review of the complex terrain literature suggests some other generalizations borne out by field programs:

1. Most investigators naturally compare results or inferences from data in complex terrain to results which would be expected in level terrain. These comparisons have been made because of the wealth of data and the improved understanding available in the latter case. Although it is recognized none of these scientists are necessarily implying complex terrain flow is just a perturbation on homogeneous terrain experience there is an unfortunate tendency to try and make such extrapolations. Since complex terrain flows are generally spatially nonstationary, lack turbulence equilibrium, and contain strong vertical and lateral pressure irregularities, it may be more rewarding to avoid such extrapolations and examine the phenomena independently from prior conceptions.
2. In general, turbulence levels over complex terrain are assumed to be higher than over level terrain for a given atmospheric stability classification. These levels are most likely a result of:
 - (a) Nocturnal, radiational cooling which produces surface inversions is often coupled with very low wind speeds in level terrain and is likely to result in the generation of gravity-driven drainage flows in complex terrain. These flows result in the mechanical production of turbulence near the surface.
 - (b) Topographic alteration of flow direction and speed will result in the production of shear in all directions which not only contributes to the production of

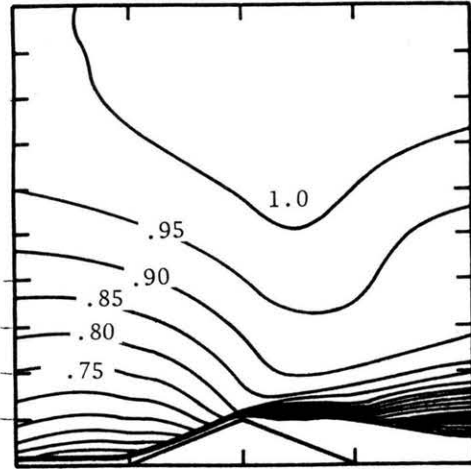
turbulence, but also results in large flow meandering resulting from the synergistic effects of plume shape distortion coupled with turbulent mixing.

(c) In level terrain, stable atmospheric conditions generally aid to suppress turbulent motions. In complex terrain, the presence of flow stratification is a key element in the production of the regions of rapid flow acceleration and deceleration, lee waves, rotors, etc., which tend to produce shearing motions, and regions of flow reversal which are conducive to turbulence production. During neutral and unstable atmospheric conditions, the effects of terrain on turbulence levels appears to be small. Evidently, convective motions dominate and suppress the influence of terrain on flow field alterations and turbulence levels.

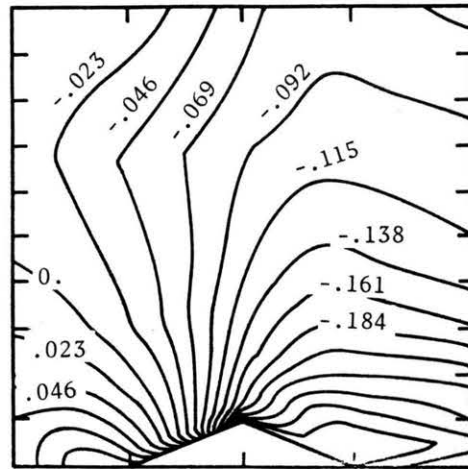
3. Lateral turbulence levels in complex terrain are generally enhanced by complex terrain to a greater extent than vertical turbulence perturbations. Observations of smoke plume meandering and splitting upon encountering terrain surfaces

are reasons cited for increase in $\overline{v'^2}$. Whether $\overline{v'^2}$ at elevated heights above the terrain is disproportionately larger is not known.

4. When the atmosphere is stably stratified, generalizations are more difficult. The flow over smooth two-dimensional terrain objects is expected to decelerate upwind and accelerate downwind of the object. Air parcels downwind of a ridge may be rapidly dispersed upward (or even upwind) by rotor waves or other eddy motions associated with the lee side flow dynamics.
5. Thermal and topographic effects in complex terrain appear to increase scalar transport rates and turbulence in regions of complex terrain over those which might be expected over level terrain. Terrain features can, however, contribute to large scale stagnation of air flow in lower regions and this can result in no-wind conditions if stagnation persists for several days.

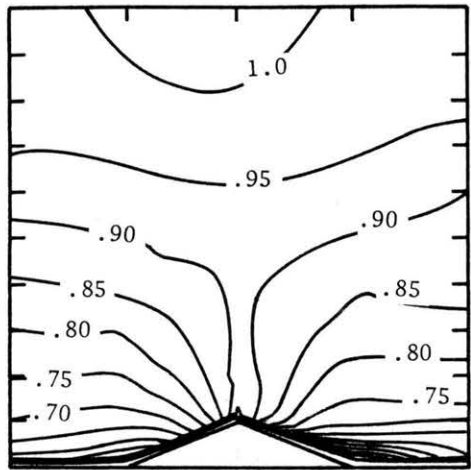


a) Velocity contours, $h/L_u = 1/3$
contour interval $\Delta u/u_\infty(\delta) = .05$

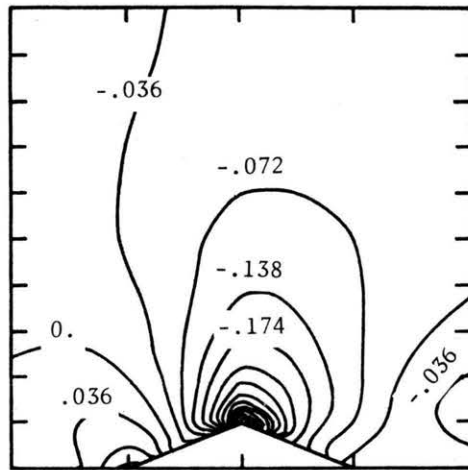


a) Static pressure contours
 $h/L_u = 1/3$
Contour interval $\Delta C_p = .023$

$h/\delta = .1, h/L_u = h/L_d = 1/4$



b) Velocity contours $h/L_u = 1/4$
interval, $\Delta u/u_\infty(\delta) = .05$



b) Static pressure contours
 $h/L_u = 1/4$
contour interval, $\Delta C_p = .036$

$h/\delta = .1, h/L_u = h/L_d = 1/3$

Figure 4-1. Mean Velocity and Static Pressure Contours Over Triangular Hills

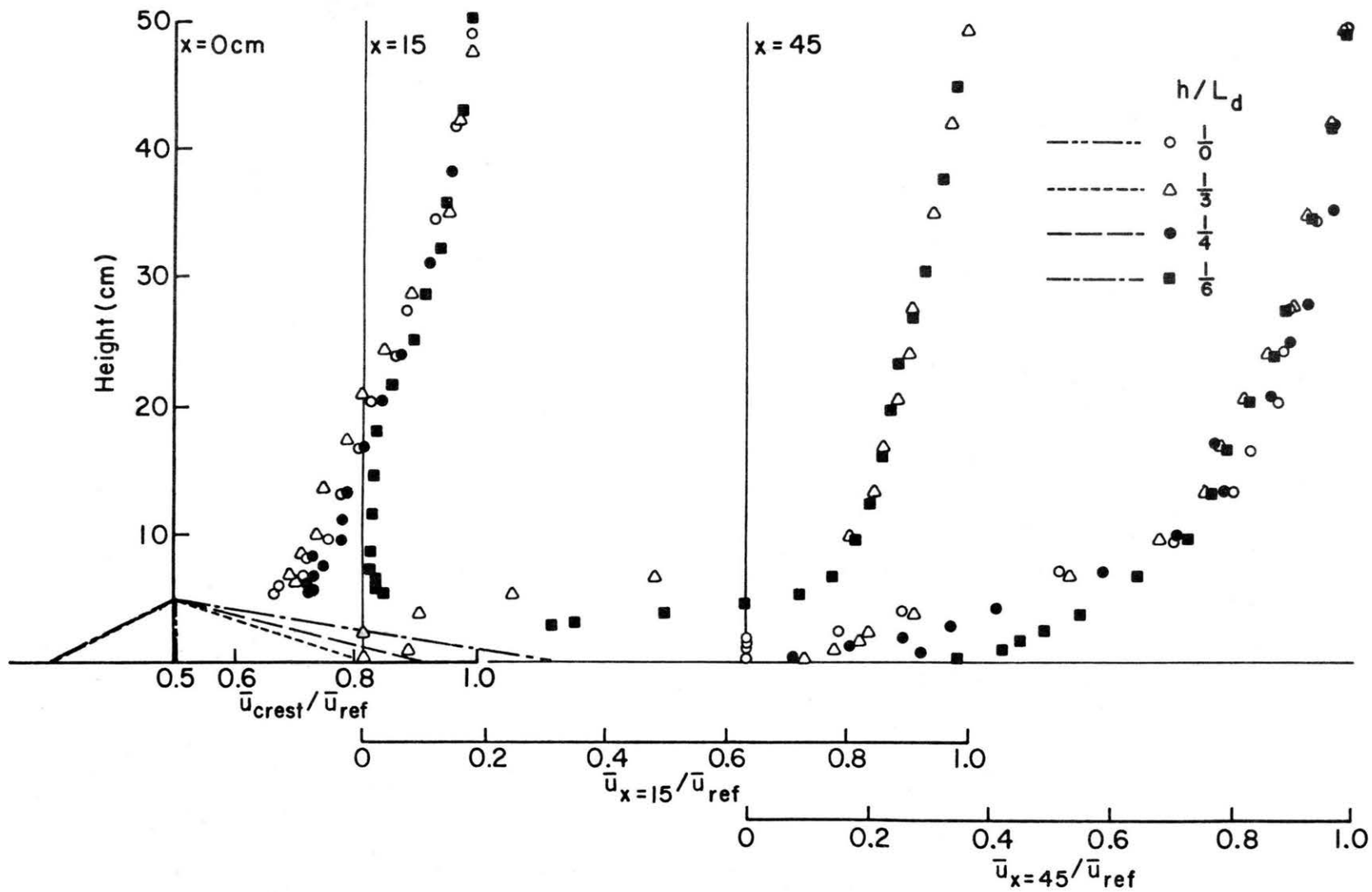


Figure 4-2. The Effect of Downwind Slope on Vertical Velocity Profiles Downwind of the Crest

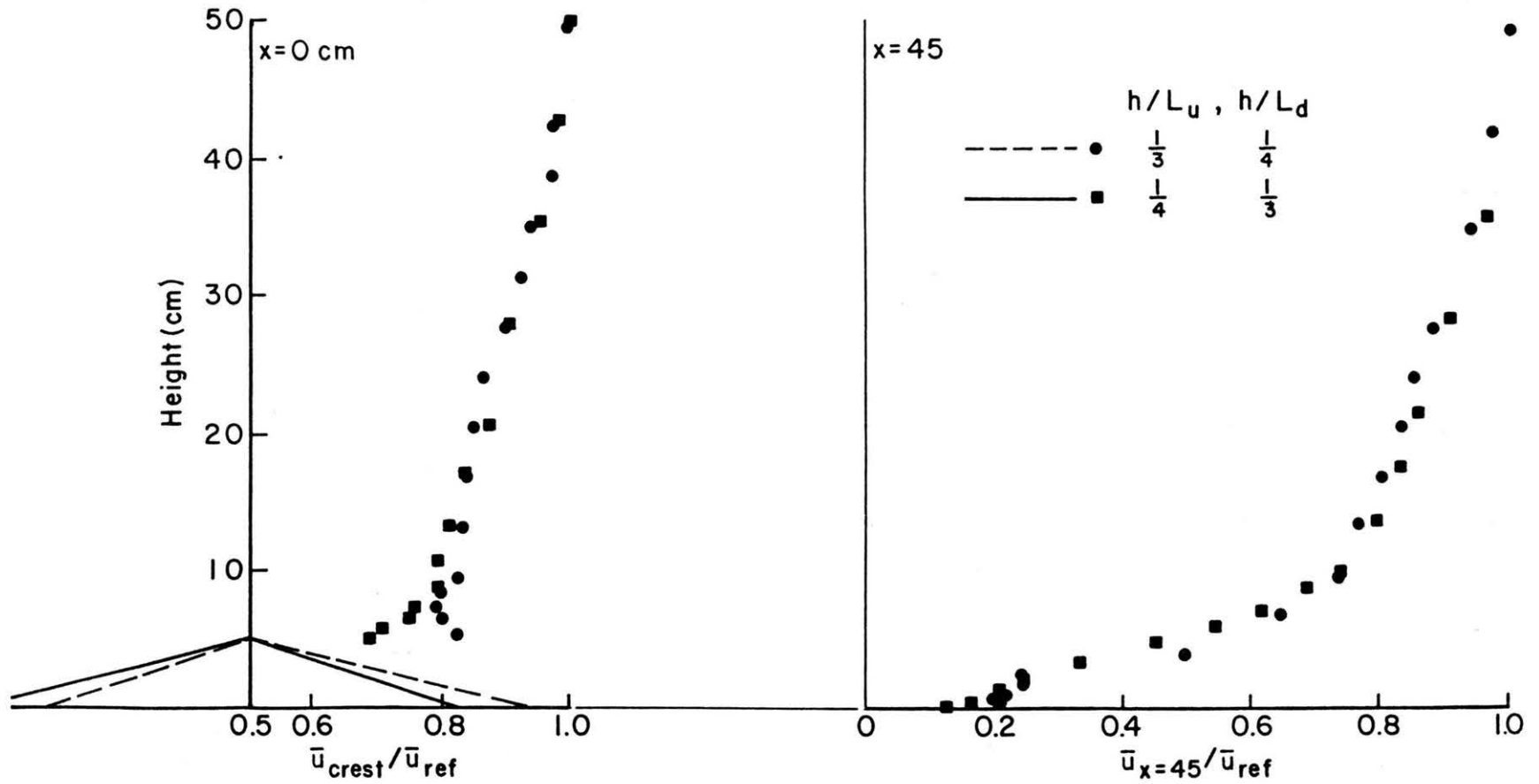


Figure 4-3. The Effect of Upwind and Downwind Slope or the Effect of Opposite Wind Directions

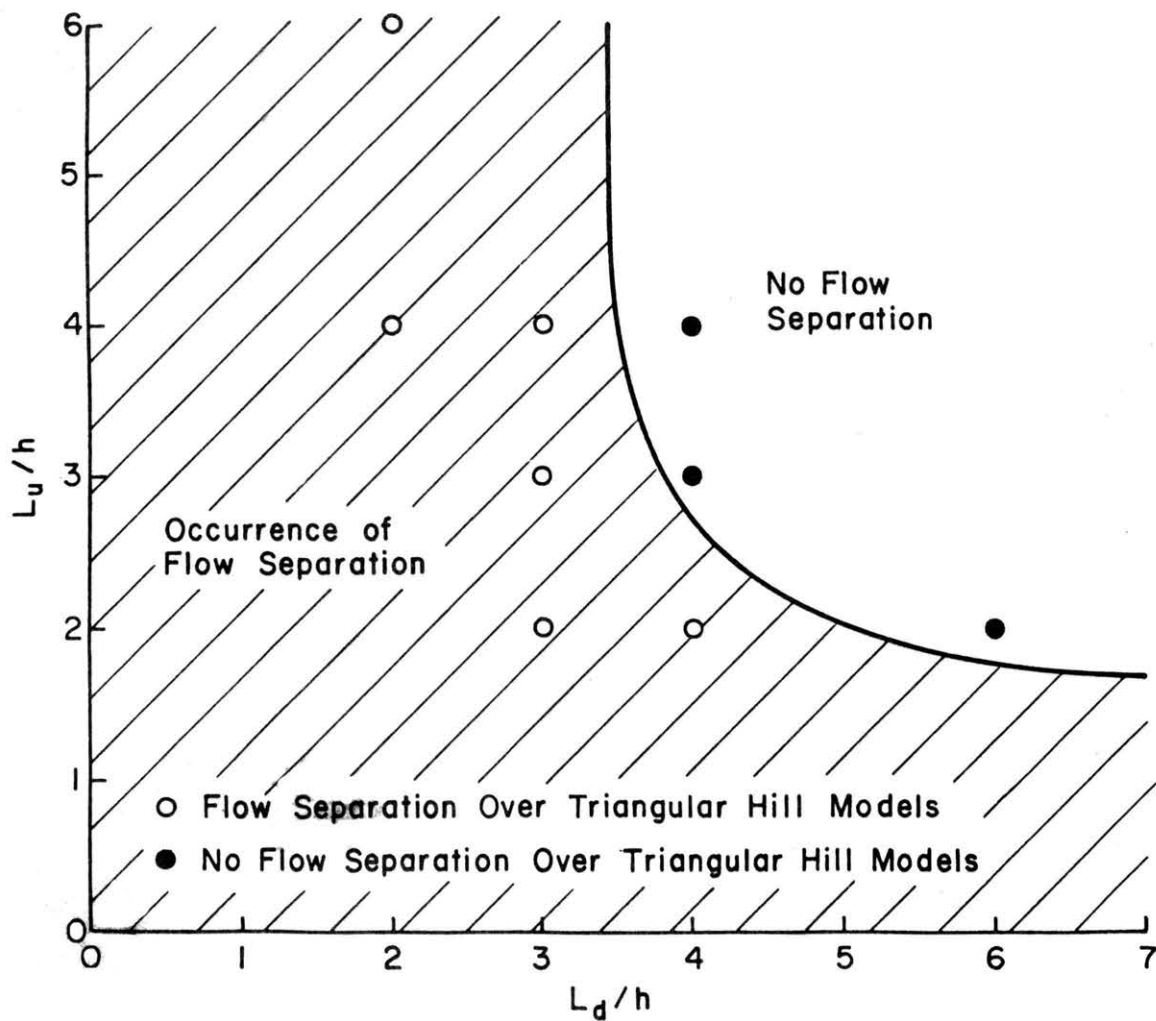


Figure 4-4. Criterion for Flow Separation Over Two-Dimensional Triangular Hills

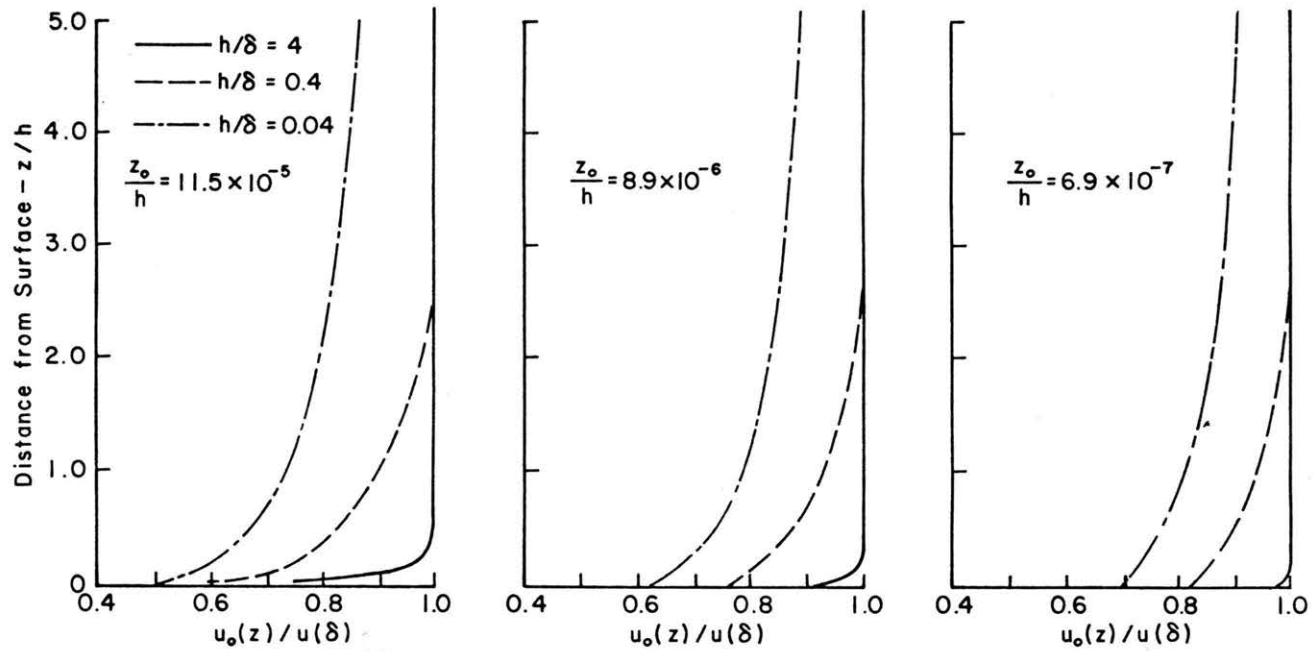


Figure 4-5. Upstream Approach Profiles for Numerical Inviscid Flow Calculation

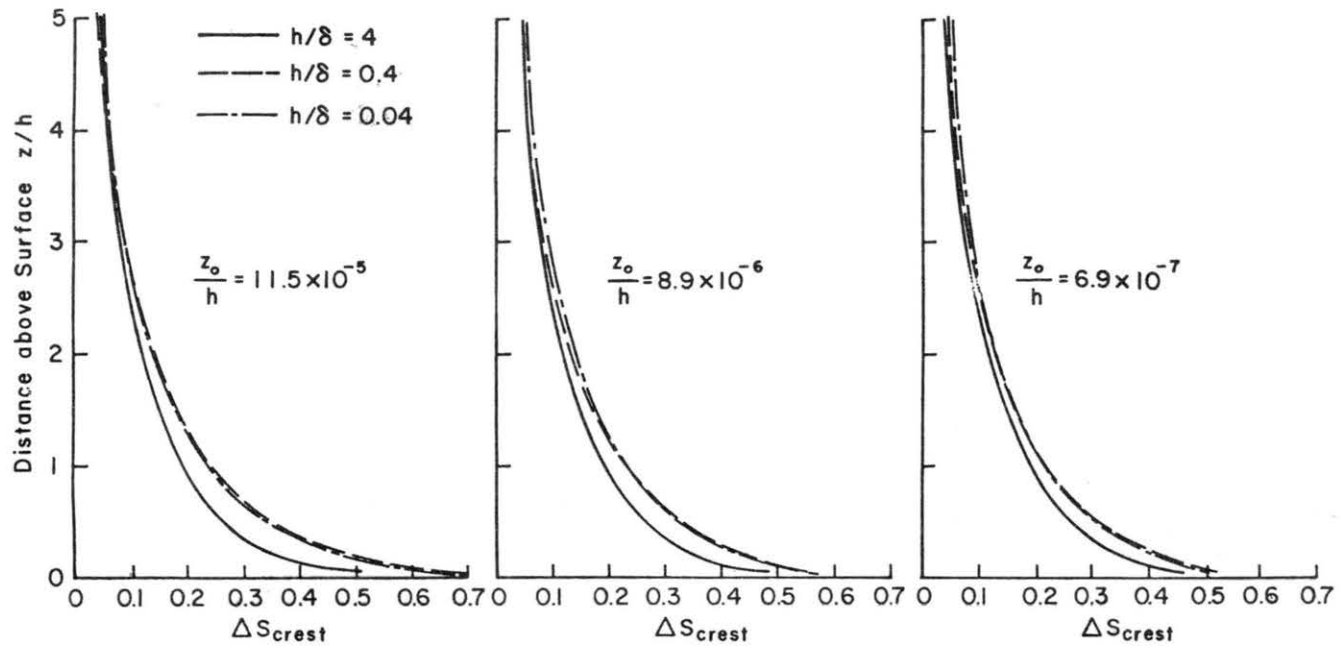
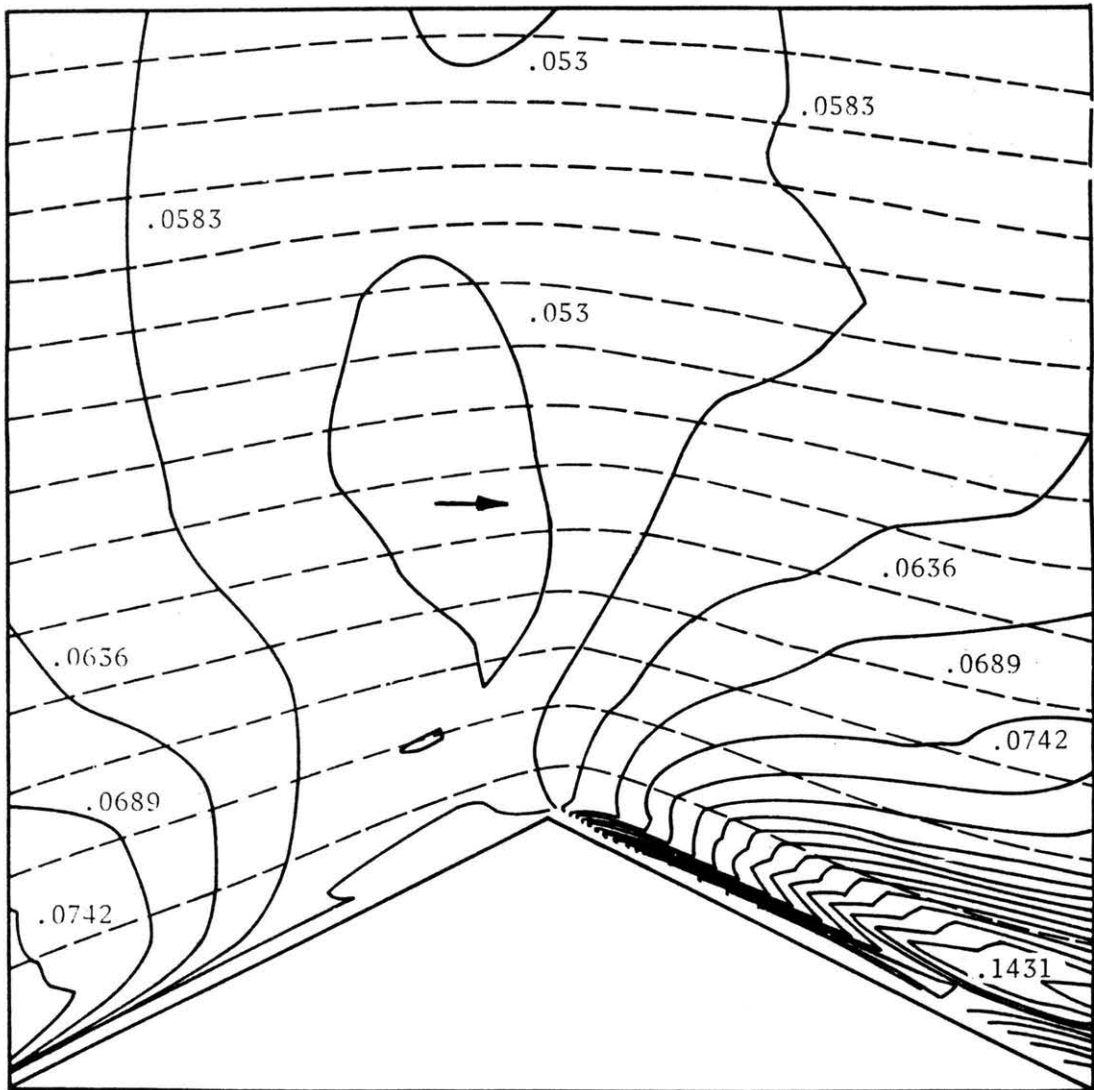


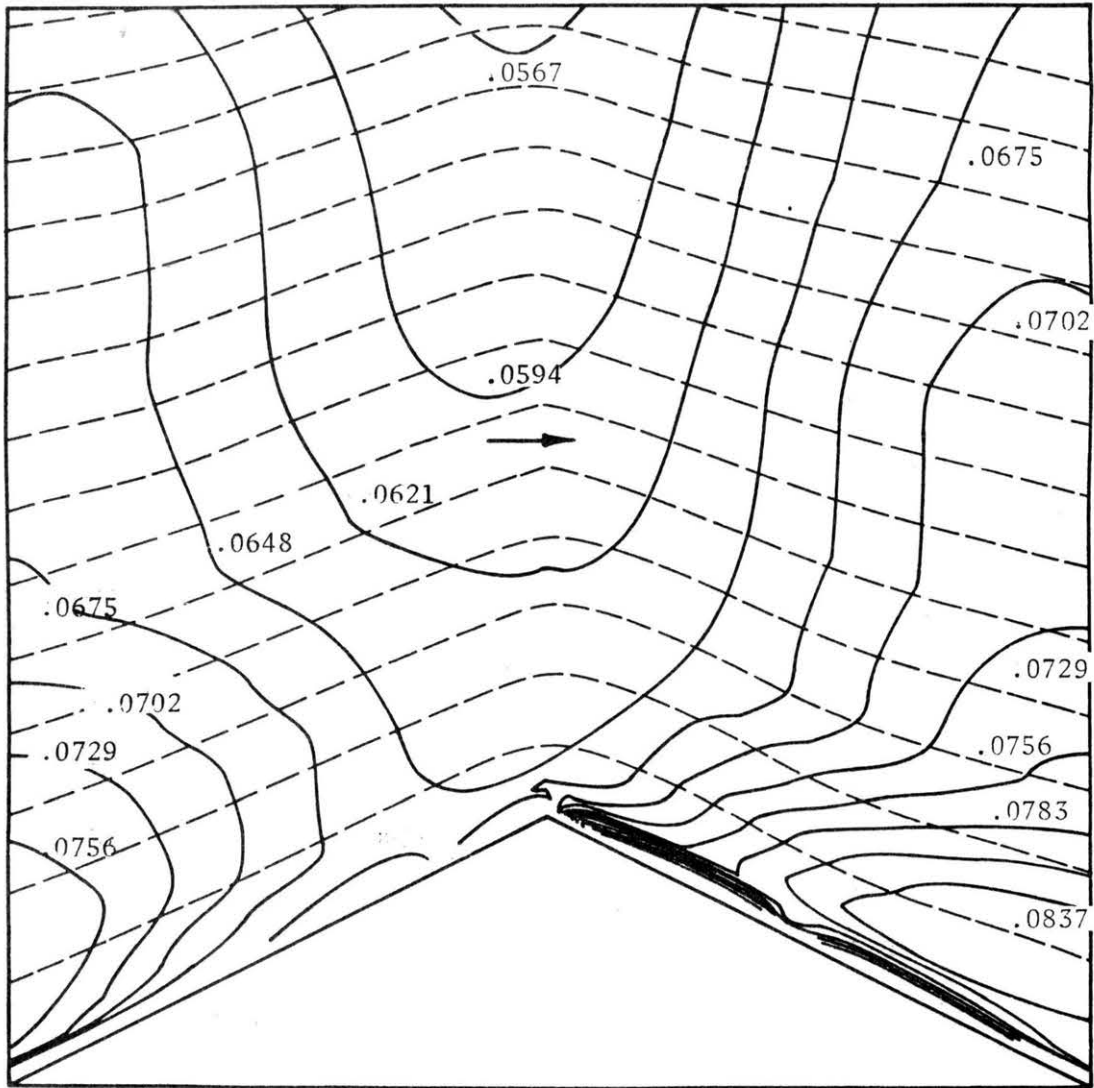
Figure 4-6. Fractional Speedup Ratios Predicted From Numerical Flow Calculations



Contour interval $\Delta \bar{u}^T / u(\delta) = .0053$

$h/\delta = .1$, $h/L_u = h/L_d = 1/4$, $z_o/h = 1.5 \times 10^{-4}$ (standard case)

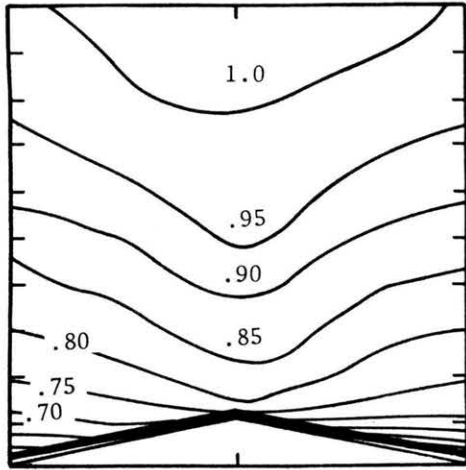
Figure 4-7a. Contour of Longitudinal Turbulence Intensity With Superimposed Streamlines (broken lines)



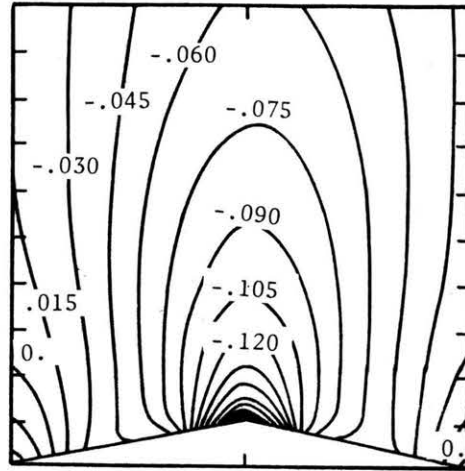
Contour interval $\Delta \overline{u^2}/u_\infty(\delta) = .0027$

$h/\delta = .1, h/L_u = h/L_d = 1/20, z_o/h = 1.5 \times 10^{-4}$ (standard case)

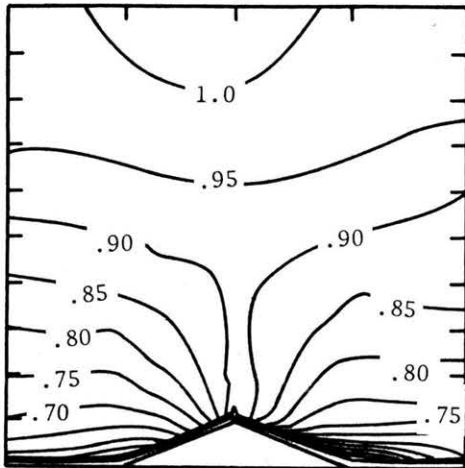
Figure 4-7b. Contours of Longitudinal Turbulence Intensity With Superimposed Streamlines (broken lines)



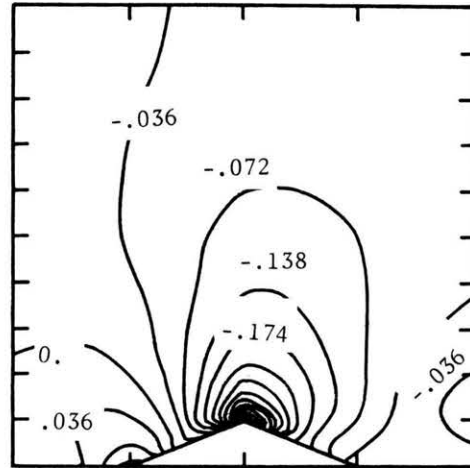
a) Velocity contours $h/L_u = 1/20$
Contour interval $\Delta u/u_\infty(\delta) = .05$



a) Static pressure contours
 $h/L_u = 1/20 \Delta C_p = .015$



b) Velocity contours $h/L_u = 1/4$
Contour interval $\Delta u/u_\infty(\delta) = .05$



b) Static pressure contours
 $h/L_u = 1/4 \Delta C_p = .036$

Figure 4-8. Mean Velocity Contours Over Triangular Hills

- a. $h/\delta = .1 \quad h/L_u = h/L_d = 1/4$
b. $h/\delta = .1 \quad h/L_u = h/L_d = 1/20$

Figure 4-9. Static Pressure Contours Over Triangular Hills

- a. $h/\delta = .1 \quad h/L_u = h/L_d = 1/4$
b. $h/\delta = .1 \quad h/L_u = h/L_d = 1/20$

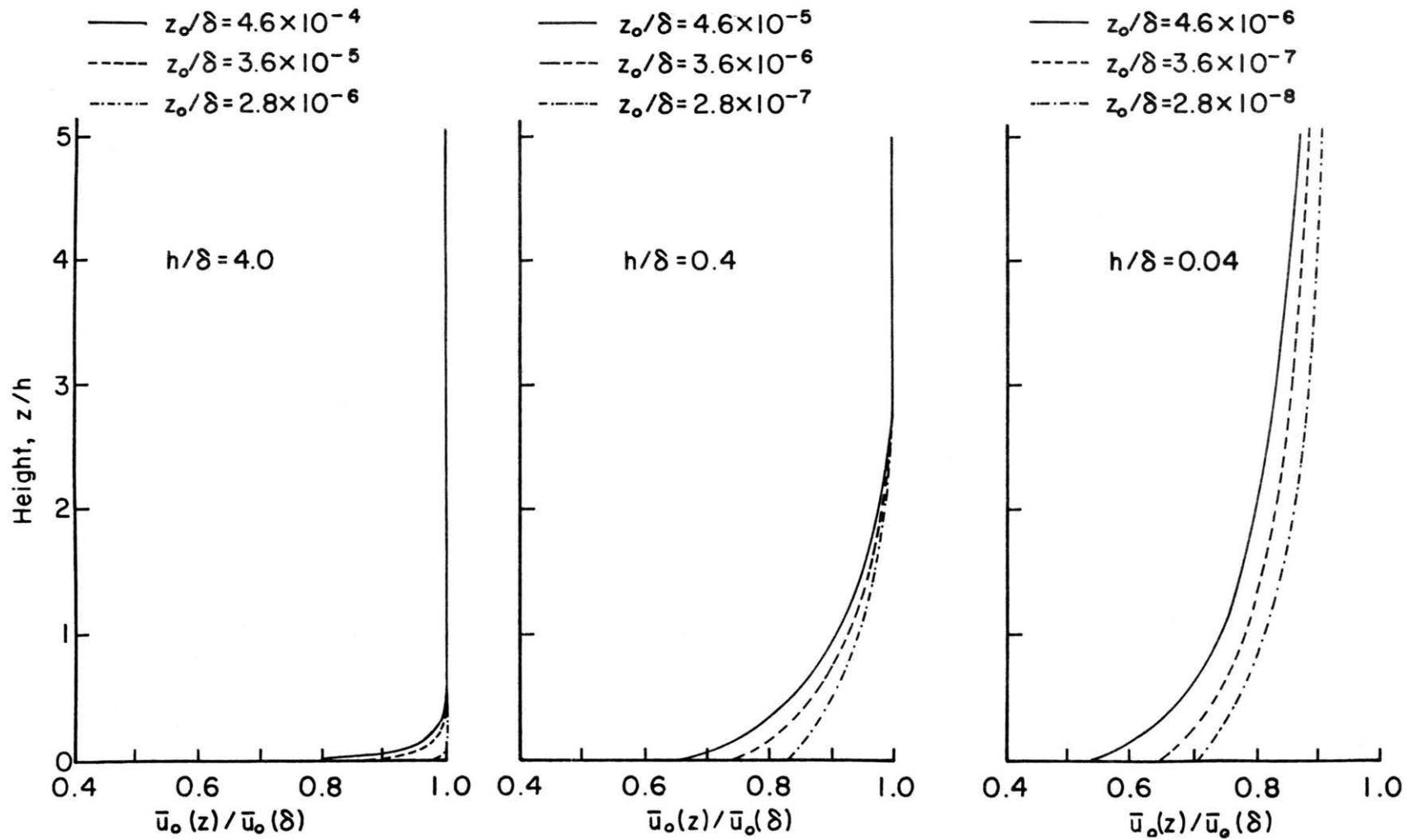


Figure 4-10. Approach Velocity Profiles for Numerical Inviscid Flow Calculations

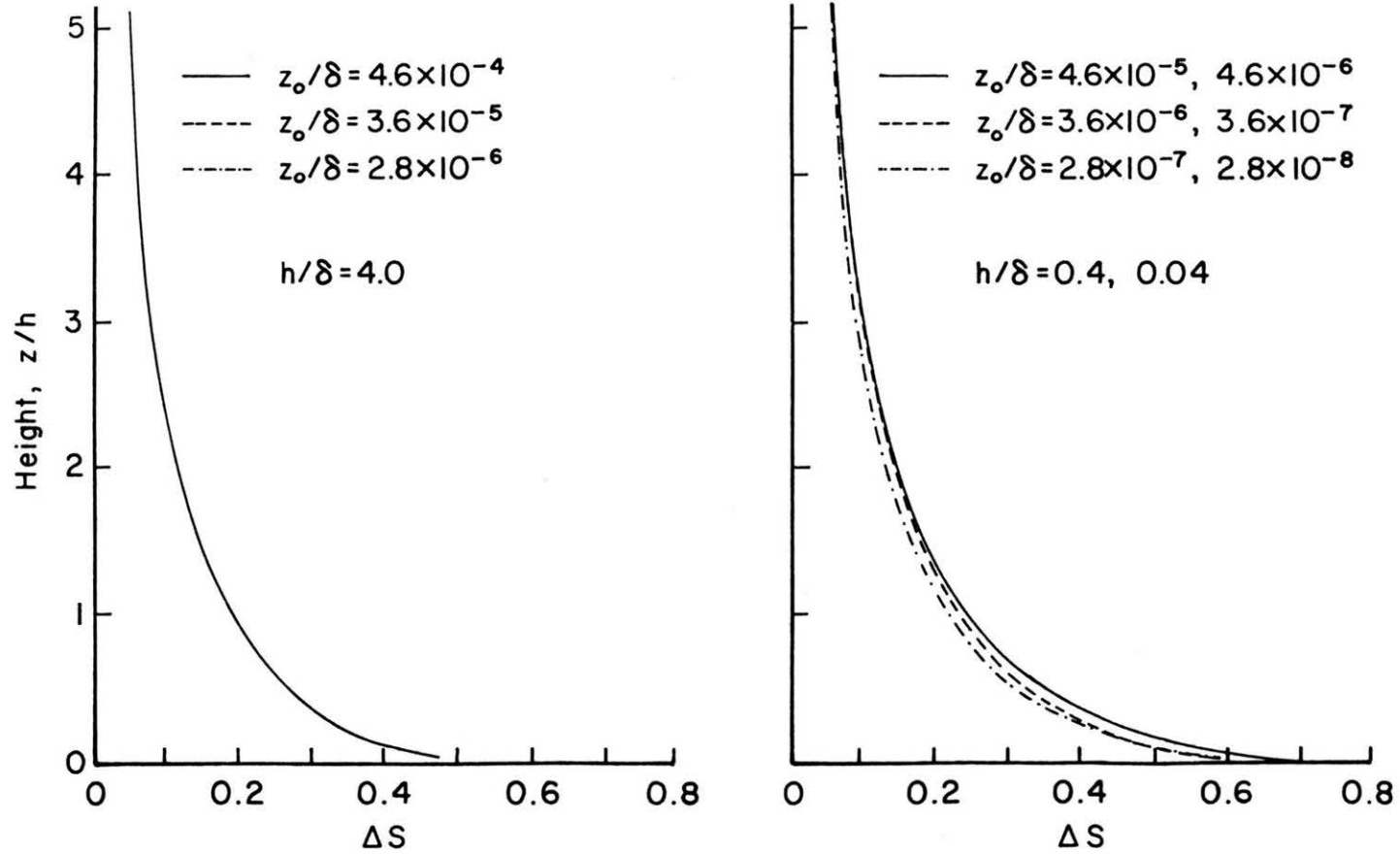
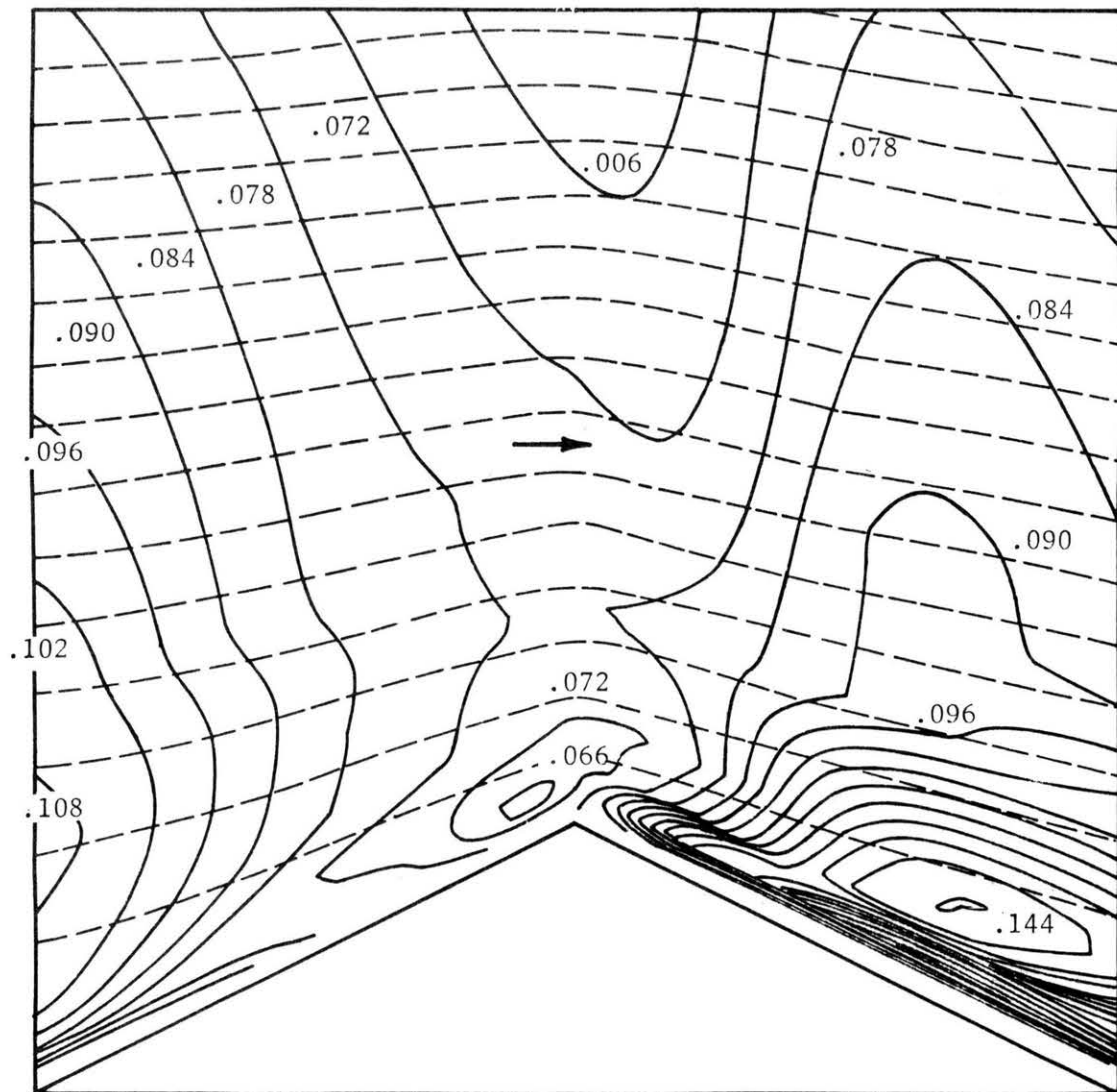


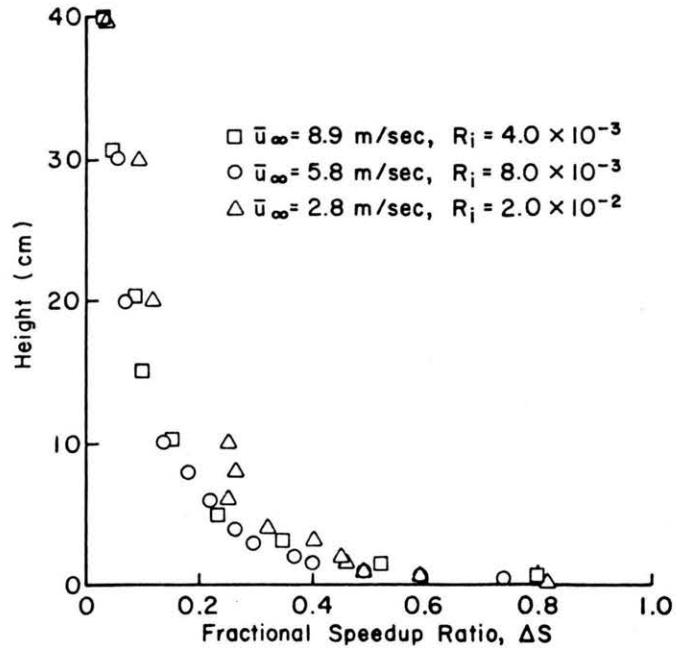
Figure 4-11. Fractional Speedup Ratios Predicted From Numerical Inviscid Flow Calculations



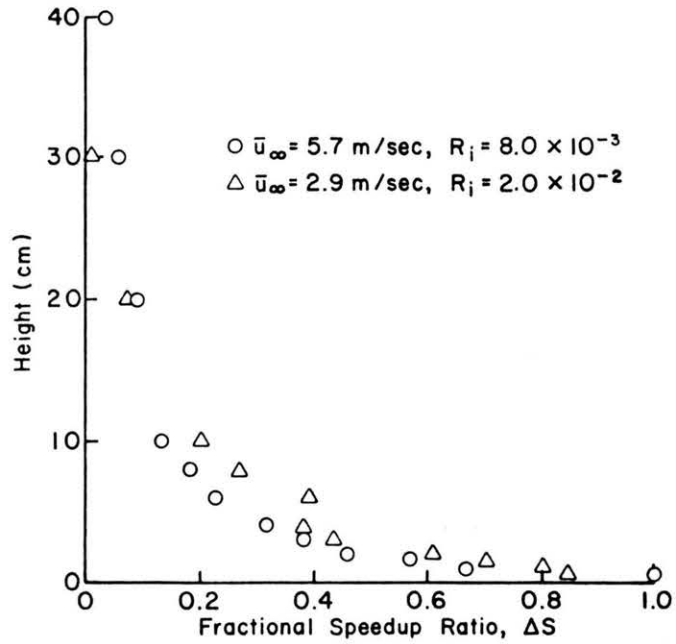
Contour Interval $\Delta u'/u(\delta) = .0060$

Figure 4-12. Contour of Longitudinal Turbulence Intensity With Superimposed Streamlines (broken lines)

$$h/\delta = .1 \quad h/L_u = h/L_d = 1/4, \quad z_o/h = 2 \times 10^{-3}$$



a) 1 to 4 slope triangular ridge



b) 1 to 6 slope triangular ridge

Figure 4-13. Fractional Speedup Ratio Over the Ridges

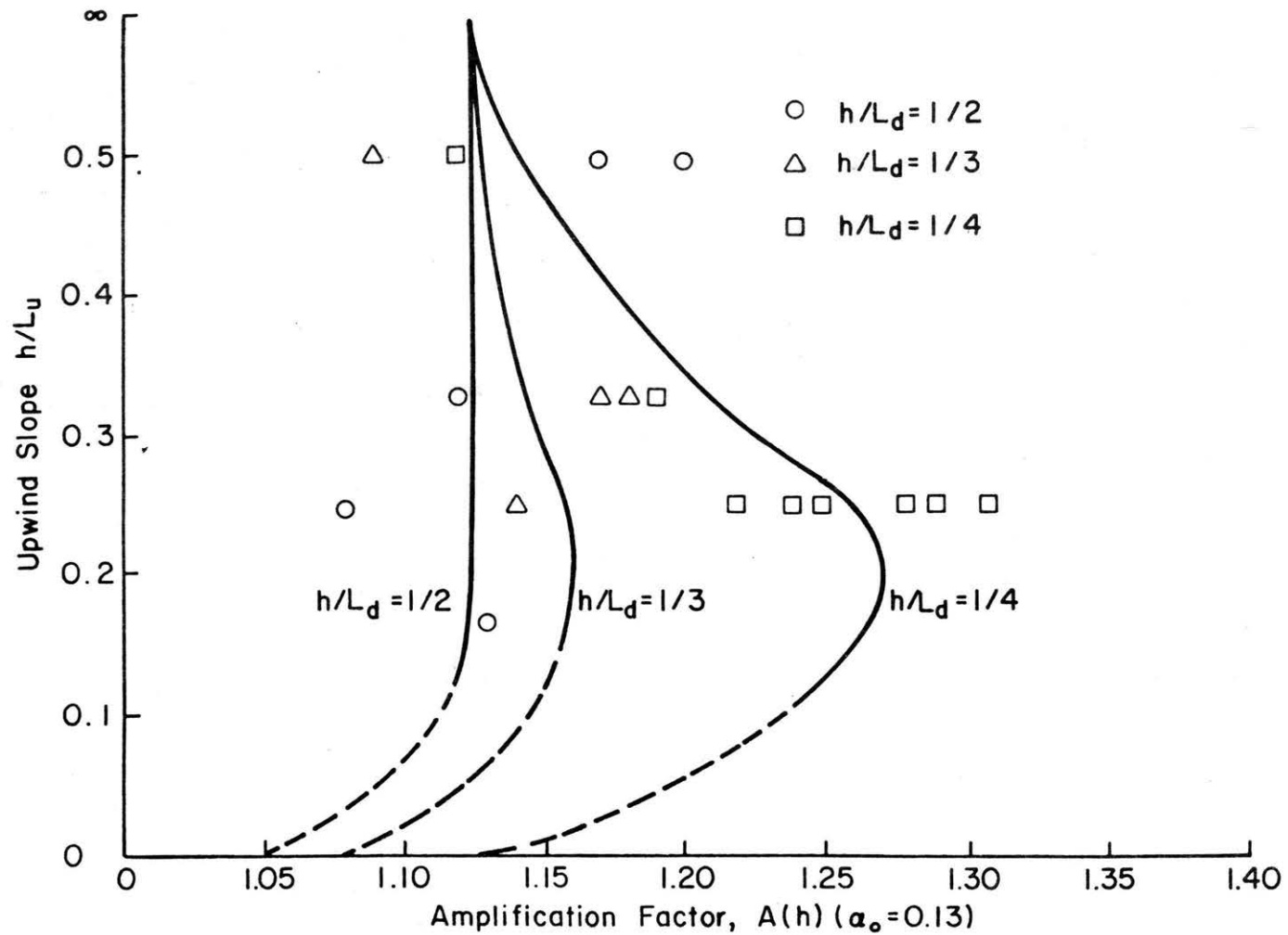


Figure 4-14. The Effect of Upwind Slope on the Speedup Factor for $\alpha_0 = 0.13$

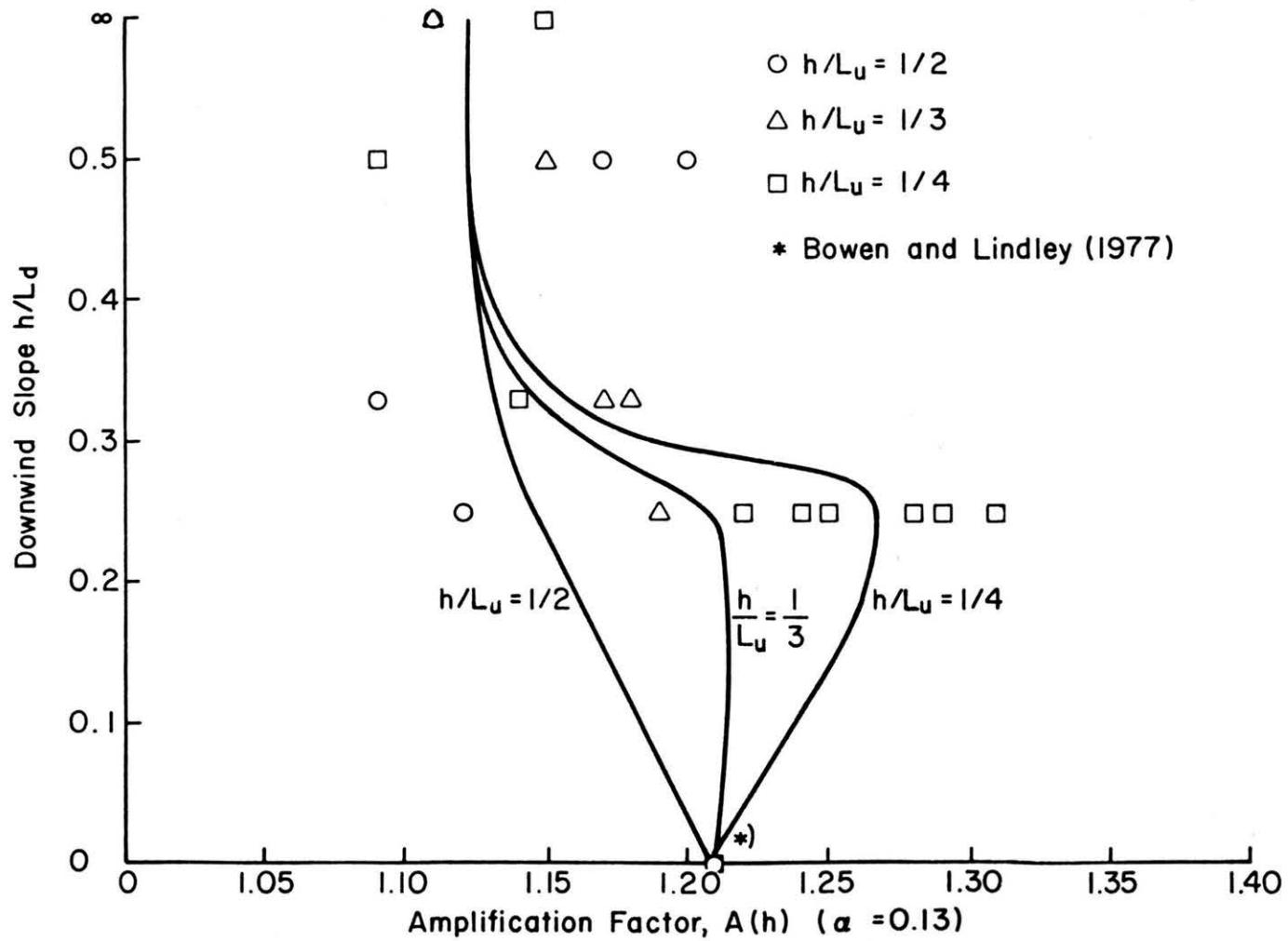


Figure 4-15. The Effect of Downwind Slope of the Speedup Factor for $\alpha_0 = 0.13$

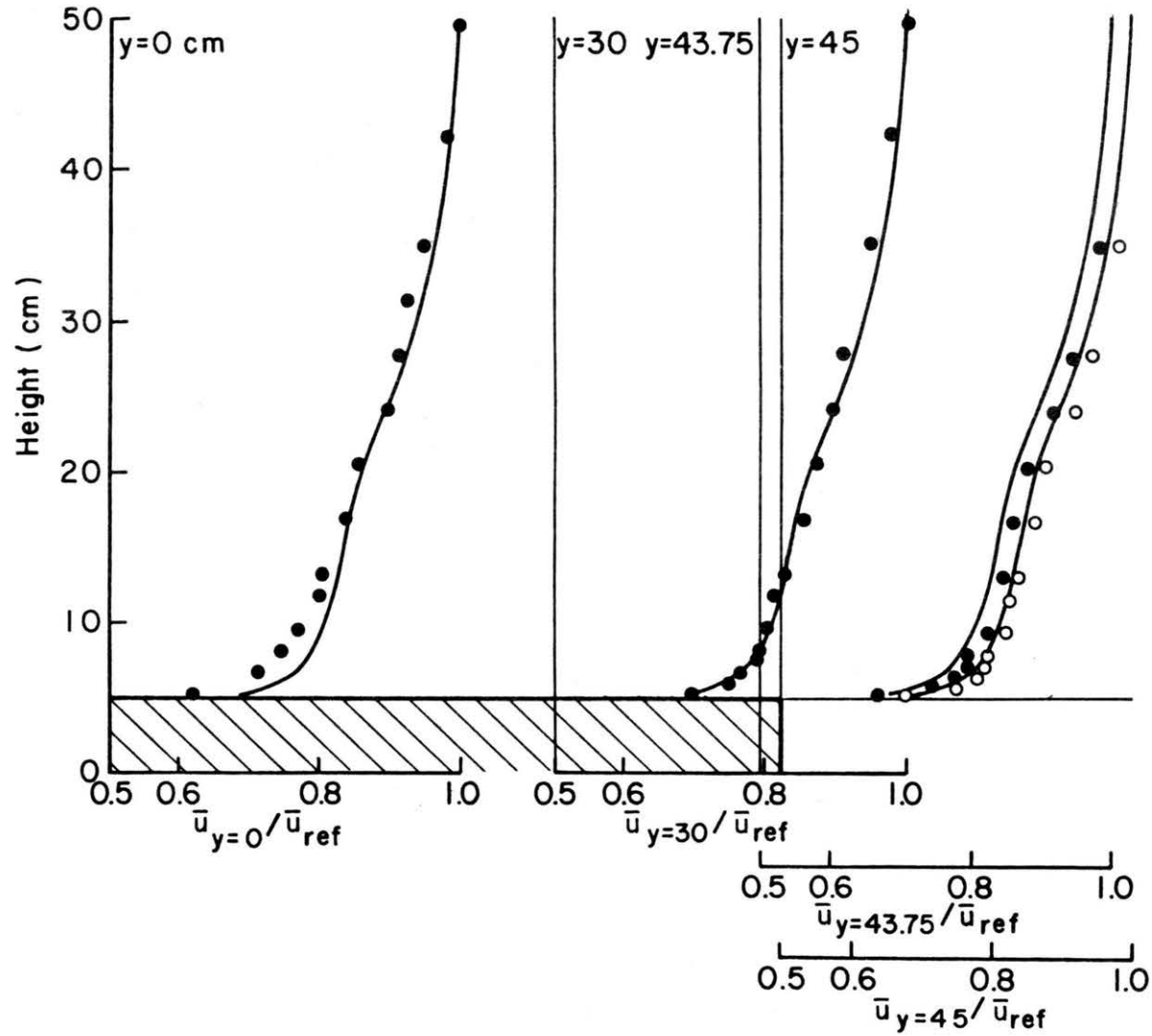


Figure 4-16. Mean Velocity Profiles Over a Ridge With Finite Width
 $W/h = 9$ $h/\delta = .1$ $h/L_u = 1/4$ and $h/L_d = 1/3$

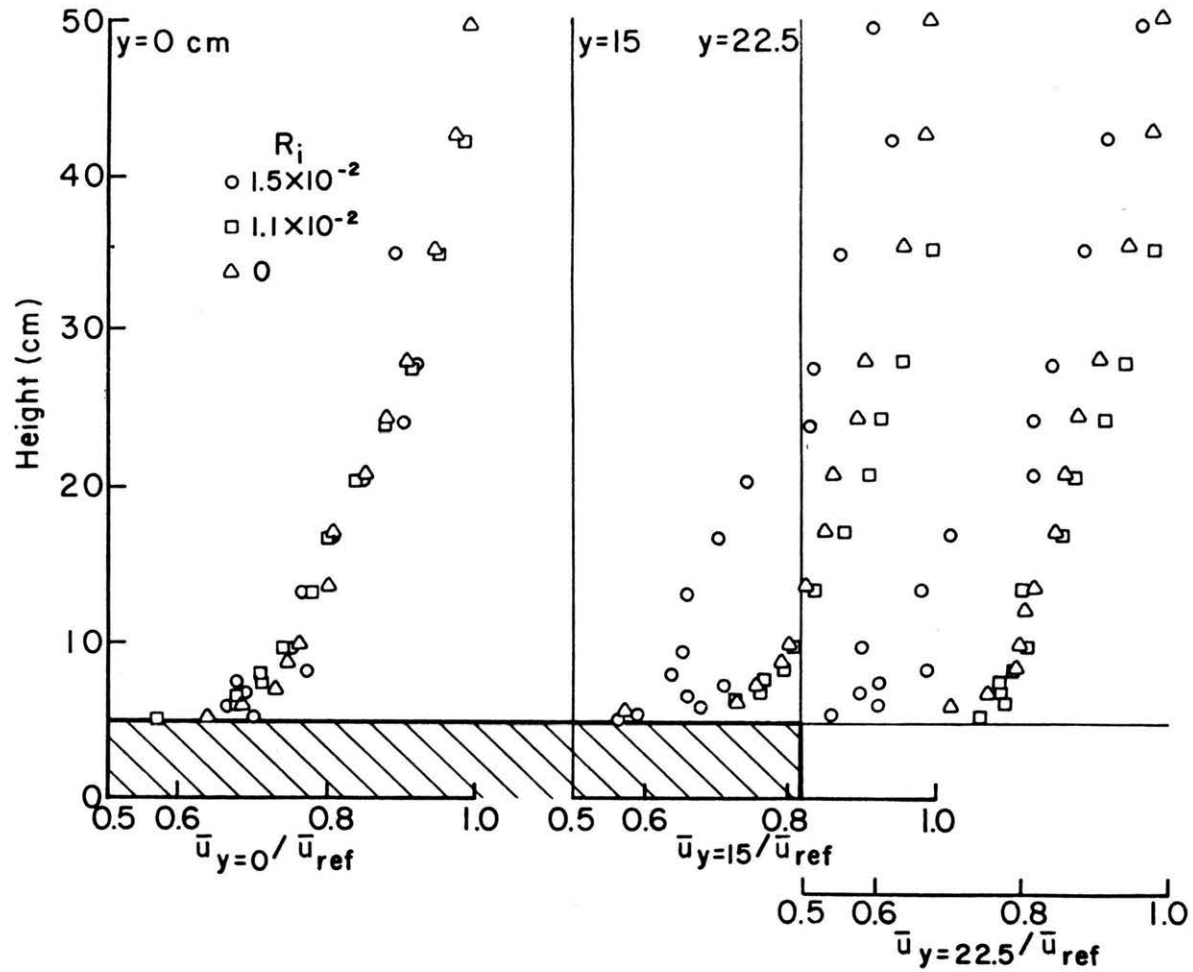


Figure 4-17. Mean Velocity Profiles Over a Ridge With Finite Width as Affected by a Stable Thermal Stratification

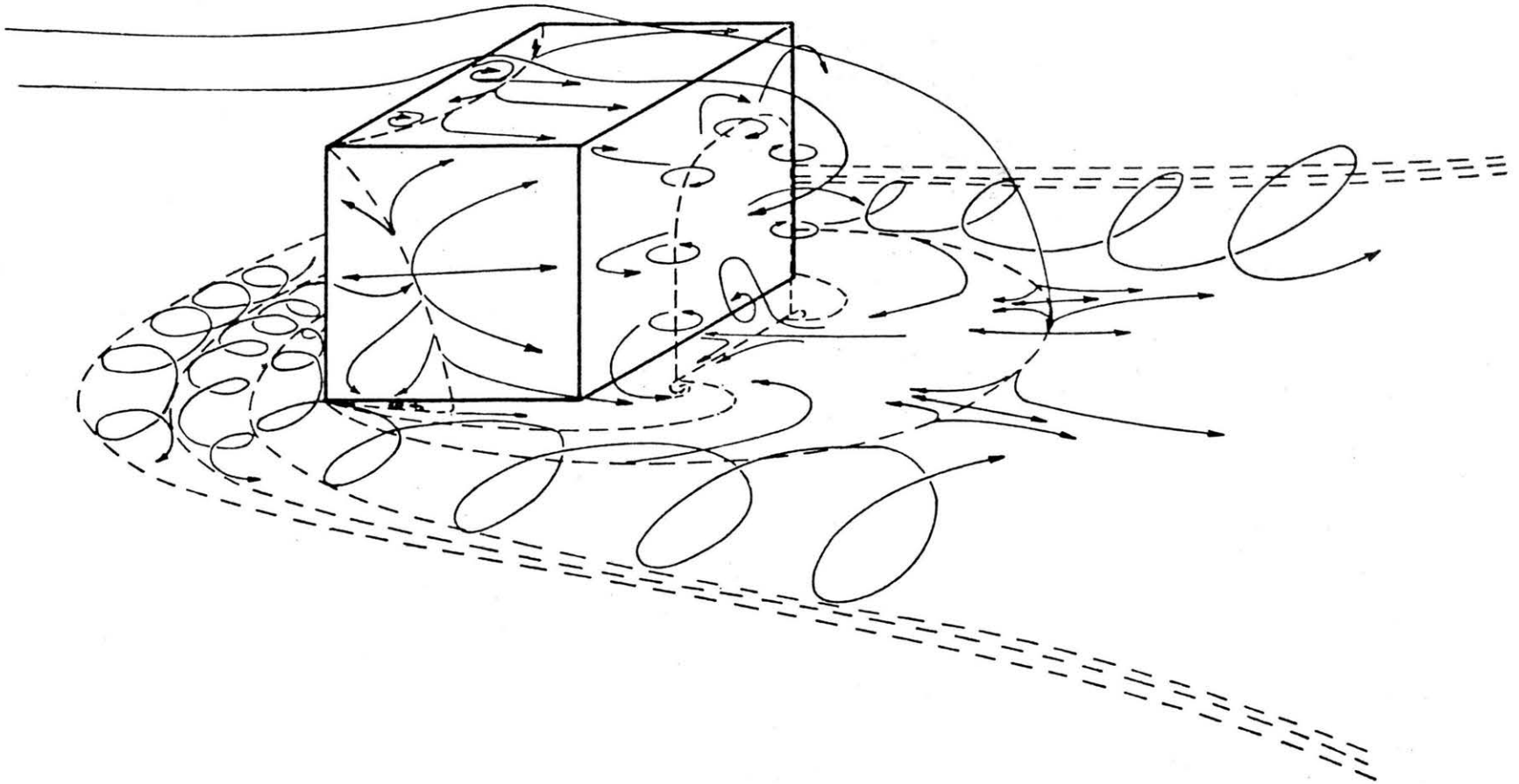


Figure 4-18. Flow Pattern Around a Rectangular Block With Reattachment of the Free Shear Layer Woo, Peterka and Cermak (1978)

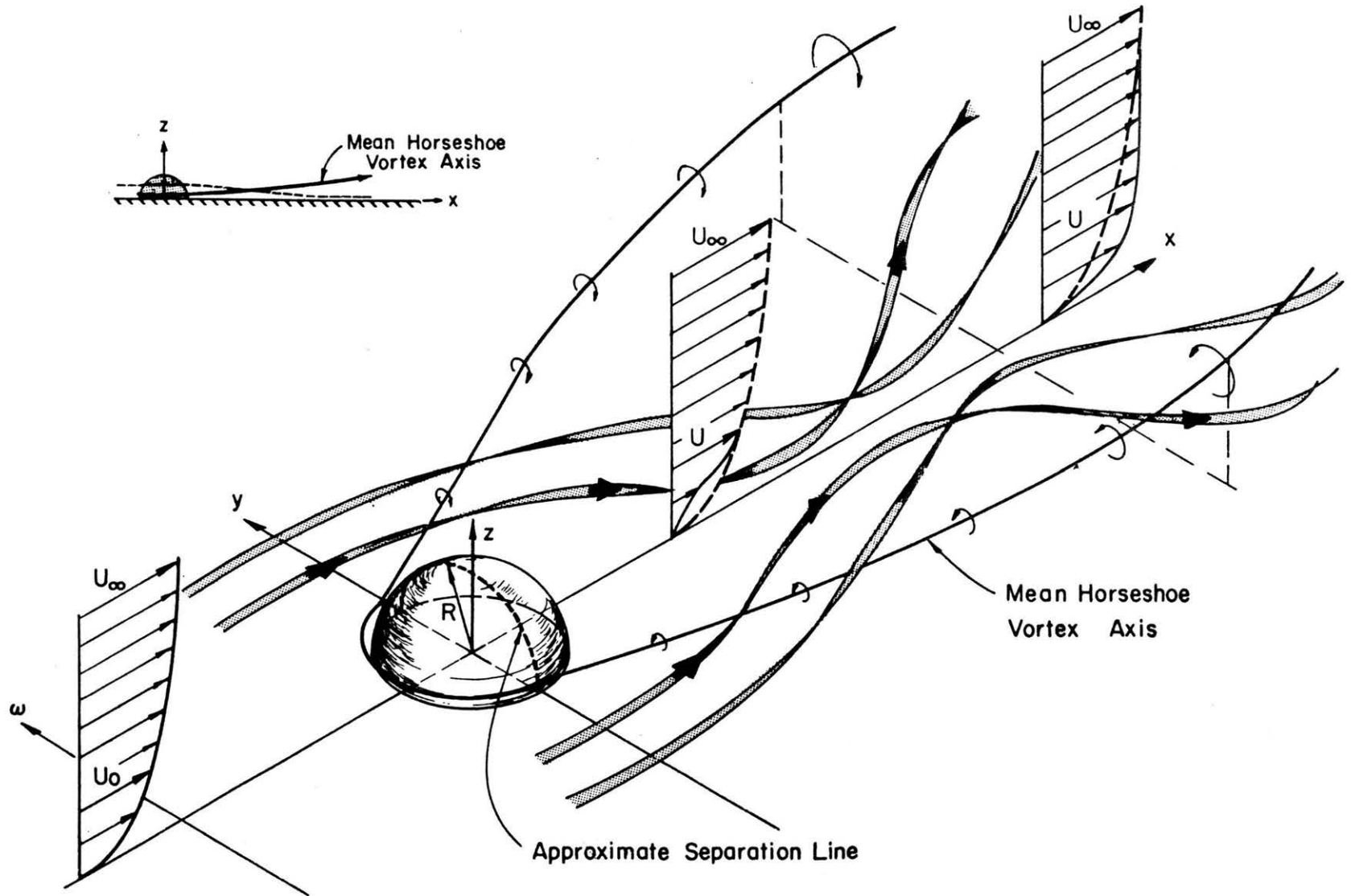


Figure 4-19. Schematic of the Vortex-Containing Wake of a Hemisphere, Hansen and Cermak (1975)

F: FENCE
 I: 2.5 ENTRANCE CONTRACTION
 S: SCREENS
 H1: HONEYCOMB 6 cm D. x 25 cm
 H2: HONEYCOMB 1 cm D. x 7.5 cm
 G: GRID 4 cm x 2 cm BARS SPACED ~13 cm x 17 cm

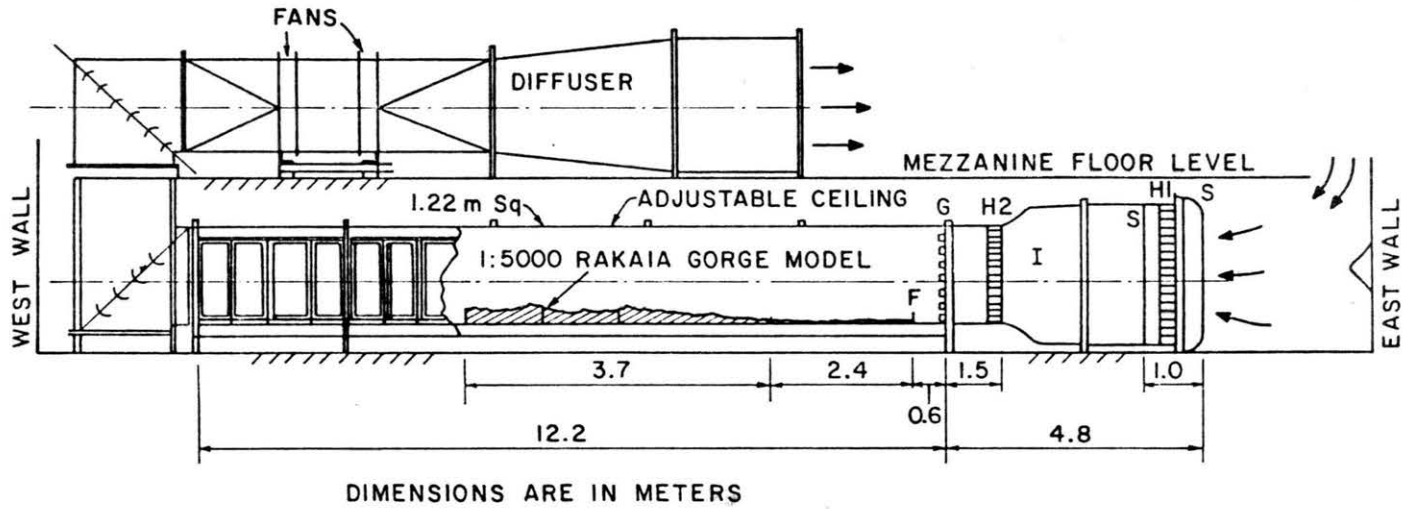


Figure 4-20. Boundary layer wind tunnel, Department of Mechanical Engineering,
 University of Canterbury.



Rakaia Gorge -
Terraced Model



Rakaia Gorge -
Contoured Model With
Pipe Cleaner Shelterbelts
(Polystyrene bead drifts)



Figure 4-21. Models of Rakaia River Gorge region looking northwest.

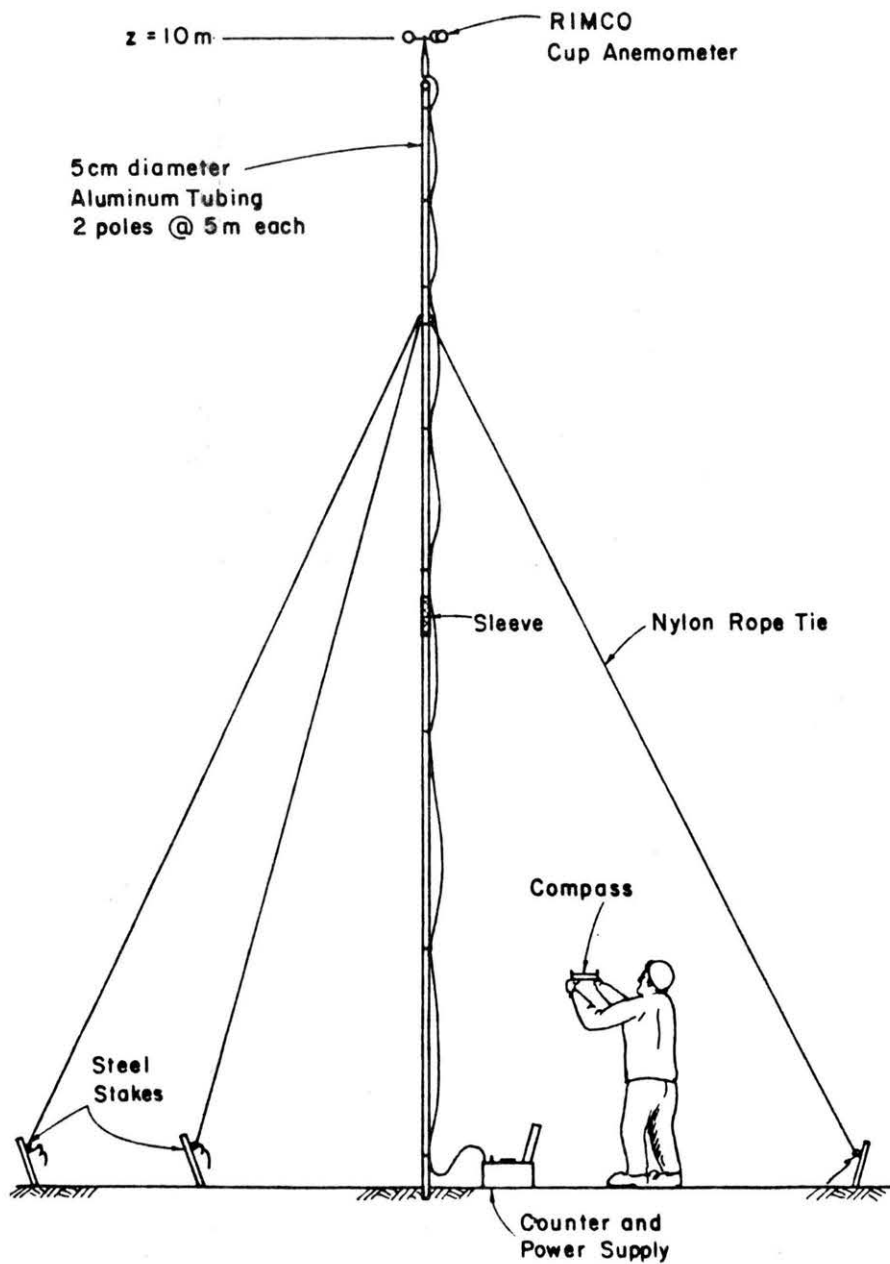


Figure 4-22. Portable tower and anemometer
 Rakaia River Gorge field experiment

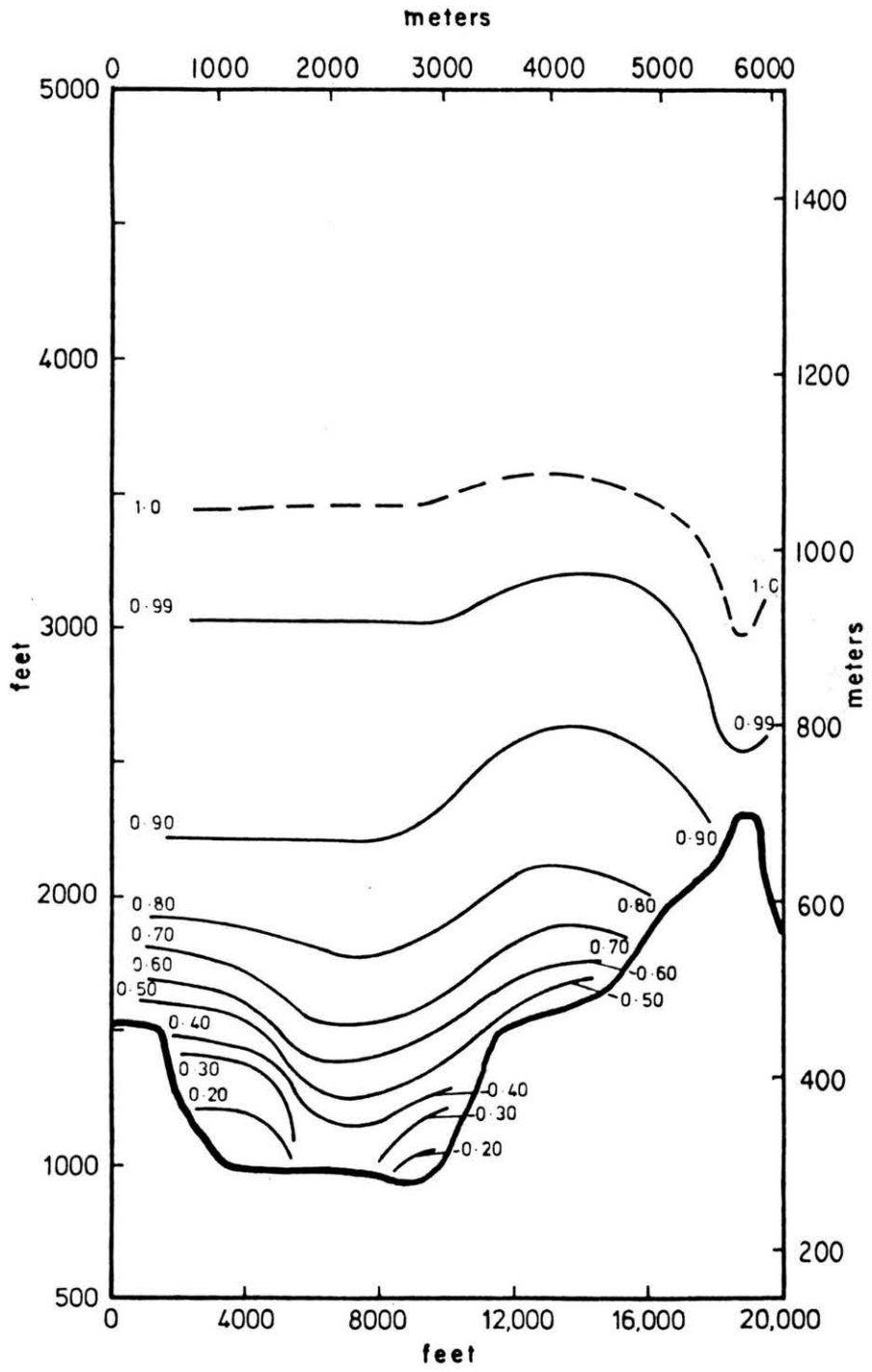


Figure 4-23. Vertical section G-G isotachs, terraced model.

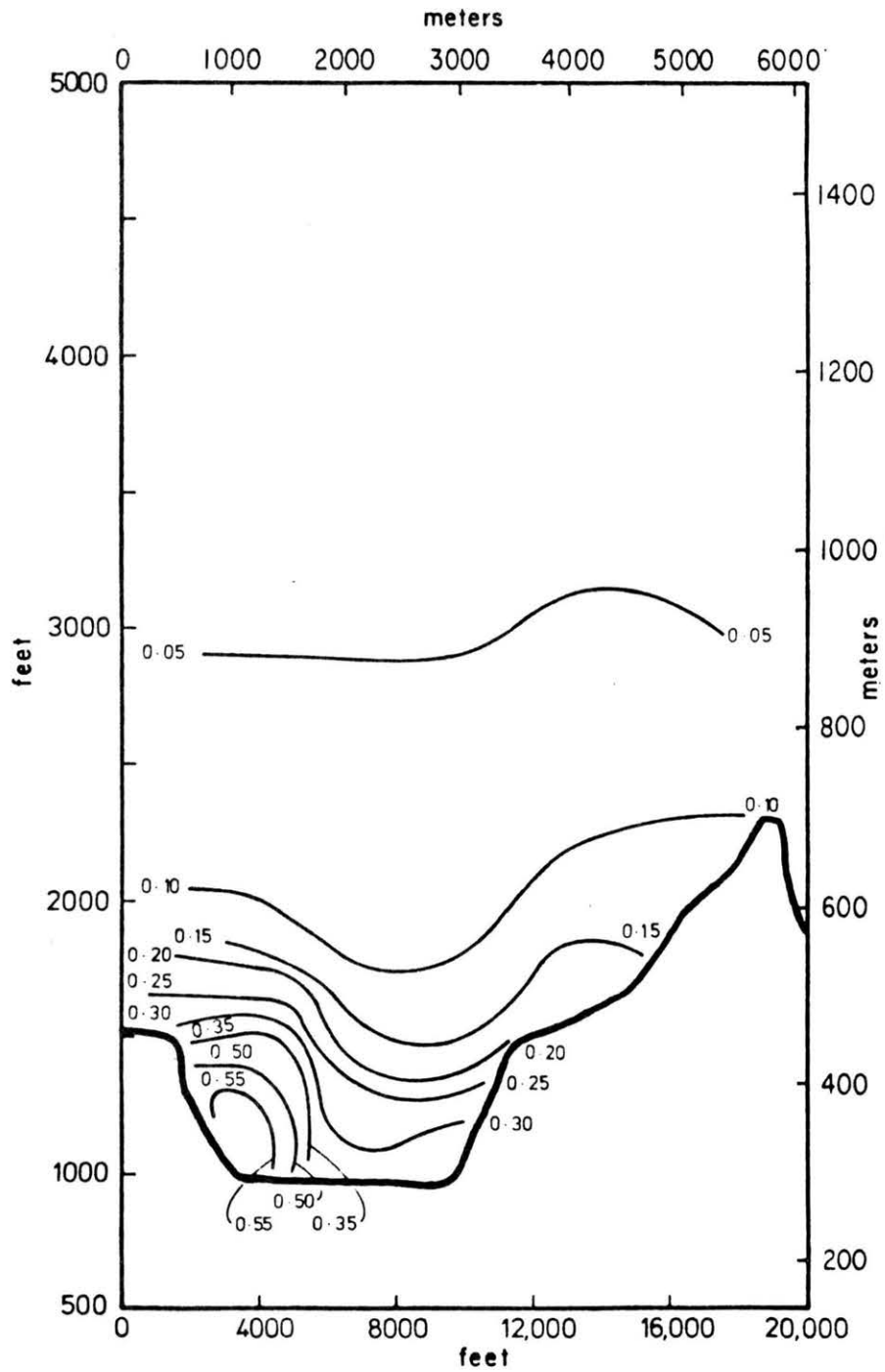


Figure 4-24. Vertical section G-G isoturbs, terraced model.

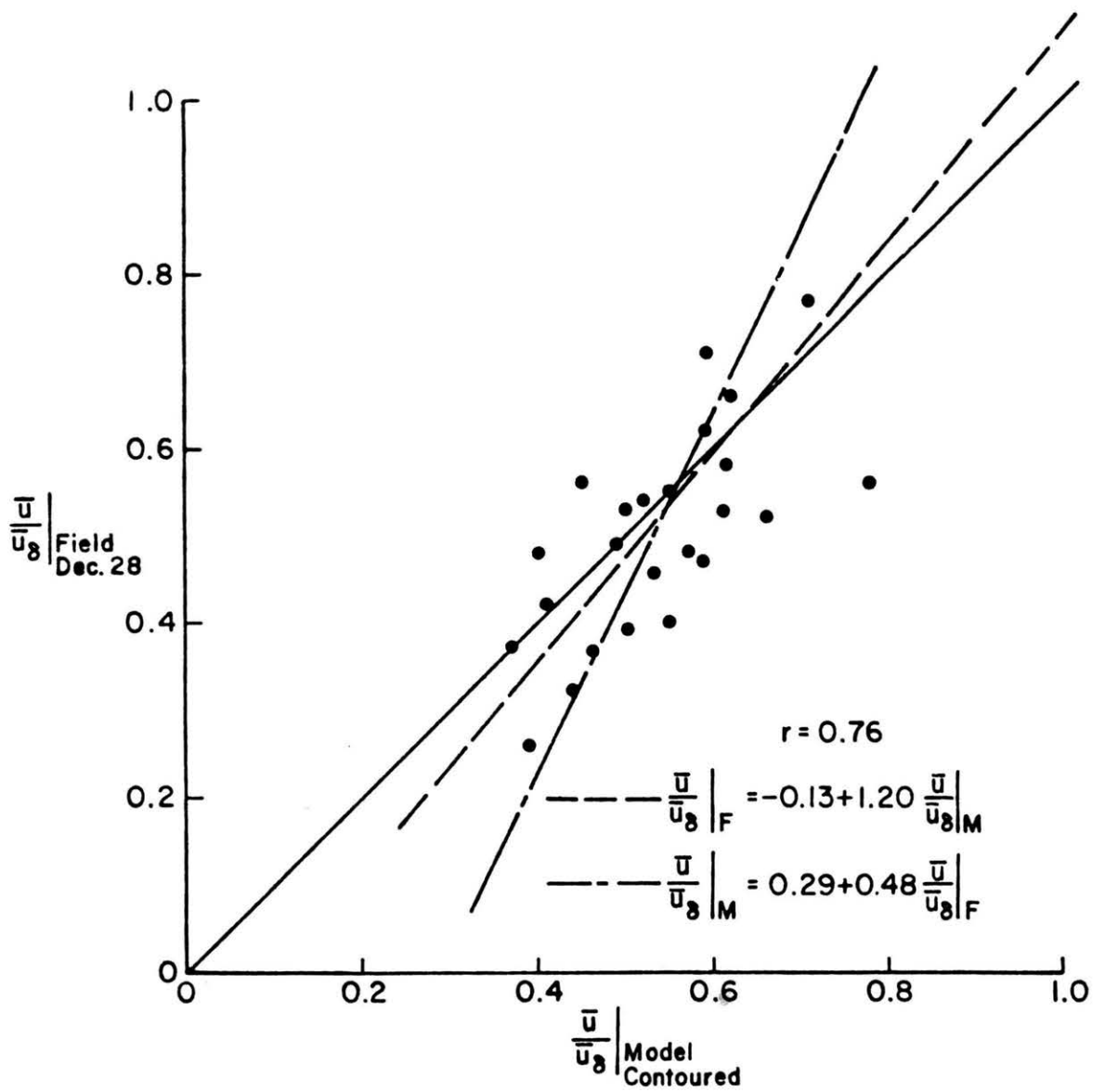


Figure 4-25. Scatter diagram field test data, December 28 versus contoured model data

5.0 SUMMARY AND RECOMMENDATIONS

Five objectives of this research program were outlined in Section 1.2 and are considered sequentially in order to draw final conclusions concerning the implications of this experimental program for WECS siting procedures.

5.1 FLOW CHARACTERISTICS PERCEIVED FROM GENERIC HILL AND RIDGE STUDIES

The first objective was to determine local wind profiles and turbulence over two- and three-dimensional idealized hills or ridges when influenced by topographical profile, surface roughness, stratification, slope or aspect ratio, and downslope hill configurations.

When one considers the results of this investigation in the context of prior experience, it is found that physical models have revealed that:

1. Except for a very small region near the surface where a low jet seems to appear, the gradient of velocity with height at ridge crest is very small for most cases studied. The results confirm the criteria preferred by Frenkiel. The variation of velocity with height above the crest tends to follow a power law with a small exponent. Thus the variation of amplification factor, A , or fractional speedup, ΔS with height may be estimated if a single value of A or ΔS at some reference height is available.

The functional variation of $A(z)$, Equation 4-10, represents results found during the wind-tunnel program within experimental accuracy. The amplification factor has been correlated with topographical parameters of slope, surface roughness, etc. Hence an ad hoc method exists to predict hill or ridge top profiles given upwind climatological data. This correlation is, of course, limited to the parameter domain for which measurements were actually performed. As h/δ decreases, or strong stable or unstable stratification occurs, the predictions may err.

Analytically it was predicted by Jackson and Hunt (1975) that the fractional speedup factor, ΔS , may be an appropriate measure of speedup for low slope hills (<1:10 to 1:20) since it was not expected to vary with height quite as much as the speedup factor, S . During laboratory measurements over steeper hills (>1:10) both amplification factor, A , and fractional speedup factor, ΔS , were found to vary substantially with height.

2. For measurements performed over a series of hill shapes, but with equivalent average slopes, when separation was absent it was determined only slight changes of fractional speedup occurred. Nonetheless, if the hill has an extended region of gentle slope (flat) near the crest then a wide flat top results in much reduced values of A and ΔS .

3. Separation at hill crest is a function of both upwind and downwind slopes. Hence, whereas a symmetric triangular shaped hill may separate an escarpment with the same upwind slope might not. Generally a highly turbulent upwind profile characterized by large power law coefficient ($\alpha > 0.2$) will not separate unless hill slopes are extreme ($h/L < 1$); nonetheless local surface features at hill crest (flat or curved surfaces versus a salient edge) may induce separation for any given approach velocity profile. Separation generally reduces crest velocities, increases turbulence, and reduces negative pressure values at the summit.
4. Three-dimensional hills did not produce speedup effects as large as similar section ridges oriented perpendicular to the wind. Speedup ratios of the order of 0.6 were observed for the three-dimensional hill as compared to 1.0 over a two-dimensional ridge. Away from the crest differences were often even larger. Thus, for neutral flow in unidirectional flow regime conditions over a three-dimensional hill are not as desirable for wind power as the comparable two-dimensional ridge.
5. Tests made over one quarter and one half span models suggest ridge end effects are limited to the immediate vicinity for neutral flow environments. Thus there may be no critical requirement that a wind power unit be mounted near the centerline of a finite aspect ratio ridge.
6. Measurements and theory suggest that mild stable or unstable stratification will decrease or increase wind velocities at hill crests respectively for the equivalent approach velocity profile. This, of course, assumes no elevated inversion or "lid" lies directly above hill crest. When air flow is constrained to move between a ridge and an elevated inversion then exactly opposite wind effects are likely. On the other hand, stable stratification tends to further reduce turbulence intensity over that observed with neutral flow fields.
7. As the fluid slows in the forward stagnation region, turbulence production near the wall decreases and the maximum appears to move outward. Near the summit the velocity gradient is large only near the surface, thus only pre-existing turbulent energy is convected over the ridge at most heights. Since longitudinal velocity on a given streamline has increased local turbulent intensity decreases by almost one-half near the surface up to $z \approx 2h$. This picture of turbulent energy rapidly convected through a flow convergence and divergence for moderate hills supports the contention by J. C. R. Hunt (1973) that turbulent diffusion from the surface region should be small and turbulent character may be determined

by the rapid distortion of vortex lines as fluid is convected over an abrupt bluff body.

The actual change in the turbulence appears to be that which could have been predicted for turbulence undergoing a contraction or strain. The turbulent component in the direction of the mean flow is reduced in magnitude near the surface, while the vertical component of turbulence is slightly increased. Since it is expected that the horizontal component of the turbulence would be the most critical in wind turbine design, the results are considered to indicate that the turbulence over the upstream face of the small, two-dimensional ridges will not be a problem.

8. Contour plots of lines of constant static pressure over ridges reveal a near symmetrical pressure distribution over shallow hills, while steeper hills display asymmetrical distributions due to flow separation. The symmetric distributions show significant changes out to distance of $\sim L$ from the crest, while the asymmetric case shows pressure changes well beyond $\sim L$ from the crest. Inviscid flow models reproduce these variations over shallow hills quite accurately. This demonstrates that for shallow hills ($h/\delta < 0.2$ and $h/l > 0.05$) there is little interaction between the turbulence, the topography, and the mean velocity other than than expected from the simple Bernoulli equation.

The concepts reviewed above are generalizations based on far more detailed information available in Bouwmeester et al. (1978). The reader is referred to this report for magnitudes of constants and specific predictive relations or correlations.

5.2 SIMILITUDE CONSTRAINTS

The second objectives addressed was to identify pertinent similarity criteria for physical modeling of flow over terrain. The third objective required a simulation verification exercise between a specific laboratory/full scale experiment. A review of previous physical modeling experience provided an index of 36 case studies relevant to terrain modeling techniques. Sixteen investigations included some field comparables. None, however, were designed to specifically test various model alternatives. Criteria for laboratory simulation of wind characteristics over irregular terrain in general are summarized in Section 3.0. Specific details of the simulation constraints on the Rakaia River Gorge verification exercise may be found in Section 4.0.

It would appear that the conventional simulation wisdom developed in the past few years is appropriate for physical modeling of flow over complex terrain. Since the flow region of interest is usually in

the lowest surface layer ($z < 100$ m) for WECS siting, great care must be taken that horizontal nonhomogeneities in roughness and terrain are faithfully reproduced. Specific conclusions suggest that:

1. An undistorted model at scales as large as 1:5000 permits resolution of velocity and turbulence details adequate to discern preferable WECS sites;
2. A wide range of scales and meteorological conditions may reasonably be simulated in existing boundary layer wind tunnel facilities; (see Performance Envelope Figure 3-1.)
3. To produce equivalent wind speeds near ground level require accurate reproduction of surface roughness, shape, and vegetation. Hence terraced models, adequate for certain dispersions simulation, are not appropriate for other purposes such as WECS site analysis; and
4. Current meteorological data in complex terrain is not yet adequate to stipulate inflow conditions to either numerical or physical models with confidence. Hence an adequate approach flow length must be provided to allow the surface layer to come to an equilibrium with underlying terrain undulations.

5.3 NUMERICAL MODELING IMPLICATIONS PERCEIVED FROM LABORATORY DATA

A fourth objective of this physical modeling program was to interpret the results in terms of their implications for WECS siting methodologies. Numerical models play an important part in the set of extrapolation tools proposed by WECS meteorological program managers for site selection. A number of the results of this measurement program may provide guidance when preparing such a numerical model program. Specific considerations are:

1. Recent field measurements as well as this measurement program suggest wind velocities in the lower surface layer are extremely sensitive to local variations in topography slope or roughness. Hence a numerical siting model should incorporate the effects of surface nonhomogeneities by having grid resolution sufficient to resolve horizontal changes at a scale of about 100 to 500 meters.
2. For a single shallow ridge or hill in deep boundary layers turbulence plays a significant role in momentum transport and profile distortion only very near the surface. Indeed over the majority of the flow region an inviscid rotational analysis will reproduce 99% of the mean velocity field behavior

if one can estimate the upwind velocity profile. Hence a complex primitive equation analysis may be unnecessary for these cases. Indeed an inviscid rotational solution of a given domain may well represent an accurate starting solution for the full equations of motion.

3. Vertical and horizontal pressure gradients both play an important part in the development of surface profiles and the occurrence of separation over hills and ridges; hence it is unlikely that a numerical or analytical analysis based upon the boundary layer equations (which assume zero vertical pressure gradients) will provide adequate physics to predict velocity or turbulence fields.
4. During flow over shallow hills or ridges in deep boundary layers the outer part of the turbulent shear stress distribution requires a very long time or distance before it can alter. It is expected then that turbulence cannot change appreciably. The actual change in turbulence which occurs appears to be that which could have been predicted for eddies undergoing a contraction or strain. Solution of a total turbulent kinetic energy equation by numerical means reveals that production and dissipation play minor roles--only advection and diffusion very near the hill surface seem significant. In any event most changes are minor as long as separation does not exist.
5. Separation upwind or downwind from a hill or escarpment crest dramatically changes the entire flow field. A numerical model which fails to incorporate the location or potential for separation will be highly misleading.

5.4 RECOMMENDATIONS FOR PHYSICAL MODELING METHODOLOGY FOR WECS SITING

The fifth objective undertaken was to consider under which circumstances physical modeling of a specific site is appropriate during a WECS siting strategy. The two constraints which are pertinent are those of characteristic time and space scales and economics.

Wind characteristics are required for WECS design and performance evaluation, siting methodologies, and WECS operational or management decisions (see Elderkin and Wendell, 1977). At this time questions still exist concerning windmill wake interactions, blade fatigue induced by flow separation over nearby topographical features such as cliffs or escarpments, and wind profiles over complex terrain. As such lore accumulates, the experience will be recorded in siting and operational handbooks such that only site unique situations need be examined in detail.

Not all scales in space and time are amenable to physical modeling. Figure 3-4 superimposes our recommendations concerning the potential domain of physical modeling upon the judgement proposed by Drake (1977). It is in the domain inclusive from 10 m to 10 km and 1 minute to 3 hours that maximum credibility exists. In this regime physical models may confidently be used to check some numerical models before their broader scale application.

Lindley (1977) proposes from 45 to 450 MW of installed WECS at Kahuku Point, Oahu, and suggests a baseline system for the California aqueduct along the Tehachaipi mountains close to 1500 MW. 75 MW clusters of windmills were proposed by Lindquist and Malver (1977) for use in Minnesota. Other large systems have been proposed for the mountains of New Zealand, Sweden, and Oregon in the United States. Once site selection has been constrained to regions of less than 10 km lateral scale, physical modeling may provide the fine scale calibration of sites that climatological or numerical models cannot obtain.

REFERENCES

- Abe, Masanao (1941) "Mountain Clouds, Their Forms and Connected Air Currents, Part II," Bull. Centr. Met. Obs, Japan 7 (3), pp. 93-145.
- Archibald, P. B. (1973) "An Analysis of the Winds of Site 300 as a Source of Power," UCLR-51469, Lawrence Livermore Laboratories, University of California, Livermore, California.
- Batchelor, G. K. (1953) "The Conditions for Dynamic Similarity of Motions of a Frictionless Perfect-Gas Atmosphere," Quarterly Journal of Royal Meteorological Society, Vol. 79, pp. 224-235.
- Bernstein, A. B. (1965) "Dimensional Analysis Applied to the Wind Distribution in the Planetary Boundary Layer," Monthly Weather Review, Vol. 93, No. 10, pp. 579-585.
- Bouwmeester, R. J. B., Meroney, R. N., and Sandborn, V. A. (1978) "Sites for Wind-Power Installations: Wind Characteristics Over Ridges," Colorado State University, Research Report No. CER77-78 RJBB-RNM-VAS51.
- Bowen, A. J., and Lindley, D. (1974) "Measurements of the Mean Wind Flow Over Various Escarpment Shapes," 5th Australian Conference on Hydraulics and Fluid Mechanics, Christchurch, New Zealand, December 9-13, 9 p.
- Bowen, A. J., and Lindley, D. (1977) "A Wind Tunnel Investigation of the Wind Speed and Turbulence Characteristics Close to the Ground Over Various Escarpment Shapes," Boundary-Layer Meteorology, 12, p. 259-271.
- Briggs, J. (1963), "Airflow Around a Model of the Rock of Gibraltar," Meteorological Office Scientific Paper No. 18, p. 20.
- Cermak, J. E. et al. (1966) "Simulation of Atmospheric Motion by Wind-Tunnel Flows," Technical Report for DA-AMC-28-043-G20 Fluid Dynamics and Diffusion Laboratory, Colorado State University, Fort Collins, Colorado, Report No. CER66JEC-VAS-ESP-GJB-HC-RNM-SI17.
- Cermak, J. E. and Peterka, J. (1966) "Simulation of Wind Fields Over Point Arguello, California, by Wind-Tunnel Flow Over a Topographic Model," Colorado State University, Fort Collins, Colorado, Report No. CER65JEC-JAP64.
- Cermak, J. E. (1970) Proceedings, Symposium on Wind Effects on High-Rise Buildings, Northwestern University, Evanston, Illinois, March 23.

REFERENCES (continued)

- Cermak, J. E. and SethuRaman, S. (1973) "Stratified Shear Flows Over a Simulated Three-Dimensional Urban Heat Island," Project THEMIS Technical Report No. 23, Colorado State University, Fort Collins, Colorado Report No. CER73-74SS-JEC4, AD-767-063.
- Cermak, J. E. (1975) "Applications of Fluid Mechanics to Wind Engineering," 1974 Freeman Scholar Lecture, ASME Journal of Fluids Engineering, Vol. 97, Series 1, No. 1, March, Colorado State University, Fort Collins, Colorado, Report No. CEP74-75JEC7.
- Cermak, J. E. and Mutter, D. G. (1978) "Physical Modeling of Atmospheric Transport of Stack Emissions at Kahe Electrical Generating Plant, Oahu, Hawaii," Colorado State University, Fort Collins, Colorado, Report No. CER77-78JEC-DGM-28a, 55 pp.
- Chang, S. C. (1966) "Velocity Distributions in the Separated Flow Behind a Wedge-Shaped Model Hill," Technical Report, Grant DA-AMC-28-043-G20, March, Colorado State University, Fort Collins, Colorado, Report No. CER65SCC66, 101 pp.
- Cherry, N. J. (1976), "Wind Energy Research Survey of New Zealand, Preliminary Analysis of Meteorological Data," New Zealand Energy Research and Development Committee, Report No. 8, Lincoln College, Christchurch, New Zealand, 31 pp.
- Chien, H., Meroney, R. N., Sandborn, V. A., and Bouwmeester, R. J. B. (1978) "Preliminary Measurements of Flow Over Model, Three-Dimension Hills," Fluid Dynamics and Diffusion Laboratory, Colorado State University Research Memorandum No. 29, CEM-77-78HCC-VAS-RNM-RJBB29, 34 pp.
- Clements, W. E. and Barr, S. (1976) "Atmospheric Transport and Dispersal at a Site Dominated by Complex Terrain," Proceedings of 3rd Symposium on Atmospheric Turbulence, Diffusion and Air Quality, Raleigh, North Carolina, October 19-22, 1976, pp. 430-435.
- Corotis, R. B. (1977) "Stochastic Modeling of Site Wind Characteristics," Department of Civil Engineering, Final Report, ERDA/PLO/2342-77/2, Northwestern University, 143 pp.
- Cook, N. J. (1977/1978) "Determination of the Model Scale Factor in Wind-Tunnel Simulations of the Adiabatic Atmospheric Boundary Layer," Journal of Industrial Aerodynamics, Vol. 2, pp. 311-321.
- Counihan, J. (1969) "An Improved Method for Simulating an Atmospheric Boundary Layer in a Wind Tunnel," Atmopsheric Environment, Vol. 3, pp. 197-214.

REFERENCES (continued)

- Counihan, J. (1973) "Simulation of an Adiabatic Urban Boundary Layer in a Wind Tunnel," Atmospheric Environment, Vol. 7, pp. 673-689.
- Counihan, J. (1973) "Flow Over Two-Dimensional Hills and Plateau in Simulated Boundary Layer Flow," Central Electric Research Laboratories, Leatherhead, Surrey, United Kingdom, Laboratory Note No. RD/L/N277/73, 17 pp.
- Counihan, J. (1975) "Review Paper: Adiabatic Atmospheric Boundary Layers: A Review and Analysis of Data From the Period 1880-1972," Atmospheric Environment, Vol. 9, pp. 871-905.
- Davidson, B. (1961) "Valley Wind Phenomena and Air Pollution Problems," Journal of the Air Pollution Control Association, Vol. 11, No. 8, pp. 364-369.
- Davidson, Ben, Gerbier, N., Pagagionakis, S. O. and Rijkvort, P. G. (1964) "Sites for Wind-Power Installations," W.M.O. Technical Note 63, WMO-NO156, TP76, 38 pp.
- de Bray, B. G. (1973) "Atmospheric Shear Flows Over Ramps and Escarpments," Industrial Aerodynamics Abstracts, 5, September-October, 4 p.
- Derickson, R. G. and Meroney, R. N. (1977) "A Simplified Physics Airflow Model for Evaluating Wind Power Sites in Complex Terrain," Proceedings of Summer Computer Simulation Conference, July 18-20, 1977, Chicago, Illinois, 14 pp.
- Drake, R. L. (1977) "Site Selection Techniques and Methodologies for WECS" Third Wind Energy Workshop, CONF770921/2, pp. 635-645.
- Field, J. H. and Warden, R. (1929) "A Survey of Air Currents in the Bay of Gibraltar, 1929-1930," Geophysics Memoirs, No. 59, Published by Her Majesty's Stationery Office, p. 84.
- Fosberg, M. A., Marlott, W. E., and Krupnak, L. (1976) "Estimating Airflow Patterns Over Complex Terrain," USDA Forest Service Research Paper RM-162, Rocky Mountain Forest and Range Experiment Station, Fort Collins, Colorado, 16 pp.
- Freeston, D. H. (1974) "Atmospheric Shear Flows Over Ramps and Escarpments," 5th Australian Conference on Hydraulics and Fluid Mechanics, Christchurch, New Zealand, December 9-13, 8 p.
- Frenkiel, J. (1962-1963) "Wind Profiles Over Hills (In Relation to Wind Power Utilization)," 88, pp. 156-169, 89, pp. 281-283.

REFERENCES (continued)

- Frenkiel, J. (1963) "Gusts Over Hills (In Relation to Wind-Power Utilization)," Quarterly Journal of the Royal Meteorological Society, 89, pp. 281-283.
- Garrison, J. A. and Cermak, J. E. (1968) "San Bruno Mountain Wind Investigation--A Wind-Tunnel Model Study," Colorado State University, Fort Collins, Colorado, Report No. CER67-68JEC-JAG58.
- Golding, E. W. (1955) The Generation of Electricity by Wind Power, Philosophical Library, New York, 318 pp.
- Graham, N. E., Taylor, G. H., Hovind, E. L., Petersen, R. L., Cermak, J. E., and Sinclair, P. C. (1968) "An Analysis of Terrain Induced Aerodynamic Disturbances Near the Kingston Steam Plant, Tennessee," North American Weather Service, Draft Report AQ-78-22.
- Halitsky, L., Tolciss, J., and Kaplan, E. L. (1962) "Wind Tunnel Study of Turbulence in the Bear Mountain Wake," Quarterly Progress Reports No. 1, 2, 3, and 4, Contract No. DA 36-039 SC-89081, Department of Meteorology and Oceanography, New York University.
- Hansen, A. Craig, and Cermak, J. E. (1975) "Vortex-Containing Wakes of Surface Obstacles, Colorado State University Report No. CER75-76ACH-JEC16, 1963 p., Fort Collins, Colorado.
- Hardy, D. M. (1977) "Wind Studies in Complex Terrain," American Wind Energy Association Conference, Boulder, Colorado, May 11-14, 1977, 38 p.
- Haugen, Duane A., ed., (1973) Workshop on Micrometeorology, American Meteorological Society, Boston, Massachusetts, 392 pp.
- Hawthorne, W. R. and Martin, M. E. (1955) "The Effect of Density Gradient and Shear on the Flow Over a Hemisphere," Proc. Royal Soc. A, Vol. 232, pp. 184-195.
- Hewson, E. Wendell, et al. (1973) "Wind Power Potential in Selected Areas of Oregon," Oregon State University (PUD73-1).
- Hidy, G. M. (1967) "Adventures in Atmospheric Simulation," Bulletin of American Meteorological Society, Vol. 48, pp. 143-161.
- Hoxit, L. R. (1973) "Variability of Planetary Boundary Layer Winds," Department of Atmospheric Science, Colorado State University, Paper No. 199, 157 pp.

REFERENCES (continued)

- Hsi, G., Binder, G. J., and Cermak, J. E. (1968) "Topographic Influences on Wind Near Green River, Utah," Technical Report, Grant DA-AMC-28-043-65-G20, for Atmospheric Science Laboratory, White Sands Missile Range, Colorado State University, Fort Collins, Colorado, Report No. CER67-68GH-GJB-JEC54.
- Huang, C. and Nickerson, E. C. (1972) "Numerical Simulation of Wind, Temperature, Shear Stress and Turbulent Energy Over Non-Homogeneous Terrain," Colorado State University, Fort Collins, Colorado, Report No. CER71-72CH-ECN23, 276 p.
- Huber, Alan H., Snyder, W. H., and Lawson, R. E. (1976) "Stack Placement in the Lee of a Mountain Ridge - A Wind Tunnel Study" Environmental Sciences Research Lab, Research Triangle Park, N. C. 44 p.
- Hunt, J. C. R. (1973) "A Theory of Turbulent Flow and Two-Dimensional Bluff Bodies," J. Fluid Mechanics 61 Part 4, pp. 625-706.
- Jackson, P. S. (1975) "A Theory for Flow Over Escarpments," Ministry of Works and Development, New Zealand, 8 p.
- Jackson, P. S. and Hunt, J. C. R. (1975) "Turbulent Wind Flow Over a Low Hill," Quarterly Journal of the Royal Meteorological Society, 101, pp. 292-955.
- Kahawita, R. A. and Meroney, R. N. (1973) "That Stability of Parallel, Quasi-Parallel, and Stationary Flows," Colorado State University, Fort Collins, Colorado, Report No. CER73-74RK-RNM12, 162 p.
- Kitabayshi, K. K. (1977) "Wind Tunnel and Field Studies of Stagnant Flow Upwind of a Ridge," Journal of the Meteorological Society of Japan, Vol. 55, No. 2, pp. 193-204.
- Kitabayshi, K. K., Orgill, M. M., and Cermak, J. E. (1971) "Laboratory Simulation of Airflow in Atmospheric Transport-Dispersion Over Elk Mountain, Wyoming," Technical Report prepared under Atmospheric Water Resources Research, Bureau of Reclamation, Contract No. 14-06-D-6455 and 14-06-6842, Colorado State University, Fort Collins, Colorado, Report No. CER70-71KKK-MMO-JEC65.
- Lin, J. T. and Binder, G. J. (1967) "Simulation of Mountain Lee Waves in a Wind Tunnel," Technical Report, Grant No. DA-AMC-28-043-65-G20, Colorado State University, Fort Collins, Colorado, Report No. CER67-68JTL-GJB24, AD-664-172.
- Lindley, C. A. (1977) "Wind Machines for the California Aqueduct," 3rd Wind Energy Workshop, Vol. 1, September 1977, Washington, D.C., CONF-770921, pp. 262-272.

REFERENCES (continued)

- Liu, H. T. and Lin, J. T. (1976) "Plume Dispersion in Stably Stratified Flow Over Complex Terrain," Flow Research, Inc., Report No. 57 or EPA-600/4-76-022, 54 pp.
- Long, R. R. (1954) "Some Aspects of the Flow of Stratified Fluids II, Experiments With a Two-Fluid System," Tellus, Vol. 6, pp. 97-115.
- Long, R. R. (1959) "A Laboratory Model of Airflow Over the Sierra Nevada Mountains," The Atmosphere and the Sea in Motion - The Rossby Memorial Volume, pp. 372-380.
- Ludwig, G. R. and Skinner, G. T. (1976) "Wind Tunnel Modeling Study of the Dispersion of SO₂ in Southern Alleghany County, Pennsylvania," Calspan Corporation, EPA Report 903/75-019.
- McVehil, G. E., Ludwig, G. R. and Sundaram, T. R. (1967) "On the Feasibility of Modeling Small Scale Atmospheric Motions," Cornell AeroLab Report ZB-2328-P-1, Buffalo, New York.
- Mari, Y., Miyata, K., and Mitsuta, Y. (1971) "A Case Study of Wind Over a Hilly Terrain," Bulletin of the Disaster Prevention Research Institute, Kyata University, Vol. 21, pp. 179-189.
- Marrs, R. W. and Marwitz, J. (1977) "Locating Areas of High Wind Energy Potential by Remote Observation of Eolian Geomorphology and Topography," 3rd Wind Energy Workshop, Vol. 1, September 1977, Washington, D.C., CONF-770921, pp. 307-317.
- Melbourne, W. H. (1977) "Development of Natural Wind Models at Monash University," 7th Australian Hydraulics and Fluid Mechanics Conference, Adelaide, Australia, December 5-9, pp. 190-194.
- Meroney, R. N. and Cermak, J. E. (1965) "Wind-Tunnel Modeling for Flow and Diffusion Over San Nicolas Island," Progress Reports for 4th and 5th Quarters, Contract No. 123 (61756) 50192A (PMR), Colorado State University, Fort Collins, Colorado.
- Meroney, R. N. and Chaudhry, F. H. (1972) "Wind Tunnel Site Analysis of Dow Chemical Facility at Rocky Flats, Colorado," Colorado State University, Fort Collins, Colorado, Report No. CER71-72RNM-FC45.
- Meroney, R. N., Cermak, J. E., Garrison, J. A., Yang, B. T., and Nayak, S. (1974) "Wind Tunnel Study of Stack Gas Dispersal at the Avon Lake Power Plant," Prepared under contract to Commonwealth Associates, Inc., April, Colorado State University, Fort Collins, Colorado, Report No. CER73-74RNM-JEC-BTY-SKN35.

REFERENCES (continued)

- Meroney, R. N., Cermak, J. E., and Yang, B. T. (1975) "Modeling of Atmospheric Transport and Fumigation at Shorelines," Boundary Layer Meteorology, Vol. 9, No. 1, pp. 69-90.
- Meroney, R. N., Cermak, J. E., and Garrison, J. A. (1975) "Wind Tunnel Study of Stack Gas Dispersal at Lansing Power Station, Units 1, 2, 3, and 4," Fluid Dynamics and Diffusion Laboratory, Colorado State University, Report No. CER74-75RNM-JEC-JAG28, 199 pp.
- Meroney, R. N., Sandborn, V. A., Bouwmeester, R., and Rider, M., (1976c) "Wind Tunnel Simulation of the Influence of Two-Dimensional Ridges on Wind Speed and Turbulence," Proceedings of International Symposium on Wind Energy Systems, St. John's College, Cambridge, England, September 7-9, 1976, Report No. CEP75-76RNM-VAS-RB-MR31.
- Meroney, R. N., Sandborn, V. A., Bouwmeester, R. J. B., and Rider, M. A. (1976a) "Sites for Wind-Power Installations: Wind-Tunnel Simulation of the Influence and Two-Dimensional Ridges on Wind Speed and Turbulence," Annual Report: First Year, NSF/RANN Contract GAER75-00702, Report ERDA/NSF-00702/75/T1, Report No. CER76-77RNM-VAS-RB-MAR5, 80 pp.
- Meroney, R. N., Sandborn, V. A., Bouwmeester, R. J. B., and Rider, M. A. (1976b) "Sites for Wind-Power Installations - Tabulated Experimental Data," Progress Report June-November 1976, ERDA Wind Energy Program Report ERDA/Y-76-S-06-2438/7611. Report No. CER76-77RNM-VAS-RB-MAR29, 60 pp.
- Meroney, R. N., Sandborn, V. A., Bouwmeester, R. J. B., and Rider, M. A. (1977) "Sites for Wind-Power Installations - Annual Report: Second Year," Department of Energy Report RLO/2438-77/1, Report No. CER77-78RNM-VAS-RB-MAR6, 186 pp.
- Meroney, R. N., Bowen, A. J., Lindley, D., and Pearse, J. R., (1978) "Wind Characteristics Over Complex Terrain: Laboratory Simulation and Field Measurements at Rakaia Gorge, New Zealand," Colorado State University Report No. CER77-78RNM29, May, 219 pp.
- Mery, P. (1969), "Reproduction en Similitude de la Diffusion dans la Cauche Limite Atmospherique," La Houille Blanche, No. 4 (Translation Air Poll. Tech. Inf. Cent. No. 1104).

REFERENCES (continued)

- Nemoto, S. (1961/1962) "Similarity Between Natural Wind in the Atmosphere and Model Wind in a Wind Tunnel," Papers in Meteorology and Geophysics, Tokyo:
Vol. 12, No. 1, pp. 30-52,
Vol. 12, No. 2, pp. 117-128,
Vol. 12, No. 2, pp. 129-154,
Vol. 13, No. 2, pp. 171-195 (1962).
- Orgill, M. M., Cermak, J. E., and Grant, L. O. (1971a) "Laboratory Simulation and Field Estimates of Atmospheric Transport-Dispersion Over Mountainous Terrain," Technical Report, Colorado State University, Fort Collins, Colorado, Report No. CER70-71MMO-JEC-LOG40, 302 pp.
- Orgill, M. M., Cermak, J. E., and Grant, L. O. (1971b) "Research and Development Technique for Estimating Airflow and Diffusion Parameters Related to the Atmospheric Water Resources Program," Final Report, Bureau of Reclamation Contract No. 14-06-D-6842, Colorado State University Report No. CER71-72MMO-JEC-LOG20, 111 pp.
- Orgill, M. M. (1977) "Survey of Wind Measurements Field Programs," Battelle, Pacific Northwest Laboratories, Report BNWL-2220, Wind-3, 53 pp.
- Orlonski, I. (1975) "A Rationale Subdivision of Scales for Atmospheric Processes," Bull. of Amer. Meteor. Soc., 56 (5), pp. 527-530.
- Orville, H. D. (1968) "Ambient Wind Effects on the Initiation of Cumulus Clouds Over Mountains," J. Atmos. Sci., Vol. 25, pp. 385-403.
- Petersen, R. L. and Cermak, J. E. (1977) "Atmospheric Transport of Hydrogen Sulfide From Proposed Geothermal Power Plants (Units 13, 14, 16, and 18) for the West Wind Direction," Fluid Dynamics and Diffusion Laboratory, Colorado State University, Research Report CER77-78RLP-LEC10, 57 pp.
- Petterssen, Sverre (1961) "Some Aspects of Wind Profiles," New Sources of Energy, Proceedings of the United Nations Conference in Rome, Vol. 7 (W/26), pp. 133-136.
- Plate, E. J. and Sheih, C. M. (1965) "Diffusion From a Continuous Point Source into the Boundary Layer Downstream From a Model Hill," Colorado State University, Fort Collins, Colorado, Report No. CER65ELP-CMS60.
- Plate, E. J. and Lin, C. W. (1965) "The Velocity Field Downstream From a Two-Dimensional Model Hill--Part 2," Colorado State University, Fort Collins, Colorado, Report No. CER65EJP-CWL41) 59 pp.

REFERENCES (continued)

- Putnam, Palmer Cosslett (1948) Power From the Wind, Van Nostrand Reinhold Company, New York, 224 pp.
- Queney, P., et al. (1960) "The Airflow Over Mountains," Technical Note No. 34, World Meteorological Organization, Geneva, 135 pp.
- Rider, M. A., and Sandborn, V. A., (1977a) Boundary Layer Turbulence Over Two-Dimensional Hills, Colorado State University Report No. CER77-78MAR-VAS4, 125 pp.
- Rider, M. A., and Sandborn, V. A. (1977b) "Measurements of the Mean and Longitudinal Turbulent Velocities Over Varying Hill Shapes," Colorado State University, Report No. CEM77-78MAR-VAS28, 30 pp.
- Riley, J. J., Liu, H. T., and Geller, E. W. (1976) "A Numerical and Experimental Study of Stably Stratified Flow Around Complex Terrain," Flow Research Inc., Report EPA-600/4-76-021 for U.S. Environmental Protection Agency, 30 pp.
- Sacre, C. (1974) "Theoretical Estimation of the Properties of Airflow Over a 2-Dimensional Hill," Centre Scientifique et Technique du Batement, Nantes, France, 30 pp.
- Sacre, C. (1975) "Numerical Method for Near Calculation of the Excess Velocity of the Wind on a Hill," Centre Scientifique et Technique du Batement, Nantes, France, 26 pp.
- Scorer, R. S. (1952) "Mountain-Gap Winds: A Study of Surface Wind at Gibraltar," Quarterly Journal of the Royal Meteorological Society, Imperial College, London, Vol. 78, pp. 53-61.
- Scorer, R. S. (1978) Environmental Aerodynamics, Ellis Horwood Limited, Chichester, 487 pp.
- Snyder, W. H. (1972) "Similarity Criteria for the Application of Fluid Models to the Study of Air Pollution Meteorology," Boundary Layer Meteorology, Vol. 3, pp. 113-134.
- Sturrock, J. W. (1972) "Aerodynamic Structures of Shelterbelts in New Zealand - 2: Medium-height to Tall Shelterbelts in Mid Canterbury," New Zealand Journal of Science, Vol. 15, No. 2, pp. 113-140.
- Traci, R. M., Phillips, G. T., Patmaik, P. C., and Freeman, B. E. (1977) "The Utility of Mathematical Wind Field Models in a WECS Siting Methodology: A Case Study," 3rd Wind Energy Workshop, Vol. 2, September 1977, Washington, D. C., CONF-770921, pp. 677-688.

REFERENCES (continued)

- Ukejurchi, N., Sakara, H., Okamoto, H., and Ide, Y. (1967) "Study on Stack Gas Diffusion," Mitsubishi Tech. Bull., No. 52, pp. 1-13.
- Woo, H. G. C., Peterka, J. A., and Cermak, J. E. (1976) "Wind-Tunnel Measurements in the Wake of Structures," Colorado State University Report No. CER75-76HGCW-JAP-JEC40, 225 pp.
- Yamada, Tetsuji, and Meroney, Robert N. (1971) "Numerical and Wind Tunnel Simulation of Response of Stratified Shear Layers to Nonhomogeneous Surface Features," Project THEMIS TR No. 9, Colorado State University, Fort Collins, Colorado, Report No. CER70-71TY-RNM62.
- Zrajevsky, I. M., Doroshenko, V. N., and Chapik, N. G. (1968) "Investigation of the Effect of Various Types of Relief on the Characteristics of an Airstream in a Wind Tunnel," Trudi Glnvaya Geofizicheskoya Observatoriya, No. 207 (In Russian).